Available online at www.sciencedirect.com
SCIENCE DIRECT®
Progress in Energy and Combustion Science 30 (2004) 175–217
PROGRESS IN ENERGY AND COMBUSTION SCIENCE
www.elsevier.com/locate/pecs

Optimization of thermal systems based on finite-time thermodynamics and thermoeconomics

Ahmet Durmayaz[a], Oguz Salim Sogut[b], Bahri Sahin[c,*], Hasbi Yavuz[d]

[a]*Department of Mechanical Engineering, Istanbul Technical University, Gumussuyu TR-34439, Istanbul, Turkey*
[b]*Department of Naval Architecture and Ocean Engineering, Istanbul Technical University, Maslak TR-34469, Istanbul, Turkey*
[c]*Department of Naval Architecture, Yildiz Technical University, Besiktas TR-34349, Istanbul 80750, Turkey*
[d]*Institute of Energy, Istanbul Technical University, Maslak, TR-34469 Istanbul, Turkey*

Received 7 September 2003; accepted 30 October 2003

Abstract

The irreversibilities originating from finite-time and finite-size constraints are important in the real thermal system optimization. Since classical thermodynamic analysis based on thermodynamic equilibrium do not consider these constraints directly, it is necessary to consider the energy transfer between the system and its surroundings in the rate form. Finite-time thermodynamics provides a fundamental starting point for the optimization of real thermal systems including the fundamental concepts of heat transfer and fluid mechanics to classical thermodynamics. In this study, optimization studies of thermal systems, that consider various objective functions, based on finite-time thermodynamics and thermoeconomics are reviewed.
© 2004 Elsevier Ltd. All rights reserved.

Keywords: Finite-time thermodynamics; Optimization; Endoreversible; Irreversible; Heat engine; Refrigerator; Heat pump; Thermoeconomics

Contents

1. Introduction . . . 176
2. Optimization of endoreversible and irreversible Carnot heat engines . . . 178
   2.1. Optimization based on maximum power criterion . . . 178
      2.1.1. Fundamentals of power optimization . . . 178
      2.1.2. Effect of heat-transfer law models on the optimal performance . . . 181
      2.1.3. Effect of design parameters and internal irreversibility on the performance . . . 183
      2.1.4. Effect of heat leakage on the performance . . . 184
   2.2. Optimization based on other performance criteria . . . 185
      2.2.1. Power density optimization . . . 185
      2.2.2. Ecological and exergetic performance optimization . . . 186
3. Optimization of cascaded Carnot heat engine models . . . 187
4. Optimization of the other heat-engine cycles . . . 189
   4.1. The Joule–Brayton cycle . . . 189
   4.2. Stirling, Ericsson and Lorentz cycles . . . 192
   4.3. Otto, Atkinson, Diesel and dual cycles . . . 194
   4.4. Direct energy conversion systems . . . 195
5. Optimization of refrigerator and heat pump systems . . . 196
   5.1. Irreversible refrigeration and heat-pump systems . . . 197
   5.2. Cascaded refrigeration and heat-pump systems . . . 199

* Corresponding author. Tel./fax: +90-212-258-2157.
E-mail address: sahinb@yildiz.edu.tr (B. Sahin).

0360-1285/$ - see front matter © 2004 Elsevier Ltd. All rights reserved.
doi:10.1016/j.pecs.2003.10.003

5.3. Gas and magnetic refrigeration and gas heat pump systems 199
5.4. Three/four-heat-reservoir refrigeration and heat-pump systems 200
6. Finite-time thermoeconomic optimization 203
7. Final remarks and conclusions. 208
References 209

1. Introduction

In 1824, Carnot [1] proposed a cycle operating on reversibility principles. In classical thermodynamics, then, the efficiency of a reversible Carnot cycle became the upper bound of thermal efficiency for heat engines that work between the same temperature limits. This equally applies to the coefficient of performance of refrigeration cycles and heat pumps that execute a reversed Carnot cycle. When T_H and T_L denote the temperatures of hot and cold thermal reservoirs, thermal efficiency of Carnot cycle for heat engines and the coefficient of performance for refrigerators and heat pumps are expressed $\eta_C = 1 - T_L/T_H$, $COP_{ref,C} = T_L/(T_H - T_L)$ and $COP_{hp,C} = T_H/(T_H - T_L)$, respectively.

Since all processes are reversible and executed in quasi-steady fashion in a Carnot cycle, thermal efficiency and coefficients of performance mentioned above can only be approached by infinitely slow processes. Therefore, duration of the processes will be infinitely long hence it is not possible to obtain a certain amount of power $\dot{W}$ from a heat engine or of heating load $\dot{Q}_H$ from a heat pump and cooling load $\dot{Q}_L$ from a refrigerator with heat exchangers having finite heat-transfer areas, i.e. $\dot{W} = 0$, $\dot{Q}_H = 0$ and $\dot{Q}_L = 0$ for $0 < A < \infty$, respectively. If we require certain amount of power output in a heat engine, heating load in a heat pump or cooling load in a refrigerator executing an ideal Carnot cycle, the necessary heat exchanger area would be infinitely large, i.e. $A \to \infty$ for $\dot{W} > 0$, $\dot{Q}_H > 0$ and $\dot{Q}_L > 0$, respectively.

Thus, the Carnot thermal efficiency and coefficients of performance do not have great significance and are poor guides to the performances of real heat engines, heat pumps and refrigerators. In practice, all thermodynamic processes take place in finite-size devices in finite-time, therefore, it is impossible to meet thermodynamic equilibrium and hence irreversibility conditions between the system and the surroundings. For this reason, the reversible Carnot cycle cannot be considered as a comparison standard for practical heat engines from the view of output rate (power output for a heat engine, cooling load for a refrigerator and heating load for a heat pump) on size perspective, although it gives an upper bound for thermal efficiency.

In order to obtain a certain amount of power with finite-size devices, Chambadal [2,3], Novikov [4,5] (Novikov's analysis was reprinted in some engineering textbooks [6,7]) and Curzon–Ahlborn [8] extended the reversible Carnot cycle to an endoreversible Carnot cycle by taking the irreversibility of finite-time heat transfer into account and investigated the *m*aximum *p*ower (mp) conditions. They obtained the efficiency of an endoreversible Carnot heat engine at maximum power output. Curzon–Ahlborn [8] claimed that "this result has the interesting property that it serves as quite an accurate guide to the best observed performance of real heat engines". However, it should be noted that this expression is valid for the heat engines to be designed regarding the maximum power output objective. The proper optimization criteria to be chosen for the optimum design of the heat engines may differ depending on their purposes and working conditions. For example, for power plants, in which fuel consumption is the main concern, the maximum thermal efficiency criterion is very important whereas for aerospace vehicles and naval ships, for which propulsion is of great importance, the maximum power output criterion is significant. On the other hand, for ship propulsion systems, both fuel consumption and thrust gain may be equally important, therefore, in such a case both the maximum power and the maximum thermal efficiency criteria have to be considered in the design. Additionally, size reduction, economical and ecological objectives are considered as other important criteria in the design of real heat engines. In this perspective, many optimization studies for heat engines based on the endoreversible and irreversible models have been carried out in literature by considering essentially finite-time and finite-size constraints for various heat-transfer modes.

As a common result of these studies, it can be concluded that the optimal thermal efficiency η_{opt} and optimal power $\dot{W}_{opt}$ for various objectives considering different criteria must be positioned between maximum power and the reversible Carnot heat engine conditions, i.e. $\eta_{mp} \leq \eta_{opt} < \eta_C$ and $\dot{W}_{max} \geq \dot{W}_{opt} > \dot{W}_C = 0$ where η_{mp} is the thermal efficiency at maximum power $\dot{W}_{max}$. It must be noted that the Carnot efficiency and the efficiency at maximum power constitute the upper and lower bounds of the thermal efficiency for a given class of heat engines, respectively. It can also be concluded that the efficiency of the reversible Carnot heat engine cycle is the upper limit for the thermal efficiencies of all heat engines whereas the maximized power output of the endoreversible Carnot heat engine is the maximum power limit.

Identifying the performance limits of thermal systems and optimizing thermodynamic processes and cycles including finite-time, finite-rate and finite-size constraints, which were called as finite-time thermodynamics (FTT), endoreversible thermodynamics, entropy generation minimization (EGM) or thermodynamic

Nomenclature

a	weight coefficient
A	area (m^2)
b	$U_H A_H/UA$, thermal conductance allocation parameter; weight coefficient
C	thermal capacitance or thermal conductance (W/K); cost
E	ecological optimization function
f	relative fuel cost parameter
F	view factor
g	economical market conductance
G	ζ_H/ζ_L
h	heat-transfer coefficient (W/m^2 K)
i	internal irreversibility parameter
k	a/b, ratio of weight coefficients
m	mass (kg)
n	an exponent related to heat-transfer mode
$\dot{N}$	goods flow rate (1/s)
p	price
P	pressure (Pa); profit
$\dot{q}$	$\dot{Q}/A$, specific cooling or heating load (W/m^2)
Q	heat transfer (J)
$\dot{Q}$	heat-transfer rate, cooling or heating load (W)
r	b/a
R	cycle internal irreversibility parameter; ideal gas constant (J/kg K)
s, S	entropy (J/kg K), (J/K)
t	time (s)
T	temperature (K)
U	overall heat-transfer coefficient (W/m^2 K)
V	volume (m^3); economic reservoir
$V\dot{N}$	price flow rate
w	W/m, specific work (J/kg)
W	work (J)
$\dot{w}$	$\dot{W}/A$, specific power (W/m^2)
$\dot{W}$	power (W); tax flow rate; revenue rate

Greek letters

α	general heat-transfer coefficient; absorption coefficient
β	external irreversibility parameter
χ	T_W/T_H
ε	emittance coefficient (%); effectiveness of heat exchangers (%)
η	thermal efficiency (%); tax rate
γ	constant to consider the total time spent in isentropic processes
Γ	total cost of conductance
ω	$\dot{W}/C$, economic objective function
ϕ	dimensionless heat-transfer rate
ψ	T_C/T_W
σ	Stefan–Boltzmann constant, ($= 5.669 \times 10^{-8}$ W/m^2 K^4)
τ	T_L/T_H
τ_1	T_{W2}/T_H
τ_2	T_L/T_{C1}
ζ	unit conductance cost for heat exchangers

Subscripts

A	absorber
avg	average
c	convective
C	Carnot; cold; condenser
cas, max	maximum for cascaded cycle
c–c	convective heat transfer–convective heat transfer
cy	cycle
CNCA	Chambadal–Novikov–Curzon–Ahlborn
d	density in power density concept
e	energy consumption
ecn	economy
eq	equivalent
f	flame
g	generation
gas	gas
H	related to high temperature reservoir
hp	heat pump
i	investment
irr	irreversible
l	leakage
L	related to low temperature reservoir
max	maximum
me	at maximum ecological function conditions
mef	at maximum efficiency conditions
min	minimum
mp	at maximum power conditions
mpd	at maximum power density conditions
opt	optimum
r	radiative
r–c	radiative heat transfer–convective heat transfer
ref	refrigerator
rev	reversible
r–r	radiative heat transfer–radiative heat transfer
R	regenerator
T	total
th	thermal
V	at constant volume
W	warm
0	surroundings
1–8	end points for the processes

Superscripts

n	non-zero integer
·	rate

Abbreviations

COP	coefficient of performance
EGM	entropy generation minimization
FTT	finite-time thermodynamics
LMTD	logarithmic mean temperature difference
MHD	magnetohydrodynamic

modelling and optimization in physics and engineering literature, have been the subject of many books including Bejan [9], Andresen [10], Sieniutycz and Salamon [11], De Vos [12], Bejan [13], Bejan et al. [14], Bejan and Mamut [15], Wu et al. [16], Berry et al. [17], Radcenco [18], and in many review articles including Sieniutycz and Shiner [19], Bejan [20], Chen et al. [21] and Hoffmann et al. [22]. This subject has also been included in some classical thermodynamics textbooks such as, El-Wakil [7], Bejan [23], Van Wylen et al. [24] and Winterbone [25].

In this study, the publications in literature on the perspective of FTT and thermoeconomics theories for the optimization of heat engines, heat pumps and refrigerators based on a variety of objective functions from late 1950s to present are reviewed by using a tutorial style of writing.

2. Optimization of endoreversible and irreversible Carnot heat engines

The studies on the fundamentals of FTT analysis and some applications to the optimization of endoreversible and irreversible Carnot heat engines which cover different performance criteria will be reviewed in this section.

2.1. Optimization based on maximum power criterion

The studies on the optimization of endoreversible and irreversible Carnot heat engines based on maximum power criterion together with the effects of heat-transfer laws, design parameters, internal irreversibilities and heat leakage are reviewed in the following sections.

2.1.1. Fundamentals of power optimization

Chambadal and Novikov derived independently that the hot end temperature of a power plant could be optimized to maximize the power output. Chambadal's model [2,3] of an externally irreversible Carnot heat engine can be shown in Fig. 1 with (1–2–3–4–1) cycle and a constant temperature heat source at T_H. In his model, there is only one optimization parameter which is T_W. It can easily be expressed that the power output may be maximized when

$$T_{W,opt} = \sqrt{T_H T_L}. \tag{1}$$

which corresponds to the thermal efficiency at maximum power of

$$\eta_{mp} = 1 - \sqrt{\frac{T_L}{T_H}}. \tag{2}$$

Novikov's model [4,5] of an irreversible Carnot heat engine is also shown in Fig. 1 however, with $(1-2-3-4_{irr}-1)$ cycle and a constant temperature heat source at T_H. The external irreversibility is due to the finite-temperature difference between the heat source temperature of T_H and the working fluid temperature of T_W. The internal irreversibility in the expansion process of $3-4_{irr}$ is also considered. Novikov accounted for the internal irreversibility with the parameter i and expressed the heat rejected to the ambient as

$$\dot{Q}_L = (1+i)\dot{Q}_{L,rev}, \tag{3}$$

where

$$1 + i = \frac{s_{4_{irr}} - s_1}{s_4 - s_1}. \tag{4}$$

The rest of the heat engine is considered to operate reversibly. Novikov derived the optimum working fluid temperature at hot side as

$$T_{W,opt} = \sqrt{(1+i)T_H T_L} \tag{5}$$

and the corresponding thermal efficiency at maximum power as

$$\eta_{mp} = 1 - \sqrt{\frac{(1+i)T_L}{T_H}}. \tag{6}$$

When the expansion process is executed reversibly ($i = 0$), Chambadal's result given by Eqs. (1) and (2) can be recovered.

Curzon and Ahlborn [8] rediscovered the Chambadal's efficiency formula given in Eq. (2) [2,3]. They extended the Chambadal's work taking into account of the cold side

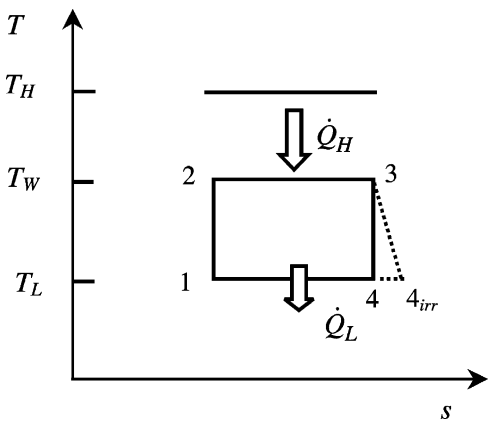

Fig. 1. Chambadal's and Novikov's heat-engine model.

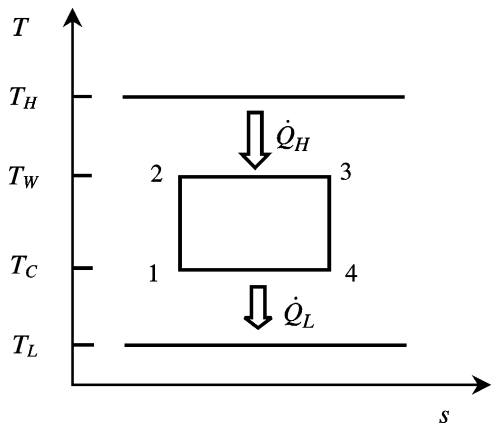

Fig. 2. Endoreversible Carnot heat-engine model.

external irreversibility between the temperatures of working fluid and heat sink as well as the hot side external irreversibility. The Carnot heat engine with external irreversibilities described in their work can be shown in Fig. 2.

In their work, they assumed that finite-time heat fluxes between heat reservoirs and the working fluid are proportional to their temperature difference where the overall heat-transfer coefficients are the proportionality constants. The assumed proportionality between convective heat-transfer rate and temperature difference may be called as 'linear heat-transfer law' which is sometimes referred to as 'Newton's law of cooling'. Time required to complete the cycle is defined as the total time spent in isothermal processes weighted by a constant, γ, to consider the total time spent in isentropic processes. The power output of the cycle is expressed as an objective function where the optimization parameters are the finite temperature differences in the heat exchangers. They obtained the maximum power output of the cycle as

$$\dot{W}_{\max} = \frac{U_H A_H U_L A_L (\sqrt{T_H} - \sqrt{T_L})^2}{\gamma(\sqrt{U_H A_H} + \sqrt{U_L A_L})^2}. \tag{7}$$

They deduced in their work that the thermal efficiency of a Carnot heat engine at maximum power with heat transfer irreversibilities does not depend on the heat-transfer coefficients. It depends only on the temperature of the heat reservoirs. They claimed that this result serves as a quite an accurate guide to the best observed performance of real heat engines. The thermal efficiency of cycle at maximum power output given in Eq. (2) may be called the Chambadal–Novikov–Curzon–Ahlborn efficiency or CNCA efficiency η_{CNCA} as it was suggested by Bejan [20].

Andresen et al. [26] developed a general description for processes involving work and heat interaction in terms of rates for continuous processes or of cycle averages for periodic processes. The description was applied to heat engines having irreversibilities to determine their maximum power and maximum efficiency. Salamon et al. [27] developed an algorithm to construct potentials that define the extremal values of work for processes with arbitrary constraints. They proved an existence theorem for potentials of quasi-static processes and claimed that this theorem extends the capability of thermodynamics from reversible processes to one class of time-dependent processes. Gutkowicz-Krusin et al. [28] analyzed the power and efficiency of a Carnot heat engine subject to finite-rate heat transfer between the ideal gas working fluid and thermal reservoirs, and maximized the power output with respect to working fluid temperatures in the limit of large compression ratio. They generalized the result of their model to any heat engine operating between the same two thermal reservoirs. Considering different heat-transfer processes, they found that the bounds on the efficiencies at maximum power output depend on the rate process.

Optimization of a class of cyclic heat engines with only external thermal resistance losses without assuming any specific power cycle were carried out in Rubin [29–31] for systems without and with volume constraints to find their optimal operating configuration for specific performance goals. Salamon et al. [32] considered the problem of minimum entropy production in an endoreversible Carnot heat engine and showed that for such engines, minimizing the total entropy production is equivalent to minimizing the loss of availability. Andresen and Gordon [33] derived optimal heating and cooling strategies for minimizing entropy generation for a common class of finite-time heat-transfer processes. Salamon and Nitzan [34] investigated the optimal operation of an endoreversible Carnot heat engine for different choices of the objective functions including maximum power, maximum efficiency, maximum effectiveness, minimum entropy production, minimum loss of availability and maximum profit. Rubin and Andresen [35] showed that endoreversible engines can be staged to form a two-stage cascaded endoreversible heat engine and that its optimization also yields the CNCA efficiency. The generalization of a Carnot heat engine with finite-rate heat transfer from finite-capacity heat source was presented theoretically together with numerical examples by Ondrechen et al. [36].

Rebhan and Ahlborn [37] examined the influence of the relative variation of the heat addition and rejection times on the maximum power output and maximum efficiency.

Wu [38] and Wu and Walker [39] have also considered an endoreversible Carnot heat engine. They assumed that the total cycle time consisted only the time required to complete the isothermal processes neglecting the time spent in isentropic processes. They considered power output as an objective function and maximum and minimum working fluid temperatures as optimization parameters. The power output of the cycle is

$$\dot{W} = \frac{W}{t_{cy}} = \frac{Q_H - Q_L}{t_{cy}}, \tag{8}$$

where W is the work output of the cycle and

$$\dot{Q}_H = \frac{Q_H}{t_H} = U_H A_H (T_H - T_W), \tag{9}$$

$$\dot{Q}_L = \frac{Q_L}{t_L} = U_L A_L (T_C - T_L). \tag{10}$$

Neglecting the time spent in adiabatic branches, i.e. $\gamma = 1$, and by the aid of Figs. 2 and 3, the total time required to complete the cycle is

$$t_{cy} = t_H + t_L + t_{12} + t_{34} \approx t_H + t_L. \tag{11}$$

Substituting t_H and t_L from Eqs. (9) and (10) into Eq. (8), the power output is written

$$\dot{W} = \frac{\dot{Q}_H t_H - \dot{Q}_L t_L}{t_H + t_L}. \tag{12}$$

The working fluid temperatures T_W and T_C are defined as the optimization parameters. Maximizing $\dot{W}$ with respect to T_W and T_C under the second law constraint yields

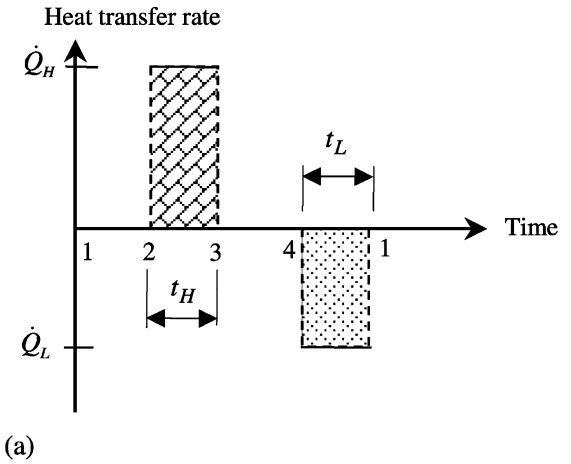

(a)

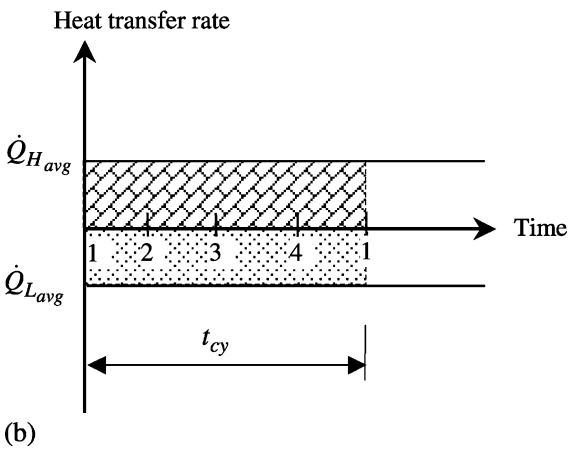

(b)

Fig. 3. Operation of an endoreversible Carnot heat engine (a) with sequential processes (b) with simultaneous processes [43].

the maximum power output for the operation of a Carnot heat engine with sequential (or reciprocating) processes given by Eq. (7) considering the time constant $\gamma = 1$. The thermal efficiency at maximum power output, η_{mp}, given by Eq. (2) is also identically recovered from this analysis. Therefore, in their work, it is illustrated that η_{mp} does not depend on either the overall heat-transfer coefficients or surface areas of the heat exchangers.

Many other authors have done similar analysis of the endoreversible Carnot cycle and obtained CNCA efficiency given by Eq. (2), however, a different expression for $\dot{W}_{max}$ was obtained in many of these studies [40,41]. Instead of Eq. (7), an alternative expression for $\dot{W}_{max}$ is given as

$$\dot{W}_{max} = U_H A_H U_L A_L \frac{(\sqrt{T_H} - \sqrt{T_L})^2}{U_H A_H + U_L A_L}, \tag{13}$$

for the maximum power output of the operation of a Carnot heat engine with simultaneous processes (used as the steady-state operation in literature). Eq. (13) gives a larger $\dot{W}_{max}$ than that of Eq. (7).

Bejan's [42] steady-state approach yields the power output for steady-state operation of a heat engine with simultaneous processes as

$$\dot{W} = \dot{Q}_H - \dot{Q}_L. \tag{14}$$

In terms of power, the second law of thermodynamics can be written as

$$\frac{\dot{Q}_H}{T_W} = \frac{\dot{Q}_L}{T_C}, \tag{15}$$

which is used as a constraint in the power optimization process for the operation of a heat engine with simultaneous processes. Using this constraint, the power optimization may be carried out for just only one working fluid temperature, either T_W or T_C. In his study, Bejan considered a steady-state power plant model in which the irreversibilities are due to three sources: the hot-end heat exchanger, the cold-end heat exchanger and the heat leaking through the plant to the ambient.

The sequential and steady-state operation approaches are compared in Wu et al.'s study [43]. It is shown that thermal efficiency at maximum power is the same for both types of engines. However, the power production in steady-state operation with simultaneous processes given by Eq. (14) is larger than that of operation with sequential processes given by Eq. (12). The source of discrepancy is shown in Fig. 3. In Wu's approach the four processes of the Carnot cycle take place sequentially as in a reciprocating engine whereas in Bejan's approach, the heat addition and heat rejection processes are assumed to take place simultaneously and are continuous in time as in a thermal power plant. (Note that $\dot{Q}_H t_H = \dot{Q}_{H_{avg}} t_{cy}$ and $\dot{Q}_L t_L = \dot{Q}_{L_{avg}} t_{cy}$).

Wu [44] considered a reversible Carnot cycle coupled to a heat source and heat sink having finite-heat capacity, shown in Fig. 4. In this study, an operation of a Carnot heat engine with sequential processes is adopted. The rate of heat

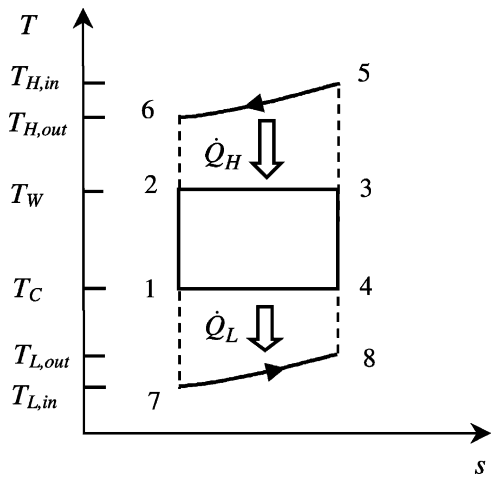

Fig. 4. Endoreversible Carnot heat-engine model with finite thermal capacity rates.

transfer between the reservoirs and the working fluid is proportional to the logarithmic mean temperature differences, $\mathrm{LMTD_H}$ and $\mathrm{LMTD_L}$. The heat-transfer rates are

$$\dot{Q}_{\mathrm{H}} = \frac{Q_{\mathrm{H}}}{t_{\mathrm{H}}} = U_{\mathrm{H}} A_{\mathrm{H}} (\mathrm{LMTD_H}), \tag{16}$$

$$\dot{Q}_{\mathrm{L}} = \frac{Q_{\mathrm{L}}}{t_{\mathrm{L}}} = U_{\mathrm{L}} A_{\mathrm{L}} (\mathrm{LMTD_L}), \tag{17}$$

where

$$\mathrm{LMTD_H} = \frac{(T_5 - T_{\mathrm{W}}) - (T_6 - T_{\mathrm{W}})}{\ln\left[\dfrac{(T_5 - T_{\mathrm{W}})}{(T_6 - T_{\mathrm{W}})}\right]}, \tag{18}$$

$$\mathrm{LMTD_L} = \frac{(T_{\mathrm{C}} - T_7) - (T_{\mathrm{C}} - T_8)}{\ln\left[\dfrac{(T_{\mathrm{C}} - T_7)}{(T_{\mathrm{C}} - T_8)}\right]}. \tag{19}$$

The power optimization of this heat engine is performed in the similar lines of an earlier paper of Wu [38]. He provided a numerical example and as a conclusion he obtained a thermal efficiency which is smaller that of a reversible Carnot heat engine.

Nulton et al. [45] examined a category of thermodynamic processes conducted over a finite interval of time and derived mathematical inequalities, relating the total cycle time and the net entropy change of the thermal reservoirs, to which such processes must conform. In their following work, Pathria et al. [46] focused on one of those inequalities which pertains to a cyclic process representing a heat engine or a refrigerator. They recast this inequality in terms of the more practical quantities, the power output and the degradation (which denotes the average rate at which the entropy of the universe increases during the cycle) associated with the process. They showed that the thermal efficiency of a heat engine and the temperature ratio of the working fluid can be written in terms of the slope of lines passing through the origin in the power output versus degradation plane. They also extended their work to include the influence of an external heat leak between the two thermal reservoirs.

Gordon [47] analysed heat engines considering finite-rate heat transfer and finite-capacity thermal reservoirs. He showed that the efficiency at maximum power is not always simply a function of the thermal reservoir temperatures only, but rather can depend on other system variables such as reservoir capacity (in the case of finite-capacity thermal reservoirs) or working fluid specific heats (in the case of the Diesel and Atkinson cycles). He also explained that the Curzon–Ahlborn problem is a special case of one general class of problems restricted to Carnot-like heat engines with linear irreversibilities in which losses and heat transfer are finite in time and linear in temperature differences.

De Mey and De Vos [48] showed that some endoreversible systems provided with linear thermal resistors have other efficiencies at maximum power output conditions than CNCA efficiency. Therefore, CNCA efficiency formula does not have a general validity as an optimum efficiency for endoreversible systems.

Bejan [20,23,49] extended the heat-transfer principle of power maximization in power plants with heat-transfer irreversibilities to fluid flow and showed that power extracted from a flow can be maximized by selecting the optimal flow rate, or optimal pressure drops upstream and downstream of the actual work-producing device. He demonstrated the analogy between maximum power conditions for fluid (mechanical) power conversion versus thermal (thermomechanical) power conversion. Bejan and Errera [50] outlined the solution to the fundamental problem of how to extract maximum power from a hot single-phase stream when the total heat-transfer surface area is fixed. Vargas and Bejan [51] considered the fundamental problem of matching thermodynamically two streams, one hot and the other cold, with the presence of phase change along both streams and determined the optimum thermodynamic match by maximizing the power generation (or minimizing the entropy generation). They showed that the thermodynamic optimum is associated with a characteristic ratio between the flow rates of the two streams, and a way of dividing the total heat-transfer area between the two heat exchangers.

2.1.2. Effect of heat-transfer law models on the optimal performance

Many authors studied the performance of endoreversible cycles based on linear heat-transfer law and derived some significant results [8,30,52]. For example, the famous CNCA efficiency, which depends only on the temperature of the heat reservoirs, was obtained for two-heat-reservoir cycle at maximum power condition for each analysis. De Vos [40], Orlov [53], Gutkowicz-Krusin et al. [28] and Yan and Chen [54] studied the effect of heat-transfer law on the performance of endoreversible cycles. Castans [55], Jeter [56], De Vos and Pauwels [57] applied

the Stefan–Boltzmann thermal radiation law to the performance analysis of solar energy conversion systems. In the application of the Stefan–Boltzmann thermal radiation law, the radiative heat-transfer rates from heat source and to heat sink, when they are assumed to have infinite heat capacity rates, can be expressed as

$$\dot{Q}_H = A_W F_{WH} \sigma (T_H^4 - T_W^4) = A_W h_{W,r} (T_H^4 - T_W^4) = A_H h_{H,r} (T_H^4 - T_W^4), \quad (20)$$

$$\dot{Q}_L = A_C F_{CL} \sigma (T_C^4 - T_L^4) = A_C h_{C,r} (T_C^4 - T_L^4) = A_L h_{L,r} (T_C^4 - T_L^4), \quad (21)$$

where F_{WH} and F_{CL} are the view factors of emitter and collector when black body radiation is considered, σ is the Stefan–Boltzman constant and $h_{W,r}$, $h_{H,r}$, $h_{C,r}$ and $h_{L,r}$ are the radiative heat-transfer coefficients.

De Vos [40], Chen and Yan [58] and Gordon [59] discussed the effect of a class of heat-transfer laws given by

$$\dot{Q} = \frac{Q}{t_{cy}} = \alpha (T_1^n - T_2^n), \quad (22)$$

on the performance of endoreversible cycles systematically (n is a non-zero integer and $n = -1$ for linear-phenomenological heat-transfer law, $n = 1$ for linear heat-transfer law, $n = 4$ for the Stefan–Boltzmann thermal radiation law) where heat is transferred from thermal source/working fluid at temperature T_1 to working fluid/thermal source at T_2 and α is a general heat-transfer coefficient. They revealed the dependence of performance on the heat-transfer law and the heat-transfer coefficient and derived a universal expression for different common heat-transfer laws and concluded that the value of maximum power depends on both the source temperatures and the heat-transfer coefficient. This conclusion also applies to the efficiency at maximum power except for the linear heat-transfer law.

Heat engines must be designed somewhere between the two limits of (1) maximum efficiency, which corresponds to Carnot efficiency or reversible operation, at zero power, and (2) maximum power point. Each of these limits implies a specific dependence of heat engine efficiency on the temperatures of the hot and cold reservoirs between which the heat engine operates. Gordon [59] analyzed the endoreversible cyclic heat engine problem for maximum power output operation when the functional form of the temperature dependence of heat transfer is a variable. He proved that the efficiency at maximum power output is in general dependent on the heat transfer and that a type of symmetry exists relative to the functional temperature dependence of linear heat conduction. He showed that the CNCA efficiency actually is not a fundamental upper limit on the efficiency of an endoreversible heat engine operating at maximum power output condition and further this upper limit depends on the heat-transfer mechanism. Gordon [60] illustrated that the optimal operating temperature for solar-driven heat engines and solar collectors is relatively insensitive to the engine design point. Gordon and Zarmi [61] also showed that certain systems in nature can be analyzed effectively as heat engines, such as the generation of the earth's winds. They analyzed a wind heat engine model in which the earth's atmosphere is viewed as the working fluid of a heat engine, solar radiation is the heat input, the energy in the earth's winds is the work output and heat is rejected to the surrounding universe. By the aid of FTT, they determined the maximum average power as well as the average maximum and minimum temperatures of the working fluid and found a theoretical upper bound for annual average wind energy.

Agnew et al. [62] optimized an endoreversible Carnot cycle with convective heat transfer following linear heat-transfer law for the case of maximum specific work output and reaffirmed the CNCA efficiency. They also investigated the dependency of the efficiency at maximum power on different modes of heat transfer.

Erbay and Yavuz [63] performed an analysis of an endoreversible Carnot heat engine with the consideration of combined radiation and convection heat transfer between the working fluid and hot and cold heat reservoirs

$$\dot{Q}_H = U_H A_H (T_H - T_W) + A_H \sigma (\varepsilon_H T_H^4 - \alpha_H T_W^4), \quad (23)$$

$$\dot{Q}_L = U_L A_L (T_C - T_L) + A_L \sigma (\varepsilon_L T_C^4 - \alpha_L T_L^4), \quad (24)$$

where α_H and α_L are absorption coefficients and ε_H and ε_L are emittance coefficients for heat source and heat sink sides, respectively. They showed that the power output of the heat engine is strongly dependent on the temperature and emittance ratios of the heat reservoirs.

Badescu [64] proposed a model of a space power station composed of an endoreversible Carnot heat engine driven by solar energy. He obtained the maximum power output and the optimum ratio between the solar collector and radiator areas.

Sahin [65] carried out an analysis for a solar driven endoreversible Carnot heat engine to investigate the collective role of the radiation heat transfer from the high temperature reservoir and convection heat transfer to the low temperature reservoir and determined the limits of efficiency and power generation numerically. He concluded that the CNCA efficiency is not a fundamental upper limit on the efficiency of heat engines operating at *mp* conditions. This upper limit is a function of the temperatures of the working fluid and heat reservoirs, heat-transfer mechanisms and relevant system parameters. With the definition of an external irreversibility parameter $\beta_{r-c} = h_{H-r} A_H T_H^3 / h_L A_L$, he plotted the variation of efficiencies η_{CNCA}, η_{mp} and η_C with respect to β_{r-c} for a constant value of the temperature ratio τ as given in Fig. 5. Since τ is taken to be constant, η_{CNCA} and η_C are constant. As a result of employing different, i.e. radiative and convective, heat-transfer mechanisms between the working fluid and heat reservoirs, it can be seen in Fig. 5 that η_{mp} is less than the Carnot efficiency

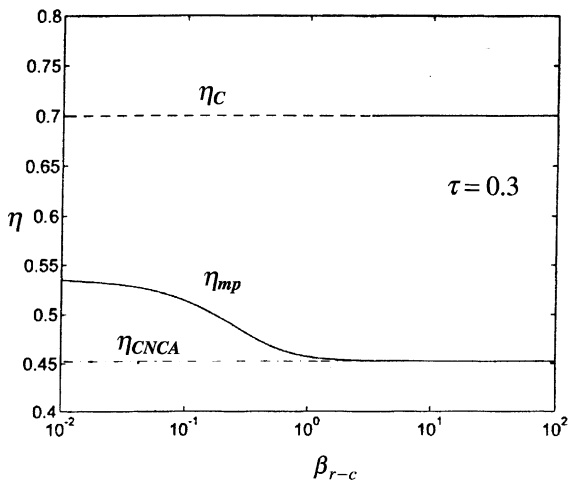

Fig. 5. Variation of efficiencies with respect to the external irreversibility parameter β_{r-c} [65].

$\eta_C = 1 - \tau$ but higher than the Chambadal–Novikov–Curzon–Ahlborn efficiency $\eta_{CNCA} = 1 - \sqrt{\tau}$ for the whole range of β_{r-c} values. Although their difference is very small for high values of β_{r-c}, η_{mp} tends to increase for small values of β_{r-c}. The variation of efficiencies with respect to the temperature ratio τ for a constant value of β_{r-c} is also shown in Fig. 6. For comparison the Carnot efficiency and the Chambadal–Novikov–Curzon–Ahlborn efficiency are also displayed. The comments made for Fig. 5 is also valid for Fig. 6 for all values of τ.

2.1.3. Effect of design parameters and internal irreversibility on the performance

Andresen et al. [26] considered the effect of friction, thermal resistance and heat leakage to determine the maximum power and maximum efficiency of heat engines with two or three heat reservoirs. For a general class of heat engines operating at maximum power output conditions, in which the generic sources of irreversibility are the finite-rate heat transfer and friction only, and Gordon and Huleihil [66] investigated the time-dependent driving function that maximize power when heat input and heat rejection are constraint to be non-isothermal (such as at constant volume, constant pressure or on a polytropic branch) and the impact of frictional losses on the engine's power–efficiency characteristics, i.e. maximum power output and corresponding efficiency.

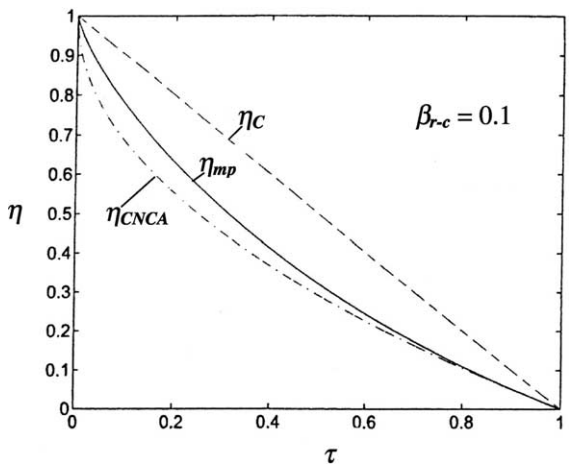

Fig. 6. Variation of efficiencies with respect to the temperature ratio τ [65].

Although, the Curzon and Ahlborn efficiency is independent of the plant size, Goktun et al. [67] reported that for radiative heat transfer at both hot and cold reservoir sides, the thermal efficiency depends on the external irreversibility parameter β_{r-r} which is the ratio of $h_{H,r}A_H$ to $h_{L,r}A_L$. They defined $\psi = T_C/T_W$ as an optimization parameter and expressed the power output as a function of β_{r-r} and ψ. The optimization for power output is carried out with the constraint of $\dot{Q}_H/\dot{Q}_L = T_W/T_C$. They concluded that increasing the heat-transfer area of the cold side rather than that of the hot side improves the thermal efficiency.

Wu and Kiang [68] introduced that the internal irreversibilities of a Carnot heat engine can be characterized by a single parameter named as the cycle-irreversibility parameter. This parameter represents the ratio of entropy generation in isothermal branches of the cycle, shown in Fig. 7.

The cycle-irreversibility parameter is defined as

$$R = \frac{s_3 - s_{2_{irr}}}{s_{4_{irr}} - s_1}, \tag{25}$$

and by the aid of Eq. (15)

$$\frac{\dot{Q}_H}{T_W} - R\frac{\dot{Q}_L}{T_C} = 0, \tag{26}$$

is obtained as the second law of thermodynamics constraint with $0 < R < 1$.

A steady-state operation with simultaneous processes of the heat engine is considered and it is concluded that the cycle-irreversibility parameter R appears in both maximum power and efficiency equations. Since this parameter is less than unity, the equations clearly show that the engine with

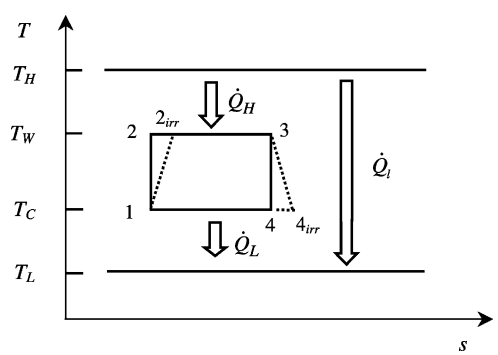

Fig. 7. Irreversible Carnot heat-engine model with heat leakage.

internal irreversibilities delivers less power and has a lower efficiency when compared with an endoreversible Carnot engine. Considering the internal irreversibilities, the thermal efficiency of an irreversible Carnot heat engine is expressed as

$$\eta_{\mathrm{mp}} = 1 - \sqrt{\frac{T_{\mathrm{L}}}{RT_{\mathrm{H}}}}. \tag{27}$$

Chen et al. [69] determined the efficiency of the irreversible radiant Carnot heat engine at maximum specific power output and corresponding optimal temperatures of working fluid and heat-transfer areas.

Goktun [70] extended their work [67] to include the internal irreversibility parameter R and used the external irreversibility parameter $\beta_{\mathrm{c-c}}$ as an optimization parameter together with ψ. He concluded that for maximum power output, the heat exchangers optimum size ratio $\beta_{\mathrm{c-c,opt}}$ must be less than unity when $R < 1$ that corresponds to an irreversible heat engine whereas $\beta_{\mathrm{c-c,opt}} = 1$ when $R = 1$ that corresponds to an endoreversible heat engine.

Ozkaynak et al. [71] extended the analysis given by Goktun et al. [67] to include internal irreversibilities with a cycle-irreversibility parameter R given by Eq. (25). β is generalized in a way that radiative–radiative or convective–convective heat-transfer mechanisms could be selected independently for the heat transfer between heat reservoirs and working fluid for hot and cold sides by the definitions of $\beta_{\mathrm{r-r}}$ and $\beta_{\mathrm{c-c}}$, respectively. Ozkaynak [72] also investigated the optimal efficiency of an internally and externally irreversible, solar-powered heat engine with radiative heat transfer from the heat source and convective heat transfer to the heat sink. He defined an optimization parameter $\chi = T_{\mathrm{W}}/T_{\mathrm{H}}$ for this case and used the external irreversibility parameter $\beta_{\mathrm{r-c}}$ and the cycle-internal-irreversibility parameter R as in Eq. (25). The non-dimensional power output is optimized with respect to χ and it is concluded that the external irreversibility parameter must be less than 0.5 for optimum thermal efficiency and maximum power output. It is also noted that increasing the cycle-irreversibility parameter R improves the thermal efficiency and maximum power output.

Ait-Ali [73] studied an irreversible Carnot-like power cycle with internal irreversibility. He considered that the generic source of internal irreversibility generates entropy at a rate being proportional to the external thermal conductance and the engine temperature ratio. He optimized the cycle for maximum power and maximum efficiency and compared the performances to those of the endoreversible cycle. He concluded that the condenser thermal conductance that takes place between the low temperature heat reservoir and the working fluid, is always higher than the boiler thermal conductance that takes place between the high temperature heat reservoir and the working fluid. He also concluded that the respective sizes of the thermal conductances and therefore the sizes of the corresponding heat-transfer areas appear to be a critical design point for maximum efficiency.

Bejan [74] investigated alternatives to the usual thermodynamic optimization formulation. The alternatives were the improvement of the thermodynamic performance of a system subject to physical size constraints, i.e. the power maximization, and the minimization of the physical size subject to specified thermodynamic performance, i.e. the surface minimization. He showed that both optimization approaches lead to the same physical configuration (the same physical design).

Salah El Din [75] studied the performance of irreversible Carnot heat engines with variable temperature heat reservoirs. He concluded that the optimal temperature ratio of working fluid at hot and cold sides and the efficiency at maximum power are functions of the inlet temperatures to the heat exchangers instead of the average temperatures of the inlet and outlet temperatures of thermal reservoirs.

2.1.4. Effect of heat leakage on the performance

Following the works of Andresen et al. [26], Bejan [42] and Pathria et al. [46] regarding the effect of heat leakage on the performance, Gordon and Huleihil [76] derived the power–efficiency relations, determined their upper bounds and plotted generalized curves for heat engine performance for several types of heat engines with frictional losses, specifically: Brayton cycle, Rankine cycle and cycles with sizeable heat leaks, such as thermoelectric generators.

Chen [77] extended the studies on the irreversible Carnot heat engine with external and internal irreversibilities such as Wu and Kiang [68], considering the heat leakage, $\dot{Q}_{\mathrm{L}} = C_{\mathrm{l}}(T_{\mathrm{H}} - T_{\mathrm{L}})$ from the heat source to the heat sink (i.e. ambient) for a Carnot heat engine with sequential processes shown in Fig. 7. C_{l} is the thermal conductance, i.e. heat-transfer area times the overall heat-transfer coefficient based on that area.

In contrast to Chen's [77] approach of sequential operation, Chen et al. [78] considered an irreversible Carnot heat engine which executes simultaneous processes with heat leakage to the ambient. They also included the effect of the ratio of heat-transfer areas into their optimization study.

Chen et al. [79] took a step further Bejan's work [42] to determine the power versus efficiency characteristics at maximum power and at maximum efficiency conditions for an endoreversible Carnot heat engine with simultaneous processes considering internal heat leakage. In this study, the maximum power output, $\dot{W}_{\mathrm{max}}$, the maximum efficiency, ν_{max}, the efficiency at maximum power output, η_{mp} and the power output at maximum efficiency, $\dot{W}_{\mathrm{mef}}$ are calculated. The functional relationship of the power output with the efficiency of the heat engine is established and shown in Figs. 8 and 9 for an irreversible Carnot heat engine without and with heat leakage, respectively. Fig. 8 clearly shows that when heat leakage is not present, large difference exists between η_{mp} and η_{max}. It must also be noted that the power

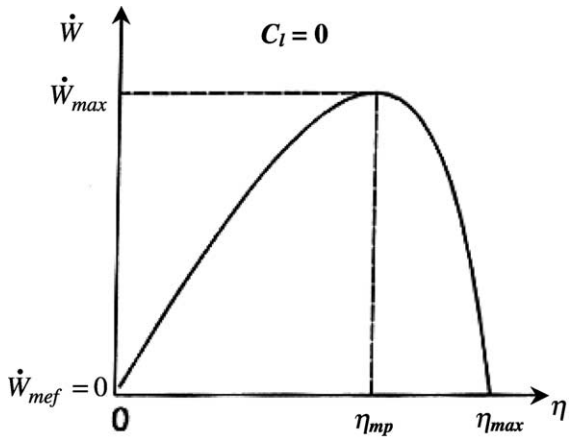

Fig. 8. The power output versus thermal efficiency of an irreversible Carnot heat engine [79].

output at maximum efficiency is equal to zero, i.e. $\dot{W}_{\mathrm{mef}} = 0$. As it is seen in Fig. 9, when heat leakage is considered, the power output versus efficiency curve becomes loop-shaped. Fig. 9 can be interpreted that when the efficiency is less than η_{mp}, the power output of the heat engine decreases as the efficiency decreases and when the power output is less than $\dot{W}_{\mathrm{mef}}$, the efficiency of the heat engine also decreases as the power output decreases. The rational regions of the efficiency and the power output of the heat engine are obviously between η_{mp} and η_{max} or $\dot{W}_{\mathrm{max}}$ and $\dot{W}_{\mathrm{mef}}$, respectively. It can be concluded that the heat engine should be operated between η_{mp} and η_{max} and $\dot{W}_{\mathrm{max}}$ and $\dot{W}_{\mathrm{mef}}$.

De Vos [40] had considered an endoreversible Carnot heat engine with generalized heat-transfer modes depending on different heat-transfer laws. Moukalled et al. [80] generalized the De Vos model by adding a heat leak term from the hot working fluid to the cold working fluid and

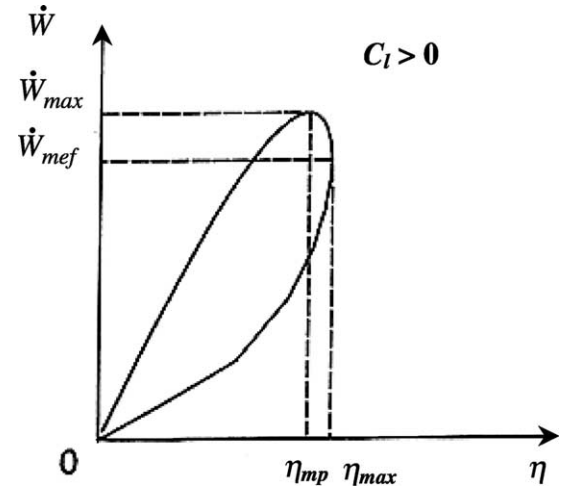

Fig. 9. The power output versus thermal efficiency of an irreversible Carnot heat engine with heat leakage [79].

investigated the variation of the thermal efficiency at maximum power as functions of the ratio of heat-transfer coefficients between the heat reservoirs and the working fluid, the ratio of cold to hot reservoir temperatures and heat leak contribution. Moukalled et al. [81] later extended this work to obtain a universal model for the performance analysis of endoreversible Carnot-like heat engines with heat leak at maximum power conditions. They developed a model to accommodate combined modes of different heat-transfer power laws.

2.2. Optimization based on other performance criteria

Optimization based on the other performance criteria such as, power density, ecological and exergetic performance is reviewed in the following sections following the review of the studies on the optimization of endoreversible and irreversible Carnot heat engines based on maximum power criterion together with the effects of heat-transfer laws, design parameters, internal irreversibilities and heat leakage.

2.2.1. Power density optimization

The performance analysis based on maximum power output does not include effects of engine size. To include the effect of engine size, Sahin et al. [82] suggested a new performance analysis criterion called *m*aximum *p*ower *d*ensity (*mpd*) which was defined as the ratio of power to the maximum specific volume in the cycle.

Sahin et al. [83] carried out an analysis using maximum power density criterion for an endoreversible Carnot heat engine. The model of the endoreversible Carnot heat engine they considered is shown again in Fig. 2. In the cycle, the working fluid has maximum specific volume or maximum volume V_{max} and minimum pressure at the end-point 4 shown in Fig. 2, i.e. $V_{\mathrm{max}} = V_4$. The power *d*ensity (d) is defined as the power given in Eq. (14) divided by the maximum volume in the cycle which is in the form of

$$\dot{W}_{\mathrm{d}} = \frac{\dot{Q}_{\mathrm{H}} - \dot{Q}_{\mathrm{L}}}{V_{\mathrm{max}}}. \tag{28}$$

The total thermal conductance is fixed, which is $U_{\mathrm{H}}A_{\mathrm{H}} + U_{\mathrm{L}}A_{\mathrm{L}} = UA = \text{constant}$, as an additional constraint to the fulfillment of the second law of thermodynamics for the cycle. Employing the ideal gas assumption, the maximum volume in the cycle, which characterizes the engine size, is expressed as $V_{\mathrm{max}} = mR_{\mathrm{gas}}T_{\mathrm{C}}/P_{\mathrm{min}}$ where m is mass, R_{gas} is gas constant and P_{min} is the minimum pressure of the working fluid. Defining a thermal conductance allocation parameter, $b = U_{\mathrm{H}}A_{\mathrm{H}}/UA$ and assuming that P_{min} is constant, the power density is optimized with respect to T_{C} and T_{W} to give the maximum power density $\dot{W}_{d,\mathrm{max}}$ and the efficiency at maximum power density, η_{mpd}. The effect of the conductance allocation parameter b on the efficiency at maximum power density for $\tau = 0.2$ is shown in Fig. 10. It can be seen from Fig. 10 that as $b \rightarrow 1$, η_{mpd} approaches

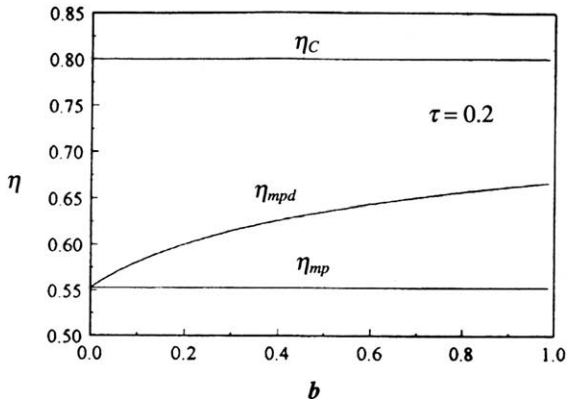

Fig. 10. Effect of conductance allocation parameter b on the thermal efficiency [83].

$1 - 2\tau/(1+\tau)$ and when $b = 0$ then $\eta_{\mathrm{mpd}} = 1 - \sqrt{\tau} = \eta_{\mathrm{mp}}$. Therefore,

$$\eta_{\mathrm{mp}} = 1 - \sqrt{\tau} \le \eta_{\mathrm{mpd}} \le (1 - 2\tau/(1+\tau)) \le \eta_{\mathrm{C}} = 1 - \tau, \tag{29}$$

for $0 \le b \le 1$ and the conclusion is that the thermal efficiency at maximum power density is greater than the thermal efficiency at maximum power.

Kodal et al. [84] carried out a comparative performance analysis of irreversible Carnot heat engines under maximum power density and maximum power conditions. Their model includes three types of irreversibilities: finite-rate heat transfer, heat leakage and internal irreversibility as shown in Fig. 7. Using Eqs. (9), (10) and (26), they expressed the second law of thermodynamics constraint as

$$\frac{U_{\mathrm{H}}A_{\mathrm{H}}(T_{\mathrm{H}} - T_{\mathrm{W}})}{T_{\mathrm{W}}} - R\frac{U_{\mathrm{L}}A_{\mathrm{L}}(T_{\mathrm{C}} - T_{\mathrm{L}})}{T_{\mathrm{C}}} = 0. \tag{30}$$

They optimized power density given in Eq. (28) with respect to T_{W} and T_{C} by using Eq. (30). The maximum power density is obtained

$$\dot{W}_d = \left(\frac{U_{\mathrm{H}}A_{\mathrm{H}}P_{\min}}{mR_{\mathrm{gas}}}\right)\frac{(\sqrt{U_{\mathrm{H}}A_{\mathrm{H}} + U_{\mathrm{L}}A_{\mathrm{L}}R} - \sqrt{U_{\mathrm{H}}A_{\mathrm{H}} + U_{\mathrm{L}}A_{\mathrm{L}}\tau})^2}{U_{\mathrm{L}}A_{\mathrm{L}}\tau R}. \tag{31}$$

Then, the efficiency at mpd becomes

$$\eta_{\mathrm{mpd}} = \frac{\eta_{\mathrm{mpd},C_{\mathrm{I}}=0}}{1 + \dfrac{C_{\mathrm{I}}(1-\tau)}{U_{\mathrm{H}}A_{\mathrm{H}}\left(1 - \sqrt{\dfrac{U_{\mathrm{H}}A_{\mathrm{H}} + U_{\mathrm{L}}A_{\mathrm{L}}\tau}{U_{\mathrm{H}}A_{\mathrm{H}} + U_{\mathrm{L}}A_{\mathrm{L}}R}}\right)}}, \tag{32}$$

where

$$\eta_{\mathrm{mpd},C_{\mathrm{I}}=0} = 1 - \frac{U_{\mathrm{L}}A_{\mathrm{L}}\tau}{\sqrt{(U_{\mathrm{H}}A_{\mathrm{H}} + U_{\mathrm{L}}A_{\mathrm{L}}\tau)(U_{\mathrm{H}}A_{\mathrm{H}} + U_{\mathrm{L}}A_{\mathrm{L}}R)} - U_{\mathrm{H}}A_{\mathrm{H}}}, \tag{33}$$

is the efficiency at mpd when there is no heat leakage. They also optimized the power output given in Eq. (14) with respect to T_{W} and T_{C} by using Eq. (30) and obtained

$$\dot{W}_{\max} = \frac{U_{\mathrm{H}}A_{\mathrm{H}}U_{\mathrm{L}}A_{\mathrm{L}}T_{\mathrm{H}}(\sqrt{R} - \sqrt{\tau})^2}{U_{\mathrm{H}}A_{\mathrm{H}} + U_{\mathrm{L}}A_{\mathrm{L}}R} \tag{34}$$

and the efficiency at maximum power as

$$\eta_{\mathrm{mp}} = \frac{1 - \sqrt{\dfrac{\tau}{R}}}{1 + \dfrac{C_{\mathrm{I}}(1-\tau)(U_{\mathrm{H}}A_{\mathrm{H}} + U_{\mathrm{L}}A_{\mathrm{L}}R)}{U_{\mathrm{H}}A_{\mathrm{H}}U_{\mathrm{L}}A_{\mathrm{L}}R\left(1 - \sqrt{\dfrac{\tau}{R}}\right)}}. \tag{35}$$

The results showed that the design parameters at maximum power density lead to smaller heat engines. The analysis also showed that the thermal efficiency at mpd conditions is greater than the one at mp condition for an irreversible heat engine, however, this advantage decreases when the internal irreversibility and heat leakage increase.

2.2.2. Ecological and exergetic performance optimization

Angulo-Brown [85] proposed an ecological optimization function E which is expressed as

$$E = \dot{W} - T_{\mathrm{L}}\dot{S}_{\mathrm{g}}, \tag{36}$$

where $\dot{W}$ is the power output and $\dot{S}_{\mathrm{g}}$ is the entropy generation rate. He showed that the efficiency at *m*aximum *e*cological (*me*) function conditions is almost equal to the average of Carnot efficiency and the efficiency at maximum power that is

$$\eta_{\mathrm{me}} \approx \frac{1}{2}(\eta_{\mathrm{C}} + \eta_{\mathrm{mp}}), \tag{37}$$

for endoreversible Carnot heat engines. As a conclusion of his study, he claimed that the ecological optimization of an endoreversible Carnot heat engine gives about 80% of the maximum power but with an entropy generation of only 30% of the entropy that would be generated by the power optimization. Yan [86] discussed the results of Angulo-Brown [85] and suggested that it may be more reasonable to use $E = \dot{W} - T_0\dot{S}_{\mathrm{g}}$ if the cold reservoir temperature is not equal to the environment temperature T_0. The optimization of the ecological function is therefore claimed to represent a compromise between the power output $\dot{W}$ and the loss power $T_0\dot{S}_{\mathrm{g}}$ which is produced by entropy generation in the system and its surroundings and also between the power output and the thermal efficiency. The ecological criterion is also applied to an irreversible Carnot heat engine with finite thermal capacitance rates of the heat reservoirs and finite total conductance of the heat exchangers by Cheng and Chen [87].

Arias-Hernandez and Angulo-Brown [88] and Angulo-Brown et al. [89] showed that the relation given by Eq. (37)

is a general identity which can also be used both for endoreversible and irreversible Carnot heat engines by the aid of Eqs. (2) and (27), respectively. They employed both linear and non-linear heat-transfer laws in their calculations and concluded that the relation given by Eq. (37) is independent of heat-transfer laws. Ares de Parga et al. [90] used a variational procedure for obtaining the thermal efficiencies of an endoreversible Carnot heat engine in both the maximum power and maximum ecological function regimes by means of a non-linear heat-transfer law.

Velasco et al. [91] proposed two saving functions, one associated with fuel consumption and another associated with thermal pollution, as a measure of possible reductions of undesired effects in heat engine operation. They proposed two different mathematical methods where the production of electric power, the saving of fuel consumption and the reduction of thermal pollution are optimized together. They applied these functions to a Curzon–Ahlborn heat engine and obtained an optimum efficiency of $\eta_{opt} = 1 - \tau^{3/4}$.

The main task in FTT is to find the minimum irreversible loss under a finite-time constraint, therefore, the concept of exergy is always inherently involved in it. To construct a method of exergy analysis, which is different from the traditional one, Andresen et al. [92] defined the finite-time exergy function which retains the traditional exergy and simply adds that the process is restricted to operate during finite time. Mironova et al. [93] introduced a criterion of thermodynamic ideality which is the ratio of actual rate of entropy production to the minimal rate of entropy production. This ratio is closely related to the energy approach but incorporates the irreversible losses due to finite time and non-zero rates. They found the regimes with minimal entropy production for the system where chemical reactions occurs and for the set of parallel heat engines. Yan and Chen [94] derived the relationship between the rate of exergy output and COP and also between the rate of exergy output and the cooling load for an endoreversible Carnot refrigerator. They obtained the optimal rate of exergy output and the minimum rate of exergy loss. Sahin et al. [95] carried out an exergy optimization for an endoreversible cogeneration cycle using FTT. The optimum values of the design parameters of the cogeneration plant, in which heat and power are produced together, at maximum exergy output were determined. They concluded that the heat consumer temperature should be as low as possible for highexergetic performance of a cogeneration system. Sieniutycz and Von Spakovsky [96] generalized the thermal exergy to finite-time processes.

3. Optimization of cascaded Carnot heat engine models

The maximum power and the efficiency at the maximum power output of an endoreversible cascaded cycle (two single Carnot heat engine cycle in a cascade), which is shown in Fig. 11, were treated by Wu et al. [97]. They assumed that the sum of the maximum powers generated simultaneously by the individual cycles gives the maximum power output of the cascaded endoreversible cycle, i.e.

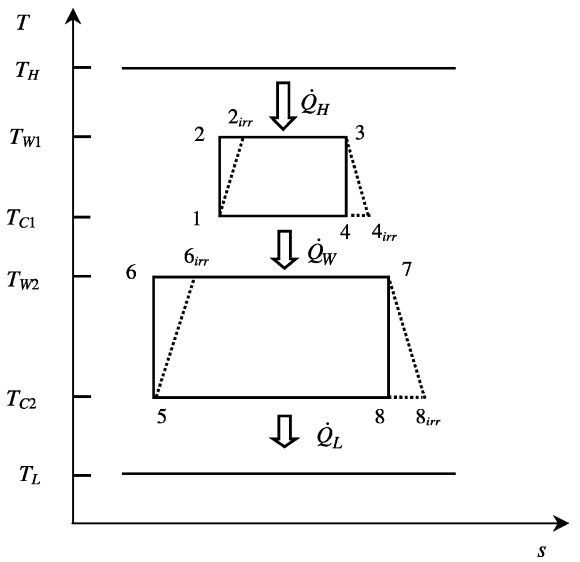

Fig. 11. Two irreversible Carnot heat-engine in a cascade.

$$\dot{W}_{cas,max} = \dot{W}_{1,max} + \dot{W}_{2,max}. \tag{38}$$

Chen and Wu [98] investigated the optimal performance of a two-stage endoreversible cascaded cycle for steady-state operation. The specific power output of the system is selected as an objective function for optimization and the maximum specific power output and the corresponding efficiency is derived. In their analysis, they first obtained the specific power output of a two-stage endoreversible cascaded heat-engine system dividing the total power output by the total heat-transfer area, i.e. $\dot{w} = \dot{W}/A$. The total heat-transfer area of the cascaded cycle is assumed to be fixed and applied as an additional constraint. The optimization of the specific power output by $\partial\dot{w}/\partial T_{W1} = 0$, $\partial\dot{w}/\partial T_{C2} = 0$ and $\partial\dot{w}/\partial\eta_{cas} = 0$ yields

$$\dot{w}_{max} = U_{eq,end}(\sqrt{T_H} - \sqrt{T_L})^2, \tag{39}$$

where $U_{eq,end}$ is defined as an equivalent overall heat-transfer coefficient for an endoreversible cascaded-cycle system. They concluded that the corresponding efficiency, which is well known CNCA efficiency, is

$$\eta_{cas,mp} = 1 - \sqrt{\frac{T_L}{T_H}} \equiv \eta_{mp}, \tag{40}$$

where $\eta_{cas,mp}$ is the thermal efficiency of the cascaded heat engine working at maximum power conditions. η_{mp} is the efficiency at maximum power for a single cycle endoreversible Carnot heat engine. They showed that a two-stage endoreversible cascaded-cycle system and a single-stage endoreversible cycle have the same efficiency when both of

them operate in the state of the maximum specific power output and at the same temperature range. They also reported that the maximum specific power output of a cascaded-cycle system is smaller than that of a single-stage endoreversible cycle because there is some loss due to irreversibility between two cycles in the cascaded-cycle system.

Chen and Wu [99] established a generalized endoreversible cycle model, based on their earlier work [98], to study the performance characteristics of an n-stage cascaded-cycle system for a two-stage endoreversible cascaded-cycle system. They generalized the results obtained from the two-stage endoreversible one Chen and Wu [98] for an arbitrarily chosen n-stage cascaded-cycle system and obtained the optimal distribution of the heat-transfer areas.

Sahin et al. [100] also studied both analytically and numerically the maximum power of an endoreversible cascaded-cycle system and its corresponding thermal efficiency subject to some design parameters. They compared their analytically and numerically derived results with each other and also with the previous studies on this topic. In their work, they claimed that the assumption of maximum power of the cascaded engine being equal to the sum of the maximum powers of the individual engines is not correct, mathematically, it should be

$$\dot{W}_{\mathrm{cas,max}} \leq \dot{W}_{1,\mathrm{max}} + \dot{W}_{2,\mathrm{max}}. \tag{41}$$

They started their performance analysis for the cascaded endoreversible engine with

$$\dot{W}_{\mathrm{cas,max}} = (\dot{W}_1 + \dot{W}_2)_{\mathrm{max}}, \tag{42}$$

since the design parameters which make the power of one of the engines maximum may not make the power of the other engine maximum. As a result, they obtained the CNCA efficiency given by Eq. (2) for thermal efficiency of a cascaded endoreversible engine at maximum power output.

Bejan [101] concluded that the power output of the cascaded-cycle power plant of finite-size can be maximized by properly balancing the sizes of the heat exchangers.

Ozkaynak [102] performed an analysis for the maximum power and efficiency at the maximum power output of an irreversible cascaded Carnot heat engine with simultaneous processes. He considered the same irreversibility parameter R for each single cycle. First, he defined a dimensionless heat-transfer rate into cycle, ϕ, and a dimensionless power output, $\dot{W}$, then maximized them with respect to ψ for a single irreversible Carnot heat engine. By the aid of the cascaded Carnot heat engines shown in Fig. 11, he defined $\tau_1 = T_{W2}/T_{\mathrm{H}}$, $\tau_2 = T_{\mathrm{L}}/T_{C1}$, $\beta_1 = h_{H2}A_{H2}/(h_{W2}A_{W2})$ and $\beta_2 = h_{W2}A_{W2}/(h_{L2}A_{L2})$. A similar approach is applied to the analysis of a cascaded Carnot heat engine defining a dimensionless power output of each irreversible cycle, $\dot{W}_1$ and $\dot{W}_2$. He derived the maximum total power output by using the assumption given in Eq. (38) by Wu et al. [97]. The overall efficiency at the maximum power output of a cascaded-heat engine is also derived as

$$\eta_{\mathrm{cas,mp}} = 1 - \frac{1}{R}\sqrt{\tau_1\tau_2}, \tag{43}$$

under consideration of

$$\eta_{\mathrm{cas,mp}} = 1 - \lfloor 1 - (\eta_1)_{\dot{W}_{1,\mathrm{max}}} \rfloor \lfloor 1 - (\eta_2)_{\dot{W}_{2,\mathrm{max}}} \rfloor, \tag{44}$$

given by Wu et al. [97] where

$$\eta_{1,\mathrm{mp}} = 1 - \sqrt{\frac{\tau_1}{R}}, \tag{45}$$

$$\eta_{2,\mathrm{mp}} = 1 - \sqrt{\frac{\tau_2}{R}}. \tag{46}$$

He compared the results with those obtained for a single cycle and concluded that a cascaded-heat engine may generate more power and is more efficient than a single cycle.

Chen [103] extended the endoreversible analysis by Chen and Wu [98] to include internal irreversibilities for a two-stage cascaded-heat-engine cycle to analyse the performance. He adopted again the specific power output of the system as an objective function for optimization and derived the maximum specific power output and the corresponding efficiency. He compared the results he obtained with those of a single-stage irreversible heat engine and also presented an optimal performance analysis of an n-stage irreversible cascaded-heat-engine system. In his model, he adopted that the cycle-irreversibility parameters for each single cycle are different, and that the total heat-transfer area of the cascaded cycle is fixed as an additional constraint. Defining a new equivalent overall heat-transfer coefficient $U_{\mathrm{eq,irr}}$ for a two-stage-cascaded irreversible heat-engine cycle, he obtained the maximum specific power output and optimal conditions as

$$\dot{w}_{\mathrm{max}} = U_{\mathrm{eq,irr}}T_{\mathrm{H}}\left(1 - \sqrt{\frac{\tau}{R_{\mathrm{T}}}}\right)^2. \tag{47}$$

He concluded that the corresponding efficiency is

$$\eta_{\mathrm{cas,mp}} = 1 - \sqrt{\frac{\tau}{R_{\mathrm{T}}}} \equiv \eta_{\mathrm{mp}}, \tag{48}$$

where η_{mp} is the efficiency at maximum power for a single cycle irreversible Carnot heat engine and $R_{\mathrm{T}} = R_1R_2$. In order to compare his results with those of Ozkaynak [102], he considered $R = R_1 = R_2$ and $R_{\mathrm{T}} = R^2$ and substituting them in Eqs. (47) and (48), he found

$$\dot{w}_{\mathrm{max}} = U_{\mathrm{eq,irr}}T_{\mathrm{H}}\left(1 - \frac{\sqrt{\tau}}{R}\right)^2, \tag{49}$$

$$\eta_{\mathrm{cas,mp}} = 1 - \frac{\sqrt{\tau}}{R}. \tag{50}$$

Chen pointed out in his work [103] that the result given by Eq. (50) is different than that of given by Ozkaynak [102] in Eq. (43). He criticized Ozkaynak [102] to employ an

erroneous assumption given in Eq. (38) in his derivation. Chen [104] also established a universal model of an arbitrary n-stage combined Carnot cycle system including heat leak and internal dissipation of the working fluid and obtained the maximum power output and corresponding efficiency and, the maximum efficiency and corresponding power output.

Sahin and Kodal [105] carried out an optimal performance analysis of a two-stage-cascaded-cycle system including internal irreversibility for steady-state operation with simultaneous processes. In their work, two different cycle-irreversibility parameters are defined. They obtained the maximum power output of the cascaded cycle similar to given by Eq. (47) with different multiplier instead of $U_{\mathrm{eq,irr}}$ definition and the efficiency at maximum power identical to given by Eq. (48). It should be noted here that Eqs. (47) and (48) were derived for maximum specific power output.

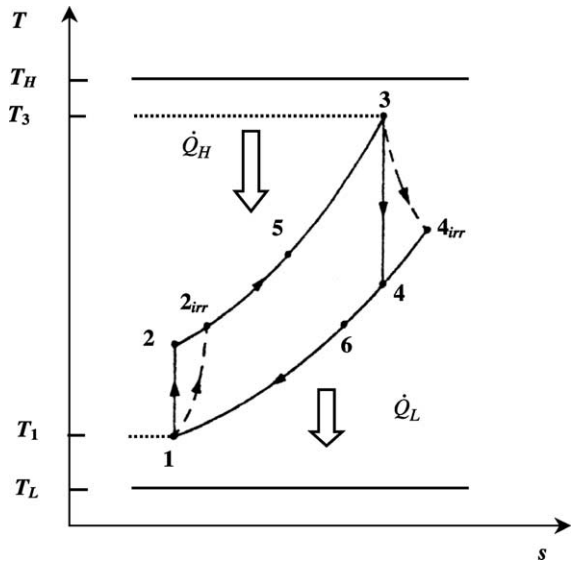

Fig. 12. The regenerative JB heat-engine model with internal irreversibilities.

4. Optimization of the other heat-engine cycles

Leff [106] showed that the reversible heat engines (Joule–Brayton, Otto, Diesel, and Atkinson) other than the Carnot heat engine operating at maximum work output have efficiencies equal to CNCA efficiency although these models involve no finite-time considerations hence no irreversibilities. Landsberg and Leff [107] later found that these important heat engine cycles can be regarded as special cases of a more universal generalized cycle.

4.1. The Joule–Brayton cycle

In 1851, James Joule proposed an 'air engine' with a piston-cylinder work producing device as a substitute for the widely used steam engine [106,108]. This engine involved adiabatically compressing atmospheric air, heating the air at constant pressure via an external heat source, expanding the air adiabatically against a work-producing piston, and exhausting it to the atmosphere. George Brayton built a piston-driven internal combustion engine based on the same model cycle for about 20 years after Joule's proposal. However, its efficiency was about 7%, therefore, it was too low to be competitive. Then, the cycle is idealized excluding the air intake and the exhaust parts as shown in Fig. 12 incorporating two constant pressure and two isentropic processes (1–2s–3–4s–1). This cycle is used as an ideal model of a continuous-combustion gas turbine engine and named as the Brayton cycle or the Joule cycle (or may be more appropriately as the Joule–Brayton cycle or briefly JB cycle).

Bejan [42] showed that the cycle efficiency of endoreversible JB cycles is independent of the distribution of the thermal conductances among hot and cold side heat exchangers and further concluded that the power output is maximized when the total thermal conductance is distributed equally. Wu and Kiang [109] and Wu [110] examined the performance of a power maximized endoreversible JB cycle. Wu and Kiang [111] also studied the efficiency under maximum power conditions by incorporating non-isentropic compression and expansion and found that these non-isentropic processes lower the power output and cycle efficiency compared to those of an endoreversible JB cycle under the same conditions. Ibrahim et al. [112] optimized the power output of Carnot and closed JB cycles for both finite and infinite thermal capacitance rates of the external fluid streams. Cheng and Chen [113] carried out a power optimization of an irreversible JB heat engine considering the irreversibility originating from heat leak between heat reservoirs in addition to the irreversibilities due to the finite thermal conductance between the working fluid and the reservoirs. They concluded that when component efficiencies are less than 100%, the optimum ratio of the hot-end heat exchanger conductance to the total conductance of the two heat exchangers will be less than 0.5 and it will be equal to 0.5 when the component efficiencies reach 100%, i.e. endoreversible JB cycle, as Bejan pointed out in his work [42]. Furthermore, this ratio decreases as the hot-to-cold reservoir temperature ratio is increased. Blank [114] studied a combined first and second law analysis to optimize the power output of JB-like cycles. He provided the pressure ratios and temperature limits for power optimization and the optimum allocation of conductances. Gandhidasan [115] performed an analysis of a closed cycle JB gas turbine plant powered by the sun. He calculated the optimum pressure ratio for maximum cycle efficiency.

Cheng and Chen [116] studied the effect of regeneration on power output and thermal efficiency of an endoreversible regenerative JB cycle and, evaluated the maximum power

output and the corresponding thermal efficiency as well as the second law efficiency. In their study, they considered an endoreversible regenerative JB cycle coupled to a heat source and a heat sink with infinite thermal capacitances as shown in Fig. 12. The rates at which heat is supplied and rejected are given by

$$\dot{Q}_H = \dot{C}_W \varepsilon_H (T_H - T_1') = \dot{C}_W (T_2 - T_1'), \tag{51}$$

$$\dot{Q}_L = \dot{C}_W \varepsilon_L (T_3' - T_L) = \dot{C}_W (T_3' - T_4) \tag{52}$$

and the regenerative heat-transfer rate is

$$\dot{Q}_R = \dot{C}_W \varepsilon_R (T_3 - T_1) = \dot{C}_W (T_1' - T_1) = \dot{C}_W (T_3 - T_3'), \tag{53}$$

where the effectiveness of hot-side heat exchanger is ε_H, that of cold-side heat exchanger is ε_L and that of regenerative heat exchanger is ε_R, the capacitance rate of working fluid is $\dot{C}_W$. The second law of thermodynamics yields

$$\frac{T_1}{T_4} = \frac{T_2}{T_3}. \tag{54}$$

By the aid of Eqs. (51) and (52) and the first law of thermodynamics the power output is written. The power output is maximized with respect to T_1 with the second law of thermodynamics constraint then, the corresponding thermal and second law efficiencies at maximum power are obtained. They illustrated the variation of efficiency with dimensionless power $\dot{W}/(\dot{C}_W T_H)$ for JB cycles with and without regeneration, as shown in Fig. 13. As a result, they claimed that pure JB cycles are better than regenerative JB cycles for maximum power and corresponding thermal efficiency as well as for maximum thermal efficiency and corresponding power.

Cheng and Chen [117] also examined the effects of intercooling on the maximum power and maximum efficiency of an endoreversible intercooled JB cycle coupled to two heat reservoirs with infinite thermal capacitance rates. They found that the maximum power output of an endoreversible intercooled JB cycle could be higher than that of an endoreversible simple one.

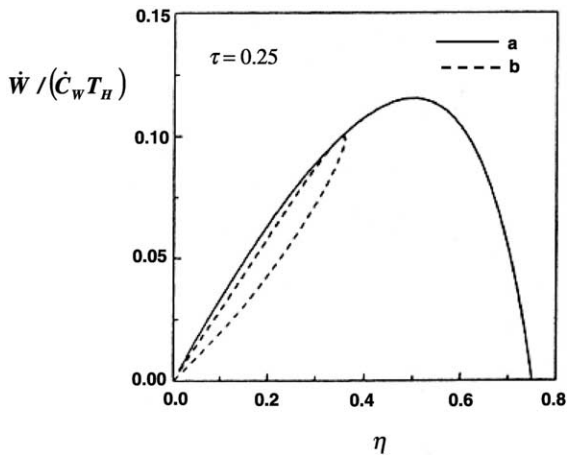

Fig. 13. Variation of dimensionless power with thermal efficiency for JB cycles (a) without and (b) within regeneration [116].

Hernandez et al. [118] and Wu et al. [119] carried out power and efficiency analyses of regenerative air-standard and endoreversible JB cycles respectively, considering the losses in the compressor and turbine by means of an isentropic efficiency term and all global irreversibilities in the heat exchanger by means of an effective efficiency and obtained optimal operating conditions. Roco et al. [120] also studied an optimum performance analysis of a regenerative JB cycle taking into account of the pressure losses in the heater and the cooler in addition to the irreversibilities due to finite temperature difference between the working fluid and heat reservoirs, turbine and compressor non-isentropic processes and the regeneration. Hernandez et al. [121] presented a general theoretical framework to study the behaviour of the power output and efficiency in terms of the pressure ratio for a regenerative gas turbine cycle with multiple reheating and intercooling stages. They considered the isentropic efficiency of the compressors and turbines as a parameter to analyse the optimal operating conditions of an air-standard regenerative JB cycle. They performed a numerical study and the numerical results show that in determining the rational regions of the efficiency and power output of the cycle ($\eta_{mp} \leq \eta_{opt} \leq \eta_{max}, \dot{W}_{max} \geq \dot{W}_{opt} \geq \dot{W}_{mef}$) the influence of thermodynamic (irreversibilities and temperatures) and technical (number of stages and pressure ratios) factors must be taken into account simultaneously. Chen et al. [122] investigated the performance of a regenerative irreversible closed JB cycle coupled to variable-temperature heat reservoirs. They derived, explicitly, the power output and the efficiency expressions of this JB cycle as functions of pressure ratios, reservoir temperatures, heat exchanger effectivenesses, compressor and turbine efficiencies, and working fluid thermal capacitance rates as a unified approach to the performance optimization studies with different constraints.

Vecchiarelli et al. [123] claimed that the hypothetical modification of gas turbine engines to include an isothermal heat addition process after the typical isobaric heat addition process, as shown in Fig. 14, may result in significant efficiency improvements of over 4% compared with conventional engines. They examined a proposed converging combustion chamber for gas turbine engines in which an isothermal heat addition takes place and concluded that the approximate heat addition in the proposed combustion chamber is feasible. Goktun and Yavuz [124] carried out a thermal efficiency analysis of the modified JB cycle explained in Vecchiarelli et al. [123] with the addition of regeneration and internal irreversibilities. As a conclusion, they reported that the effect of regenerative heat transfer on the performance of a modified JB cycle is positive for low pressure ratio values whereas it is negative for high pressure ratio values.

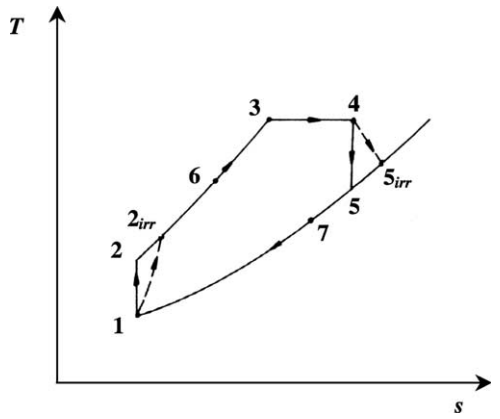

Fig. 14. JB heat-engine model with isothermal heat addition.

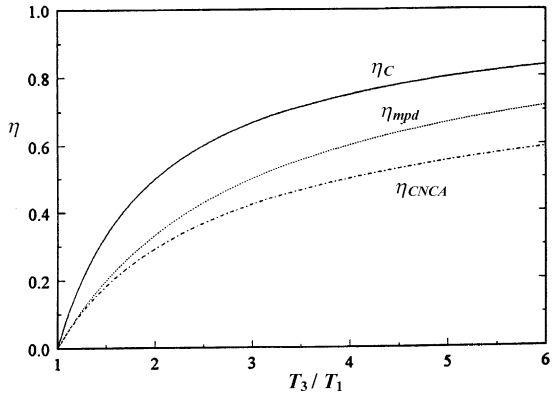

Fig. 16. Variation of efficiency at maximum power density η_{mpd}, efficiency at maximum power η_{CNCA}, and the Carnot efficiency η_C with extremal working fluid temperature ratio T_3/T_1 of the temperatures T_3 and T_1 shown in Fig. 12 for an endoreversible JB heat engine [82].

As it is explained in power density optimization of Carnot heat engine section, to include the effects of engine size in the performance analysis, Sahin et al. [82] suggested a performance criteria called mpd. In their analysis, by considering a reversible JB engine, they maximized the power density (the ratio of power to the maximum specific volume in the cycle) and found that design parameters at maximum power density lead to smaller and more efficient JB engines as shown in Figs. 15 and 16. Therefore, they stated that by maximizing the power density, one obtains lower fuel costs due to higher thermal efficiency and lower investment costs due to the use of a smaller engine. Sahin et al. [125] extended the work of Sahin et al. [82] by including irreversibilities at the compressor and the turbine of a JB engine along with considerations of pressure losses at the burner. They concluded that although the irreversibilities result in a reduction of power output and thermal efficiency, the mpd conditions still give a better performance than those at mp conditions in terms of thermal efficiency and engine size as shown in Figs. 17 and 18. Medina et al. [126] applied the mpd analysis by Sahin et al. [82,125] to a regenerative JB cycle, using a previous theoretical work, Hernandez et al. [118], where the optimal operating conditions of the heat engine are expressed in terms of the compressor and turbine isentropic efficiencies and of the heat exchanger efficiency. They showed that under mpd conditions the irreversible JB cycle is also smaller in size and requires a higher pressure ratio than that of under mp conditions. They also showed that unlike non-regenerative results, real regenerative gas turbines, i.e. when $\eta_R > 0.3$, are less efficient at mpd conditions than at mp conditions. Sahin et al. [127] carried out a comparative performance analysis based on mpd and mp criteria for a regenerative JB heat engine by inclusion of the application of reheating into the model. They showed that when the irreversibilities of turbine and compressor increase the thermal efficiency advantage of the mpd conditions decreases in comparison with mp conditions. They also showed that the application of reheating to a regenerative JB cycle increases the range of

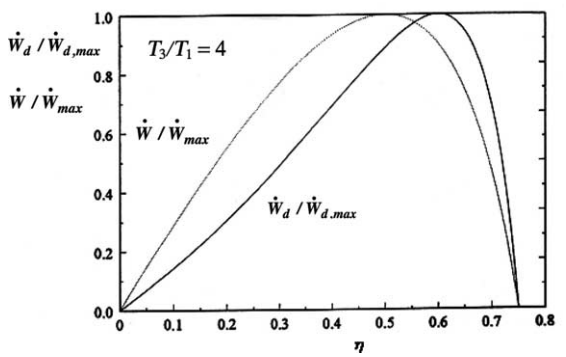

Fig. 15. Variation of normalized power density and normalized power with thermal efficiency for an endoreversible JB heat engine [82].

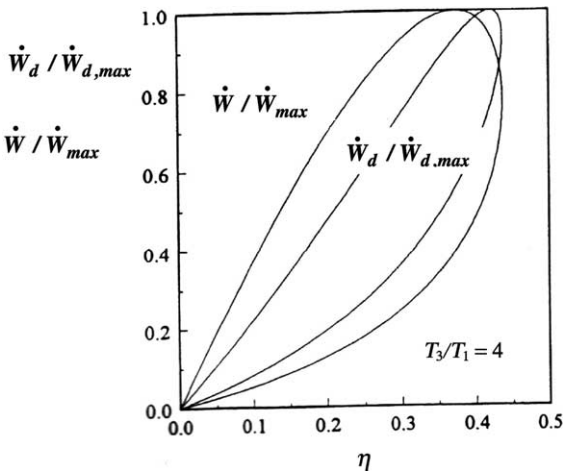

Fig. 17. Variation of normalized power density and normalized power with thermal efficiency for an irreversible JB heat engine [125].

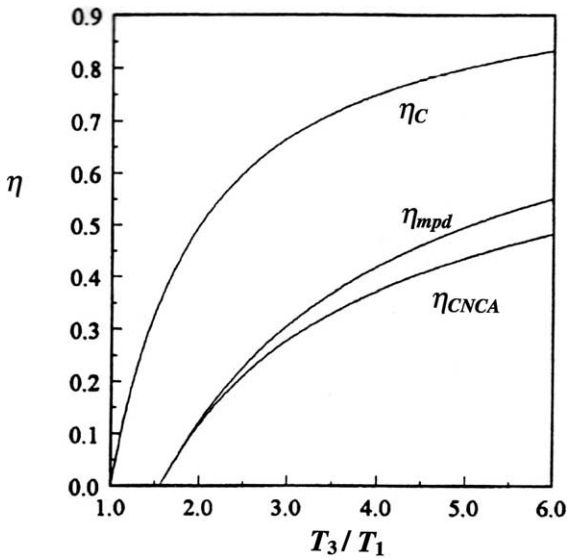

Fig. 18. Variation of efficiency at maximum power density η_{mpd}, efficiency at maximum power η_{CNCA}, and the Carnot efficiency η_C with extremal working fluid temperature ratio T_3/T_1 of the temperatures T_3 and T_1 shown in Fig. 12 for an irreversible JB heat engine [125].

the thermal efficiency advantage of the mpd conditions with increasing regenerator efficiency. Finally, they demonstrated that the smaller engine size advantage under mpd conditions is preserved with the inclusion of reheating.

Chen et al. [128] optimized the endoreversible JB cycle performance using power density as an objective function with the consideration of the finite-time heat transfer irreversibility in the hot- and cold-side heat exchangers. They carried out this work by optimizing the pressure ratio of the cycle and by optimizing the heat conductance distribution of heat exchangers assuming a fixed total heat exchanger inventory. They also carried out a performance comparison of the JB cycle examined in Ref. [128] with variable temperature heat reservoirs in Ref. [129]. Further step of their works, they [130] analyzed and optimized the performance of an irreversible regenerated closed JB cycle with variable temperature heat reservoirs using power density as an objective function. They considered heat transfer irreversibilities in the heat exchangers and the regenerator, the irreversible compression and expansion losses in the compressor and the turbine, the pressure loss at the heater, cooler and the regenerator as well as in pipes, and the effect of the finite thermal capacity rates of the heat reservoirs. Their mpd analyses may lead to higher efficiency and smaller design size of the JB engines.

Erbay et al. [131] expanded the work of the modified JB cycle with isothermal heat addition explained in Vecchiarelli et al. [123] and Goktun and Yavuz [124] to cover a numerical work using mp and mpd as objective functions. They showed that the modified JB cycle has higher efficiencies at mp and mpd conditions and also with respect to the cycle pressure ratio than those of the classical regenerative JB cycle.

Cheng and Chen [132] applied the ecological optimization criterion given in Eq. (36) to optimize the power output of an endoreversible closed JB cycle. The ecologically optimum values of the power output values and the corresponding thermal and second law efficiencies were presented. The thermal efficiency at maximum ecological function is found to be about the average of the reversible Carnot efficiency of a Carnot heat engine that works between the same temperature limits and the efficiency at maximum power as it is given in Eq. (37). They also found that the ratio of ecologically optimum power to maximum power is independent of the number of transfer units of the hot-side and the cold-side of the heat exchangers. Chen and Cheng [133] also studied the ecological optimization of an irreversible JB heat engine where the irreversibilities were assumed to originate from finite thermal conductance between the working fluid and the reservoirs, non-isentropic compression and expansion processes, and heat leaks between the reservoirs. The ecological function was optimized with respect to the thermal conductance ratio and the adiabatic temperature ratio. They concluded that the thermal conductance of the cold-side heat exchanger should be larger than that of the hot-side heat exchanger to obtain a higher ecological function also that the optimum conductance ratio and the adiabatic temperature ratio are hardly affected by the heat leaks when infinite thermal capacity of heat reservoirs are considered.

Huang et al. [134] carried out an exergy analysis based on the ecological optimization criterion for an irreversible open cycle JB engine with a finite capacity heat source. They showed that for such an irreversible JB cycle, the first and second law efficiencies can be presented as a function of the cycle pressure ratio and compressor and turbine efficiencies and that by using the ecological criterion and the second-law performance (or exergetic performance), it is possible to combine the lost work with the first law. They concluded that if the values of inlet temperature of the heating fluid, working fluid temperature at turbine inlet, source-to-cycle temperature difference and isentropic efficiency of the turbine or compressor were increased, the resulting first and second law cycle efficiencies would be higher.

4.2. Stirling, Ericsson and Lorentz cycles

In 1816, Robert Stirling lodged a patent for the first hot-air engine [135,136]. The important aspect of the air-standard Stirling engines was the use of a regenerative heat exchanger in a heat engine system for the first time. The ideal Stirling cycle consists of two isochoric and two isothermal processes. This cycle approximates the compression stroke of the real engine as an isothermal process, with irreversible heat rejection to a low-temperature sink.

The heat addition to the working fluid from the regenerator is modelled as a reversible isochoric process. The expansion stroke producing work is modelled as an isothermal process, with irreversible heat addition from a high temperature source. Finally, the heat rejection to the regenerator is modelled using a reversible isochoric process.

Ericsson introduced a power cycle in 1833 in which the primary heat addition and rejection processes take place at constant temperature and the expansion and compression processes at constant pressure having an ideal heat regeneration [137].

Badescu [138] evaluated the performances of solar converter in combination with a Stirling or Ericsson heat engine by taking into consideration the design and climatological parameters and the energy balance for the solar converter. He analyzed the influence of these parameters on both the optimum receiver temperature and the optimum efficiency of solar converter-heat engine combination at maximum power conditions. The design parameters considered in this study were concentration ratio, effective absorptance–transmittance product for solar direct radiation, receiver emissivity and overall heat-loss coefficient and the climatological parameters were global solar radiation flux and sky temperature. Ladas and Ibrahim [139] defined a finite-time parameter as the ratio of working fluid contact time to the engine time constant which evolves the heat transfer characteristics of the given Stirling engine design. They conducted a numerical study and plotted the change of power output versus the finite-time parameter, the change of power output versus efficiency and effects of regeneration on them. Senft [140] described a mathematical model of heat engines operating with an endoreversible Stirling cycle subject to internal thermal losses and mechanical friction losses and investigated the effects of these irreversibilities on the performance. Blank et al. [141] and Blank and Wu [142] conducted optimization analyses for maximum power output of endoreversible Stirling and Ericsson heat engines with perfect regeneration and provided sample parametric studies using representative data for Stirling-type engines from West [143], respectively. Blank and Wu [144,145] also studied a solar-radiant regenerative Stirling and Ericsson heat engines coupled to a heat source and heat sink by radiant heat transfer in order to obtain the finite-time maximum power output and corresponding efficiency based on higher and lower temperature bounds.

Erbay and Yavuz [146] analyzed an endoreversible Stirling engine with polytropic processes in compressor and turbine and an isochoric process in a regenerator to obtain the performance at mp and mpd conditions. Erbay and Yavuz [147,148] also analyzed irreversible Stirling and Ericsson engines with simultaneous polytropic processes in compressor and turbine, respectively. In the latter works, they considered the internal irreversibilities due to the turbine and compressor thermal efficiencies and the pressure drops present in regenerators to examine the effect of these internal irreversibilities on the performance at mp and mpd conditions for realistic Stirling and Ericsson engines. Wu et al. [149] performed an mp analysis to determine the effects of heat transfer, regeneration time and imperfect regeneration on the performance of an irreversible Stirling engine cycle with sequential processes.

Chen et al. [150] considered a combined system of a solar collector and a Stirling engine. The performance of the system was investigated based on the linearized heat loss model of the solar collector including the radiation losses and the irreversible cycle model of the Stirling engine affected by finite-rate heat transfer and regenerative losses. They determined the optimal temperature of the solar collector and the maximum efficiency of the total system.

Feidt et al. [151] proposed a general method for studying the Stirling engine based on a generalized form of heat-transfer law at source and sink. They focused on obtaining the maximum power output and investigated the influence of the different forms of heat-transfer law as well as heat losses between the hot and cold side of the machine, and partial regeneration processes on mp. Feidt et al. [152] further studied the influence of the regenerator effectiveness on the optimal heat-transfer surface conductance distribution in a Stirling engine. Costea and Feidt [153] extended the previous works on Stirling engines [151,152] by considering the influence of the linear variation of the overall heat-transfer coefficient with the temperature difference on the engine characteristics and performance, particularly on the distribution of the heat-transfer surface conductance or area among the heater and the cooler in a parametric study.

Blank [154] generalized mixed-mode heat transfer studies to determine their effects on power optimization in regenerative Stirling-like heat engines including the Carnot heat engine with sequential processes considering different types of thermal reservoir capacities. Bhattacharyya and Blank [155] developed a universal expression for optimum specific work output of regenerative reciprocating endoreversible heat engine cycles which include the Stirling and Ericsson cycles and the reciprocating Carnot cycle. In their analysis, they employed the ideal gas model with constant specific heat considering the case of ideal regenerator used by Blank et al. [141] and Blank and Wu [142], and claimed that the results are applicable to Carnot cycles with vapours and real gases. They showed that the finite-time optimum specific work (work output per unit mass) at maximum power w_{opt}, is exactly half of that obtained for the reversible cycles operating between the same temperature limits $w_{opt} = (1/2)w_{rev}$. They performed a sample calculation and concluded that the endoreversible Stirling engine will have the same thermal efficiency as the endoreversible Ericsson engine however it will have higher optimum power output while operating under the same optimized working fluid temperatures. The optimum power of the reciprocating endoreversible Carnot engine will be superior to both of these cycles.

The Lorentz cycle operates between a heat source and sink with finite heat capacity rates considering that heat is transferred irreversibly between the thermal reservoirs and the multi-component working fluid across counter-flow heat exchangers with fixed temperature differences. Gu and Lin [156] studied an endoreversible multi-stage Lorentz cycle with a non-azeotropic binary mixture, which is suitable for electricity generation, using relatively low temperatures for hot water or other fluids. Lee and Kim [157] determined the maximum power of an endoreversible Lorentz cycle and found that the maximum power of the Lorentz cycle is twice that of the Carnot cycle with finite-capacity thermal reservoirs for a given pinch-temperature difference.

4.3. Otto, Atkinson, Diesel and dual cycles

The air-standard Otto cycle incorporates an isentropic compression, an isochoric heat addition, an isentropic expansion and an isochoric heat rejection processes, sequentially. The air-standard Diesel cycle having an isentropic compression, an isobaric heat addition, an isentropic expansion and an isochoric heat rejection processes, sequentially. The air-standard dual cycle having an isentropic compression, an isochoric and an isobaric heat addition, an isentropic expansion and an isochoric heat rejection processes, sequentially.

Mozurkewich and Berry [158] used mathematical techniques from optimal-control theory to determine the optimal motion of the piston in an Otto engine. Hoffman et al. [159] performed a similar analysis for a Diesel engine. In these works, the major loss terms such as friction loss, heat leak and incomplete combustion were incorporated in a simple model based on air-standard cycle with rate-dependent loss mechanisms. Then using optimal control theory, the piston trajectory which yields maximum power output were computed as applications of the methods of FTT. Band et al. [160] and Aizenbud and Band [161] determined the optimal motion of a piston fitted to a cylinder which contained a gas pumped with a given heating rate and coupled to a heat bath during finite times. Klein [162] considered the ideal Otto and Diesel cycles and compared their volumetric compression ratios, thermal efficiencies at maximum work per cycle conditions. He derived the net work output of an air standard Otto cycle as an objective function and used the compression ratio as an optimization parameter to obtain the maximum net work output and corresponding thermal efficiency. He studied the effect of heat transfer through a cylinder wall on the work output of an Otto cycle assuming the heat transfer to the cylinder walls to be a linear function of the difference between the average gas and cylinder wall temperatures during the isometric energy release process 2–3. He concluded that the compression ratios that maximize the work of the Diesel cycle are always higher than those for the Otto cycle at the same operating conditions, although the thermal efficiencies are nearly identical, and that the compression ratios that maximize the work of the ideal Otto and Diesel cycles compare well with the compression ratios employed in corresponding production engines.

Wu and Blank [163] and Blank and Wu [164] investigated the effect of combustion on a work-optimized endoreversible Otto cycle and a power-optimized endoreversible Diesel cycle. Blank and Wu [164] maximized the net power output with respect to the cut-off ratio and their numerical study resulted in an optimum cut-off ratio value of 5.997 for the sample problem they considered. Chen [165] analyzed and optimized the power potential of a dual cycle considering the effect of combustion on power. In his work, also, he criticized the correctness of the optimum maximum temperature and the optimum cut-off ratio value findings of Blank and Wu [164]. He pointed out that the optimum maximum temperature was found higher than the adiabatic flame temperature by Blank and Wu [164]. Wu and Blank [166] also optimized the endoreversible Otto cycle with respect to both net power output and mean effective pressure (work of one cycle divided by displacement volume). Comparisons of the results show that the compression ratios for the optimization of net power output and mean effective pressure are themselves increasing functions of the maximum cycle temperature. Further, the optimization for $\dot{W}_{\mathrm{net}}$ results higher thermal efficiency than the optimization for mean effective pressure for a given maximum cycle temperature.

Orlov and Berry [167] obtained some analytical expressions for the upper bounds of power and efficiency of an internal combustion engines taking into account finite rate heat exchange with the environment and entropy production due to chemical reactions. Also, they claimed that a non-conventional internal combustion engine may have an additional heat input from the environment to produce maximum power.

Angulo-Brown et al. [168] proposed an irreversible simplified model for the air-standard Otto cycle taking into account of finite-time for heating and cooling processes and neglecting the time spent in adiabatic processes. They also considered a lumped friction-like dissipation term representing global losses. They maximized the power output, efficiency and ecological function with respect to compression ratio and showed that the optimum compression ratio values were in good agreement with those of standard values of practical Otto engines. They also showed that their model leads to loop-shaped power-versus-efficiency curves which are performance characteristics of real heat engines. Hernandez et al. [169] presented a model for an irreversible Otto engine with internally dissipative friction considering non-instantaneous adiabatic processes as a complementary to the one proposed in Angulo-Brown et al. [170]. In their work, they gave a central role to the full cycle time and piston velocity on the adiabatic branches with a pure sinusoidal law. Angulo-Brown et al. [170] extended the work of Angulo-Brown et al. [168] to include internal irreversibilities through the cycle-irreversibility parameter R

which was defined in Eq. (25). They found that R is also the ratio of the constant volume thermal capacities, i.e. $R = C_{V1}/C_{V2}$ where C_{V1} is the constant volume thermal capacity during the compression stroke and C_{V2} is the constant volume thermal capacity during the power stroke of the working fluid. They showed that the efficiency and power output of the Otto cycle can be remarkably improved choosing convenient combustibles having higher R values without changing the compression ratio and the other geometric parameters. Aragon-Gonzalez et al. [171] investigated the maximum irreversible work and efficiency of the Otto cycle considering the irreversibilities during the expansion and compression processes.

In the 1880s, James Atkinson designed and built an internal combustion engine [106]. The ideal cycle representing the operation of this engine consists of an isentropic compression, an isochoric (constant volume) heat addition with internal combustion, an isentropic expansion all the way to the lowest cycle pressure and an isobaric heat rejection processes. Chen et al. [172] carried out a comparative performance analysis of Atkinson engines at mp and mpd conditions.

Chen et al. [173] and Akash [174] carried out a performance analysis to show the heat-transfer effects on the net work output and efficiency for air-standard Diesel cycles employing the expression for heat addition to the working fluid proposed by Klein [162]. Chen et al. [175] and Lin et al. [176] also performed analyses for an air-standard Otto cycle and a dual cycle, respectively, similar to the one employed in Chen et al. [172].

Bhattacharyya [177] analyzed an irreversible Diesel cycle considering a friction-like dissipation term representing thermal and frictional losses and, optimized the power output and thermal efficiency with respect to cut-off ratio in addition to compression ratio similar to the one employed in Angulo-Brown et al. [170] for an irreversible Otto cycle. Chen et al. [178] and Wang et al. [179] also investigated the effect of friction on the performance of Diesel engines and an air-standard dual cycle, respectively.

Sahin et al. [180] introduced and optimized a new combined dual and JB power cycle model. In this theoretical model, a reciprocating heat engine with a gas turbine system is considered where the JB cycle utilizes the waste heat from the dual cycle. The optimal performance and design parameters are obtained analytically in terms of thermal efficiency, power output and engine sizes for the mpd conditions of the dual cycle and the combined cycle. Their results indicated that although a design based on the mpd criterion has the advantage of smaller size for a dual cycle, it has the disadvantage of lower power output and thermal efficiency than a classical dual cycle optimized considering mp criterion. They showed that the power and thermal efficiency disadvantages of the dual cycle working at mpd conditions can be improved considerably by the proposed combined system.

Sahin et al. [181] carried out a performance analysis and optimization based on the ecological criterion for an air-standard endoreversible internal-combustion-engine dual cycle coupled to constant temperature thermal reservoirs. The optimal performances and design parameters, such as compression ratio, pressure ratio, cut-off ratio and thermal conductance allocation ratio which maximize the ecological objective function are investigated. The obtained results are compared with those of the maximum power performance criterion.

4.4. Direct energy conversion systems

Magnetohydrodynamic energy conversion, popularly known as MHD, is one of the forms of direct energy conversion in which electricity is produced from fossil fuels without first producing mechanical energy. The process involves the use of a powerful magnetic field to create an electric field normal to the flow of an electrically conducting fluid through a channel. MHD effects can be produced with electrons in metallic liquids such as mercury and sodium or in hot gases containing ions and free electrons due to the requirement of high-temperature plasma from which the electrical energy is extracted. MHD channels, like gas turbines, may be operated on open or closed cycles. The simplest MHD power cycle is similar to a Brayton power cycle except for the irreversible process which is either a constant-velocity or a constant-Mach-number expansion in an MHD generator. Therefore, this ideal cycle consists of an MHD generator instead of turbine-generator group, in addition to a cooler, a compressor and a heater. Performance improvement can be provided by including regeneration application for preheating the working fluid at the compressor exit in the MHD power cycle.

The non-regenerative MHD power cycle efficiencies at maximum power output conditions for a constant-velocity and a constant-Mach-number type of an MHD generator were analyzed and compared with the CNCA efficiency by Aydin and Yavuz [182]. Later, Sahin et al. [183] carried out a performance analysis for a non-regenerative MHD power cycle at maximum power density for a constant-velocity-type MHD generator and compared the results with those of at maximum power conditions. Sahin et al. [184] extended these works by including a regenerator in the model and by considering the irreversibilities arising from pressure drops in the heater, regenerator and cooler together with the irreversibilities at the compressor and the electrical losses at the MHD generator.

Thermoelectric generators, refrigerators and heat pumps are also another types of direct energy conversion systems. A practical thermoelectric heat pump, in its simplest form, contains semiconductor materials, a heat source and a heat sink. A thermoelectric refrigerator describes a system in which two dissimilar materials are joined electrically and thermally for the purpose of transferring thermal energy from a heat source at temperature T_L to a heat sink at a higher temperature T_H by the input of electrical power $\dot{W}$.

Wu [185] applied the endoreversible Carnot heat engine model, shown in Fig. 2, to the FTT analysis of a solar-powered thermionic engine which is a device that converts heat directly to electricity. In this study, he considered a radiant thermionic heat engine which receives solar radiation from the sun at $T_H = 5755$ K and emits radiant heating to space at $T_L = 0$ K. The optimization of power output with respect to the emitter temperature, T_W and the collector temperature T_C is carried out and concluded that the thermal efficiency of such a heat engine is less than of a Carnot heat engine operating between the same heat reservoirs, in this case $\eta_C = 1$.

Gordon [186] analyzed the power versus efficiency relationships for thermoelectric generators having one or more sources of irreversibility, and compared the results with those of real heat engines.

Wu [187] and, Wu and Schulden [188] employed an externally irreversible model to study the performance analysis of a thermoelectric refrigerator and a thermoelectric heat pump considering the specific cooling load, heating load per unit heat exchanger surface area, as an objective function, respectively. An irreversible heat engine model is used by Ozkaynak and Goktun [189] to determine the maximum power and thermal efficiency at maximum power for a thermoelectric generator. Goktun [190,191] investigated the optimal performance of an irreversible thermoelectric generator employing a reversed Carnot-like heat engine model. He defined a device-design parameter, used a cycle-irreversibility parameter and determined the dimensionless maximum cooling load with respect to electrical current and corresponding dimensionless optimum power output and COP. Agrawal and Menon [192] considered a thermoelectric generator with zero internal resistance, vanishing heat leakage and negligible production of Thomson heat. They showed that such a generator behaves as an ideal Carnot engine or an endoreversible Carnot heat engine depending upon whether the heat transfer at junctions is reversible or finite rate. They found that the optimized power of the generator is greater than that of the endoreversible Carnot heat engine.

Nuwayhid et al. [193] performed a comparison between the EGM method and the power maximization technique by analyzing, as a typical example of direct energy conversion systems, the thermoelectric generator. They investigated the effects of heat leak, internal dissipation and finite-rate heat transfer on the performance of the generator, which is modelled as a Carnot-like heat engine. The EGM and the power maximization methods were shown to lead to the same conclusions, i.e. minimum entropy generation rate and maximum power output conditions are coincident, with the EGM method being less straightforward than the power maximization technique.

5. Optimization of refrigerator and heat pump systems

An endoreversible Carnot refrigeration cycle is a modified Carnot cycle with two isentropic and two externally irreversible isothermal processes. In this cycle, two infinitely large thermal reservoirs existing at temperatures T_H and T_L are considered to transfer heat to the refrigerator from the low temperature heat source across a temperature difference of $T_L - T_C$ and from the refrigerator to the high temperature heat sink across a temperature difference $T_W - T_H$ with a reversed Carnot cycle as shown in Fig. 19. The heat-transfer rate from the low temperature heat source to the working fluid (refrigerant), which is also called the cooling load, $\dot{Q}_L$, the heat-transfer rate from the refrigerator to the high temperature heat sink $\dot{Q}_H$ considering linear heat-transfer law can be written similar to the Eqs. (9) and (10) of endoreversible Carnot heat engine. The power input of the refrigerator can be expressed similar to the power output of a heat engine given in Eq. (8). In a complete reversible Carnot refrigeration cycle, $\dot{Q}_L$ would be zero since this cycle would take an infinitely long time to remove a finite amount of heat or it would require two infinitely large heat exchanger areas. The COP can be defined as

$$\mathrm{COP} = \frac{\dot{Q}_L}{\dot{W}}. \tag{55}$$

The modelling features used for power plants have also been used in the optimization of refrigeration plants. The model that was studied mostly is the refrigerator composed of a cold-end heat exchanger, i.e. evaporator, a reversible compartment that receives power and transfers the heat toward higher temperatures, and a room-temperature heat exchanger, i.e. condenser. This model is shown in Fig. 19 which was used first by Andresen et al. [26] who focused on the optimal temperature staging of the three compartments.

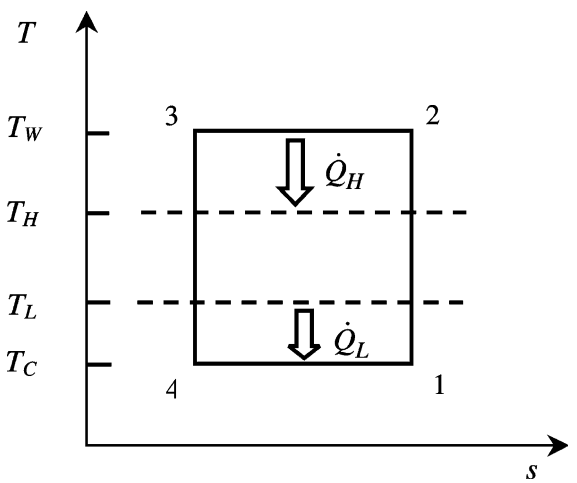

Fig. 19. Endoreversible reversed Carnot refrigerator model.

Unlike in the power plant equivalent, in a refrigerator there is no optimal warm-to-cold temperature ratio of T_W/T_C for minimum power input.

Subsequent to Curzon Ahlborn's analysis [8], Leff and Teeters [194] have noted that the straight forward calculation of Curzon Ahlborn calculation will not work for a heat pump because there is no natural maximum. Refrigeration cycles considered in the light of the Curzon–Ahlborn maximum power analysis with a specified overall heat conductance do not have a bounded solution either for minimum power input or for cooling load without specifying further criteria. Blanchard [195] has recognized this particular problem as he minimized the power input to an endoreversible heat pump for a specified heat rejection load and parallel temperature profiles in the heat exchangers.

Yan and Chen [196] studied a class of endoreversible Carnot refrigeration cycles considering a general heat-transfer law which has been adopted by De Vos [40,197] and Chen and Yan [58]. They obtained the relation between the cooling load (rate of refrigeration) $\dot{Q}_L$ and COP of these cycles, which is shown in Fig. 20, and optimized the cooling load with respect to the working fluid temperature on the cold side at constant COP. From Fig. 20, it can be observed that as expected, $\dot{Q}_L$ decreases when COP increases and $\dot{Q}_L$ approaches $\dot{Q}_{L,max}$ while COP tends to zero. However, the refrigeration cycle cannot be carried out when COP = 0. In their study, they also investigated the effect of different heat-transfer laws on the optimal performances of these cycles.

5.1. Irreversible refrigeration and heat-pump systems

Bejan [198] considered an endoreversible Carnot refrigeration plant model with internal heat-transfer irreversibility which is due to the heat transfer (heat gain) that passes directly through the machine all the way to T_L. He examined the second law efficiency dependence on refrigeration temperature levels in general, and went on to maximize the cooling load of refrigeration cycles with respect to the heat conductance allocation between the evaporator and condenser. The equal distribution of the specified heat conductance between the condenser and evaporator was found to be optimal, just as for the maximum power cycle problem.

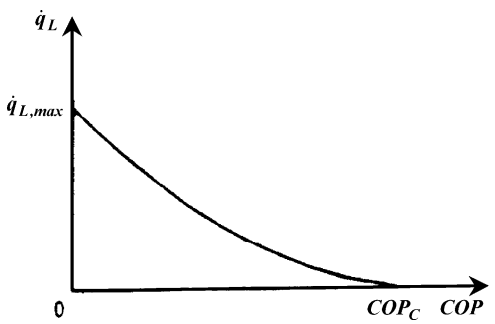

Fig. 20. Rate of refrigeration (cooling load) $\dot{Q}_L$ versus COP for the heat transport exponent $n = 1$ [194].

Klein [199] showed that for a fixed cooling load, the COP of an endoreversible refrigeration cycle is maximized when the product of the heat-transfer effectiveness and external fluid capacitance rate is equally divided between the evaporator and condenser of the cycle. Bejan [200,201] investigated the best way of allocating a finite amount of heat exchanger area between the hot and cold ends of the refrigeration plant models with heat-transfer irreversibilities. Radcenco et al. [202] carried out an optimization study for the intermittent operation of a defrosting vapour-compression-cycle refrigerator with respect to the frequency of on/off operation, and the way in which the supply of heat exchanger surface area is divided between evaporator and condenser.

The philosophy adopted by Curzon–Ahlborn [8] to maximize the power output of an endoreversible heat engine was extended by Agrawal and Menon [203] to optimize the cooling rate of an endoreversible refrigerator having a constant piston speed and it was noticed that the corresponding COP matched that of dry-air based refrigerators. Agrawal and Menon [204] also investigated the effects of the thermal gain through wall and the product loads on the overall COP and the cooling rate of a refrigerator based on an endoreversible Carnot cycle.

Grazzini [205] studied endoreversible Carnot refrigerator cycles with internal irreversibility and obtained the maximum COP and maximum exergetic efficiency as a function of the temperature difference between the cycle's hottest isotherm and the hot sink and also as a function of thermal conductivity.

Ait-Ali [206] analyzed endoreversible refrigeration cycles to optimize the maximum cooling load for refrigerators and the maximum heating load for heat pumps with a specified operating temperature range for the working fluid and a fixed total thermal conductance for the condenser and evaporator. He considered these two constraints to provide boundedness. He concluded that the optimum ratio of condenser to evaporator conductances is always greater than unity and smaller than the ratio of condenser to evaporator heat loads.

Wu [207,208] considered an endoreversible Carnot refrigerator to maximize the specific cooling load, which is the cooling load per unit area of both heat exchangers, with respect to the working fluid temperatures and further analyzed the relationship between the coefficient of performance (COP) and the cooling load, respectively.

Chiou et al. [209] performed an analysis to investigate the optimal cooling load of an endoreversible Carnot refrigeration cycle considering real heat exchangers which have finite size heat-transfer areas and heat-transfer effectiveness therefore having finite thermal capacitance rates. They calculated the optimal rate of refrigeration and expressed in terms of COP, the time ratio of refrigeration

cycle to heat-transfer processes, and the effectiveness of the heat exchangers.

Chen et al. [210] compared the optimization performance expressions of endoreversible forward and reversed Carnot cycles, i.e. heat engines and refrigerators-heat pumps, respectively, and analyzed the inherent connection between these expressions.

Ait-Ali [211] studied a Carnot-like irreversible refrigeration cycle which is modelled with two isothermal and two non-adiabatic processes. The source of internal irreversibility is characterized by a general irreversibility term which could include any heat leaks into the expansion valve, the evaporator and compressor cold volumes. Although a minimum refrigeration power objective would be more appropriate for refrigeration cycles, he optimized this cycle for maximum refrigeration power, maximum refrigeration load and maximum COP with respect to the cold refrigerant temperature considering the maximum refrigeration power is reached at nearly the same refrigeration temperature at which maximum refrigeration load is achieved. He concluded that the distinguishing feature of this internally irreversible refrigeration cycle is that it achieves a maximum value for its COP, which the endoreversible cycle does not. Ait-Ali [212] also investigated the maximum COP of internally irreversible heat pumps and refrigerators in order to obtain analytical expressions for the optimum performance parameters in terms of a cycle-irreversibility parameter similar to the one defined in Eq. (25), the thermal capacitance ratio and the temperature ratio. He showed that the effect of internal irreversibility is to decrease the condensation temperature and increase the evaporation temperature simultaneously in the heat pump mode, which leads to a lower COP and lower heating temperatures. In the refrigerator mode, the COP also decreases with respect to the cycle-irreversibility parameter but under the effect of increasing condensation temperatures and decreasing evaporation temperatures of the refrigerant. Salah El-Din [213] examined similar models of refrigerators and heat pumps as in Ref. [212] considering the constraints of fixed total thermal conductance and fixed total heat-transfer area. He concluded that the thermal conductance at the high temperature end must be greater than that of at the low temperature end when the total thermal conductance is fixed, and that the heat-transfer area at hot end must be increased when the internal irreversibilities are increased and the total heat-transfer area is fixed. He also concluded that the total heat-transfer area must be divided by the same ratio between the two ends of both the refrigerator and the heat pump. Additionally, he expressed that an optimal temperature ratio across the inner compartment of a refrigerator or a heat pump cannot be observed.

Chen [214] developed a general description for a class of irreversible refrigerators considering heat leaks between the heat reservoirs, and internal dissipations of the refrigerator, which were taken into account by using a cycle-irreversibility parameter in order to obtain the maximum COP and the COP versus cooling rate characteristics of such refrigerators. Cheng and Chen [215] applied a similar procedure to determine the maximum COP and corresponding heating load of the heat pump with the similar types of irreversibilities considered in Ref. [214].

Chen et al. [216] examined the influence of internal heat leak on the optimal performance of an endoreversible refrigerator through establishing a relationship between optimal cooling load and COP following Bejan's pioneering work [198]. Chen et al. [217] studied a class of Carnot refrigeration cycles with external heat resistance, heat leakage and finite thermal capacity reservoirs. They demonstrated the importance of finite size and finite thermal capacity of the heat reservoirs and the heat leakage upon the maximum COP, maximum cooling load and the nature of the optimum cycle for real refrigeration plants. Chen et al. [218] generalized the classical endoreversible Carnot refrigeration model incorporating irreversibilities due to heat leakage, friction, turbulence, etc. which are characterized by a constant parameter and a constant coefficient and derived the relationship between the COP and the cooling capacity.

Davis and Wu [219,220] considered an endoreversible heat-engine-driven heat-pump which is shown in Figs. 21 and 22 and an endoreversible heat-engine-driven air-conditioning system receiving heat from a geothermal source, respectively. The environment was used as the heat sink for the heat engine and as the heat source for the heat pump. To analyse such an endoreversible heat-engine-driven systems, a Rankine heat engine and a Carnot heat

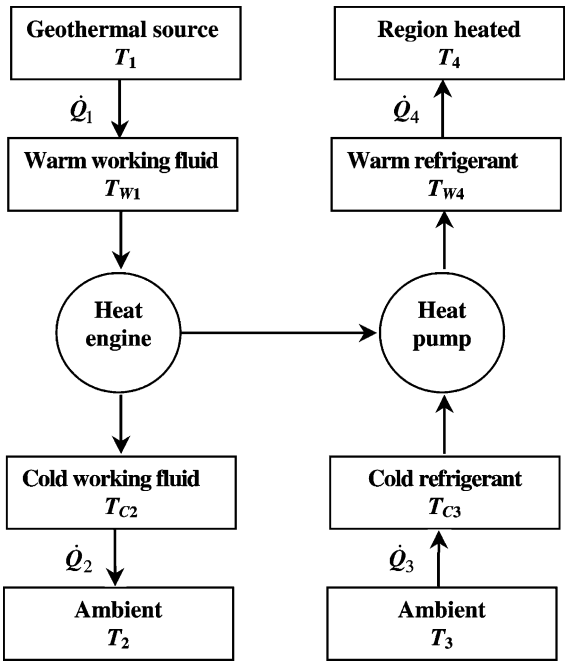

Fig. 21. Schematic of a geothermal heat-engine-driven heat pump [217,218].

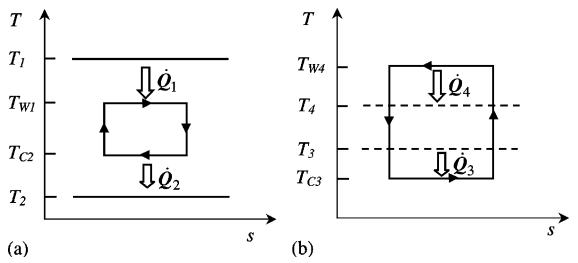

Fig. 22. Endoreversible geothermal heat-engine driven heat pump.

pump or air-conditioner cycle were used. They calculated the COP for both the completely reversible and the endoreversible systems and found that the COP of the latter is lower than that of the former.

5.2. Cascaded refrigeration and heat-pump systems

Chen and Yan [221] derived the optimal configuration for the cascaded refrigeration cycle formed by two endoreversible piston type refrigeration cycles without any intermediate reservoirs to asses the effect of finite rate heat-transfer on the performance. The results obtained in this work have shown that some of the optimum performances of a two-stage endoreversible cascaded refrigeration cycle are not identical with those of a single-stage endoreversible refrigeration cycle, e.g. given by Yan and Chen [196].

Chen et al. [222] derived a fundamental relation between optimal specific rate of refrigeration, i.e. the average rate of refrigeration per unit total heat-transfer surface area, and COP of an endoreversible two-stage refrigeration cycle without intermediate reservoirs for both a piston type (sequential processes) model and a steady flow (simultaneous processes) model. They concluded that, for the single endoreversible cycle, the optimum performance is the same for both models. However, for the cascaded cycles, there are changes for two models mentioned above and in the overall effective heat-transfer coefficients for cycles with or without intermediate reservoir. Chen et al. [223] modelled an n-stage cascaded endoreversible heat pump system to derive the relation between the optimal COP and the specific heating load and optimized the temperatures of the working fluid in the isothermal processes and the heat-transfer areas of the heat exchangers. Chen and Wu [224] performed a similar analysis to derive the relation between heating load and COP for cascaded heat pump cycles without any intermediate reservoirs.

Chen and Wu [225] modelled a two-stage and an n-stage cascaded endoreversible refrigeration systems, respectively. They derived the relation between the optimal COP and the specific cooling rate for this system, and optimized the primary performance parameters of this cascaded system, such as the temperatures of the working fluid in the isothermal processes and the heat-transfer areas of the heat exchangers. Chen et al. [226] examined the influence of a bypass heat leak on the optimum performance of an endoreversible two-stage refrigeration cycle. Chen [227, 228] investigated the performance of a two-stage and an n-stage cascaded refrigeration system analyzing the influence of multi-irreversibilities, such as finite rate heat-transfer, heat leak between the heat reservoirs and internal dissipation of the working fluid. He determined the maximum COP and the corresponding optimal working fluid temperatures, optimal distribution of heat-transfer areas and the power input of the refrigeration system for each case. Goktun [229] obtained an improved equation for the COP of an irreversible two-stage (binary working fluid) refrigeration cycle. Kaushik et al. [230] performed an analysis of irreversible cascaded refrigeration and heat pump cycles to derive a general expression for the optimum COP at minimum power input and given cooling/heating load conditions, respectively, considering the source/sink thermal reservoirs of finite thermal capacitance.

5.3. Gas and magnetic refrigeration and gas heat pump systems

The adiabatic expansion of gases can be used to produce a refrigeration effect. In the simplest form, this is accomplished by reversing the Brayton power cycle which is shown in Fig. 23. Although the Brayton refrigeration cycle with ideal heat exchangers displays the highest COP, it does not provide any cooling load with finite size heat exchangers. It only gives an upper bound that is too high to reach for any real Brayton refrigerator. Real refrigerators deliver a certain amount of cooling load with finite size heat exchangers. Therefore, to find a more meaningful bound for the characteristics of real refrigeration systems, Wu [231], Wu et al. [232] and Chen et al. [233] have examined the performance of an endoreversible Brayton refrigeration cycle coupled to constant or variable temperature heat reservoirs. To extend these works, Chen et al. [234] considered an irreversible air refrigeration cycle, coupled to constant or variable-temperature thermal reservoirs,

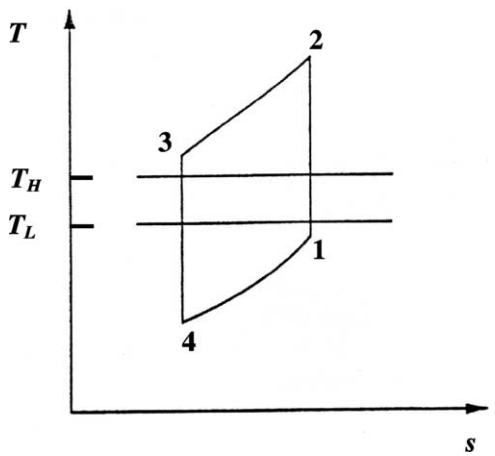

Fig. 23. Endoreversible JB refrigerator with real heat exchangers.

incorporating non-isentropic compression and expansion processes in order to make the model more realistic. They derived the relations between cooling load and pressure ratio and between COP and pressure ratio. The performance of irreversible closed regenerated Brayton refrigerator cycles with either constant- or variable-temperature thermal reservoirs are examined by Chen et al. [235] in a similar way to determine the influences of the effectiveness of the regenerator as well as the heat exchangers, the efficiencies of the expander and the compressor and the temperature ratio of the thermal reservoirs on the cooling load and the COP. Ni et al. [236] and Chen et al. [237] carried out similar analysis of endoreversible and irreversible closed regenerated Brayton heat pump cycles, respectively, for similar purposes.

The Stirling refrigeration cycle is constructed by reversing the Stirling power cycle. It consists of two isothermal and two constant generalized coordinate (polytropic) processes, such as constant volume or isomagnetic processes, and its performance is directly dependent on the working substance, which may be a gas, a magnetic material etc. in the cycle.

Yan and Chen [238] showed that a class of general magnetic refrigeration cycles of paramagnetic salt, which includes the Carnot, Stirling, and other magnetic refrigeration cycles, possess the conditions of perfect regeneration can have the same COP as the Carnot cycle for the same temperature range. Chen and Yan [239] derived the COP of the Ericsson cycle of paramagnetic salt and deduced that it cannot attain the COP of a Carnot refrigerator since it had been pointed out that a magnetic Ericsson refrigeration cycle of a simple paramagnetic salt cannot possess the condition of perfect regeneration by Yan and Chen [240]. Dai [241] claimed that the magnetic Ericsson refrigeration cycles, using the composite working substances, cannot only possess the condition of perfect regeneration but also attain or approach the COP of the Carnot refrigeration cycle. Yan [242] criticized the claims of Dai [241] and pointed out that the COP of the magnetic Ericsson cycle may not exceed the COP of a reversible Carnot refrigeration cycle for the same temperature range. Chen and Yan [243] investigated the effect of the irreversibilities due to regenerative losses on the performance of a magnetic Ericsson refrigeration cycle and calculated the maximum cooling rate.

The influences of finite-rate heat-transfer and regenerative losses on the performance of an endoreversible and that of heat leak on the performance of an irreversible Stirling refrigeration cycle considering ideal gas as the working substance were investigated by Chen and Yan [244,245] and Chen [246]. They derived the relation between the cooling rate and COP and obtained the maximum cooling rate and the corresponding COP. Petrescu et al. [247] presented an optimization analysis of heat engines, refrigerators and heat pumps operating on the Stirling cycle considering the irreversibilities due to finite-rate heat transfer, pressure losses and regeneration effectiveness. The performance characteristics of irreversible Ericsson and Stirling heat pump cycles were also evaluated by Kaushik et al. [248] considering finite thermal capacitance of thermal reservoirs.

A number of cycles other than Carnot, Brayton, Stirling and Ericsson cycles have been proposed and devices built that operate on these cycles. One of such cycles is the Rallis cycle which is a combination of the Stirling and the Ericsson cycles. It consists of two isothermal processes separated by two regenerative processes which are partly constant volume and partly constant pressure in any given combination. An optimum performance analysis of an endoreversible Rallis cycle was carried out by Wu [249] to obtain the maximum power of the Rallis heat engine, maximum heating load of the Rallis heat pump and maximum cooling load of the Rallis refrigerator.

5.4. Three/four-heat-reservoir refrigeration and heat-pump systems

An absorption refrigeration system (equivalent to three-heat-reservoir refrigeration system) or an absorption heat pump system (equivalent to three-heat-reservoir heat pump system) affected by the irreversibility of finite rate heat transfer may be modelled as a combined cycle which consists of an endoreversible heat engine and an endoreversible refrigerator or an endoreversible heat pump. A single-stage absorption refrigerator or heat pump consists primarily of a generator, an absorber, a condenser and an evaporator. It normally transfers heat between three temperature levels, but very often among four temperature levels which is shown in Fig. 24. An equivalent four temperature level combined refrigeration system is also shown in Fig. 25. In these figures, $\dot{Q}_H$ is the heat-transfer rate from the heat source at temperature T_H to the generator, $\dot{Q}_L$ is the heat-transfer rate (cooling load) from the cooled space at temperature T_L and $\dot{Q}_a$ and $\dot{Q}_C$ are the heat-transfer rates from the absorber and condenser to the heat sink at temperature T_a, respectively. T_1, T_2, T_3 and T_4 are the temperatures of the working fluid in the generator, absorber, condenser and evaporator, $\dot{W}$ is the power output of the heat engine which is the power input for the refrigerator.

Yan and Chen [250] and Chen and Yan [251] used the optimal theory of endoreversible two-heat-reservoir refrigerators and heat pumps to investigate the effect of finite rate heat-transfer on the performance of three-heat-source refrigerators and heat pumps, respectively. They determined the relation between the COP and the cooling load (rate of refrigeration), $\dot{Q}_L$ then the optimal COP and corresponding $\dot{Q}_{L,max}$ in refrigerators, and the relation between the COP and the heating load then the optimal COP and corresponding maximum heating load in heat pumps, respectively.

Wu [252] investigated the maximum cooling load of an endoreversible heat-engine-driven refrigerator model by assuming that the heat sinks of the heat engine and the refrigerator are at the same temperature. Also, Davis and

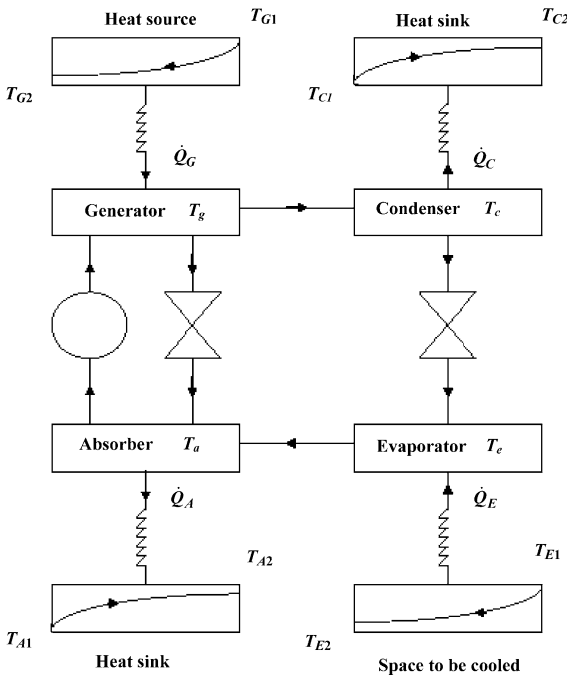

Fig. 24. Absorption refrigeration system.

Wu [253] performed an analysis for an endoreversible heat-engine-driven heat pump system utilizing low grade thermal energy. Finite-time performance analyses of irreversible heat-engine-driven heat pump systems have also been conducted by D'Accadia et al. [254,255].

Chen [256] considered an endoreversible absorption–refrigeration system which is modelled as a combined cycle of a heat engine and a refrigerator as shown in Fig. 25. He optimized the COP of the combined system with respect to heat-transfer area, the specific cooling load with respect to COP of the system, and also obtained corresponding optimal distribution of heat exchanger areas and the optimal working fluid temperatures. Chen and Andresen [257] carried out a similar analysis for an endoreversible absorption-heat pump. Chen and Schouten [258] established a general irreversible absorption–refrigeration cycle model which includes finite-rate heat transfer between the working fluid and the external heat reservoirs, heat leak from the heat sink to the cooled space, and irreversibilities due to the internal dissipations of the working fluid and used this model to calculate the maximum COP and cooling rate of the combined system for a given total heat-transfer area of the heat exchangers. The corresponding optimal temperatures of the working fluid and the optimal distribution of the heat-transfer areas are obtained. Additionally, the behaviour of the dimensionless specific cooling rate as a function of the COP is presented which is shown in Fig. 26. Chen [259,260] also reported similar performance characteristics of an irreversible absorption–refrigeration system at maximum specific cooling load and an irreversible absorption-heat pump system operating among four temperature levels, respectively.

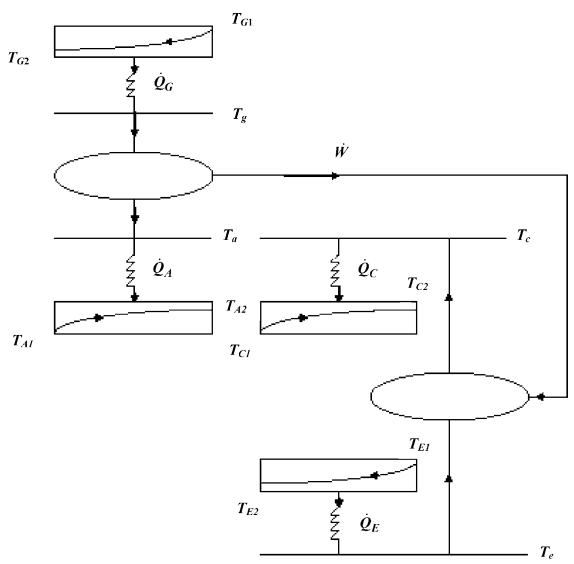

Fig. 25. Equivalent cycle of an absorption refrigeration system.

Wijeysundera [261] performed a parametric study to obtain the maximum cooling capacity, corresponding COP and the second law efficiency of an endoreversible absorption refrigerator cycle with three-heat reservoirs. Goktun [262,263] carried out similar performance analyses to determine the influence of finite-time heat transfer between the heat sources and the working fluid together with the working fluid dissipation on the optimal performance of an irreversible absorption-refrigeration system and an irreversible absorption-heat pump system operating among three temperature levels, respectively. Bhardwaj et al. [264] performed a finite time optimization analysis of an endoreversible and irreversible vapour absorption refrigeration system to determine the optimal bounds for COP and working fluid temperatures of the absorption system at the maximum cooling capacity considering the thermal reservoirs of finite thermal capacitance.

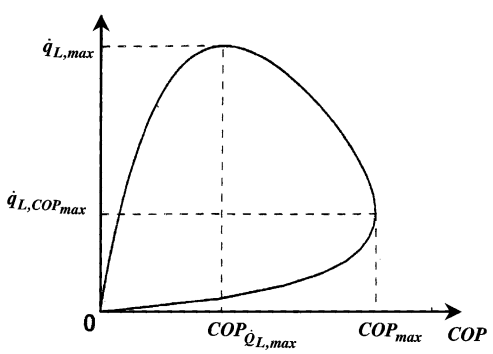

Fig. 26. The dimensionless specific cooling rate (specific cooling load) versus COP [258].

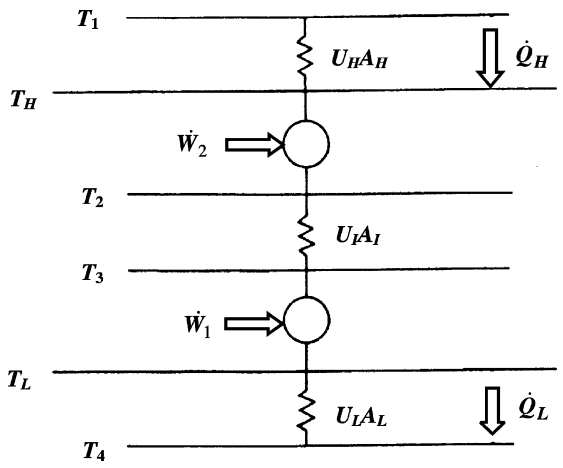

Fig. 27. Schematic of an irreversible combined vapour-compression heat pump [265].

Goktun and Yavuz [265] put forward a model of an irreversible heat-pumping cycle formed by two irreversible cascaded Carnot heat-pumping cycles with two heat reservoirs, which is shown in Fig. 27, and also described a model of an irreversible combined heat-pumping cycle formed by an irreversible vapour compression heat pump and an irreversible absorption heat pump in series with three heat reservoirs to obtain the COP of the system. Their performance results showed that the cascaded vapour compression heat-pumping cycle is more effective than the combined vapour compression–absorption cycle regardless of its greater energy consumption.

In the refrigeration systems area, the models have either power input, as analyzed in heat-engine driven refrigeration systems mentioned above, or heat input and heat rejection to the ambient. A heat-driven refrigeration plant is a refrigerator, which is driven by a heat source without work input. These plants use lowgrade heat (e.g. solar) or waste heat as the driving heat transfer. Examples of such plants are absorption refrigerators and jet ejector refrigerators. Bejan et al. [266] presented the thermodynamic optimization of heat-driven refrigeration plants. Their work based on a model that accounted for the irreversibility of the plant and the finiteness of the heat exchanger inventory (total thermal conductance). They determined the operating regime for maximum refrigeration effect, which requires that the thermal conductance be allocated in a certain way among the heat exchangers, and how the optimal performance is affected by the extreme temperature levels of the refrigeration plant.

Research into heat-driven refrigeration and heat pump systems with solar energy as heat input have been conducted by Chen [267–269], Lin and Yan [270,271] and Wu et al. [272], the other solar-driven combined systems by Goktun and Ozkaynak [273], Goktun and Yavuz [274] and Goktun [275] and also heat-engine-driven combined systems by Goktun [276] for space cooling and heating to investigate their optimal performances.

An absorption heat transformer is the second type of absorption heat pumps, in which the temperature of the heat source is lower than the temperature of the heated space. It may be described by a three-heat-reservoir cycle, which consists of three isothermal and three adiabatic processes. Chen [277] used an equivalent combined cycle model of an endoreversible absorption heat transformer, consisting of an endoreversible Carnot heat pump driven by an endoreversible Carnot heat engine and, to investigate the effect of finite-rate heat transfer on the performance of an absorption heat transformer. He obtained the maximum specific heating load and the corresponding COP of this combined cycle heat transformer. Chen [278] also established a general irreversible cycle model which includes finite-rate heat transfer, heat leak, and other irreversibilities due to the internal dissipation of the working fluid and analyzed the optimal performance of an irreversible heat transformer. Chen and Yan [279] investigated the ecological performance of a class of irreversible absorption heat transformers by employing an ecological optimization criterion proposed by Angulo-Brown [85].

To increase the availability of energy resources and decrease the environmental pollution of high-temperature waste heat, cogeneration cycles are becoming more important. Therefore, many authors have paid great attention to the theoretical analysis and their applications of cogeneration systems. Some useful performance parameters for a cogeneration system have been presented by Huang [280] and Goktun [281,282] obtained improved equations for the COP of an irreversible cogeneration refrigerator and heat pump cycles. Goktun [283] and Goktun and Ozkaynak [284] also investigated the overall system COP for a solar-powered cogeneration system.

Considering the binary fluid cascaded system normally cannot furnish cryogenic temperatures, Goktun and Yavuz [285] carried out a theoretical investigation to determine COP of the irreversible cascaded cryogenic refrigeration cycles. In their work, they introduced a model formed by four irreversible vapour compression refrigerator cycles in series and, a closed cycle solar driven irreversible combined refrigeration and power gas turbine plant using helium as the working fluid. They showed that the performances of the two cycles are almost the same for the same cooling load and cryogenic temperature, however the vapour compression refrigeration cycle in series displays a disadvantage from the energy consumption point of view.

Wu [286] has also investigated the effects of finite-rate of heat transfer on the performance of endoreversible refrigerators. Some other researchers, including Gordon [287] and Bejan [288] have also assessed the effects of finite-rate heat-transfer irreversibility together with other major irreversibilities such as heat leaks, dissipative processes inside working fluid, etc.

6. Finite-time thermoeconomic optimization

Finite-time thermoeconomic optimization is a further step in performance analysis of thermal systems based on FTT to include their economic analyses. The studies in the literature on FTT thermoeconomic optimization is quite limited and research on this topic is still in progress.

De Vos [289] introduced a thermoeconomics analysis of the Novikov plant considering the power output $\dot{W}$ per unit running cost of the plant exploitation C as an objective function. In his study, he assumed that the running cost of the plant consists of two parts: a capital cost that is proportional to the investment and, therefore, to the size of the plant and a fuel cost that is proportional to the fuel consumption, and, therefore, to the heat input rate $\dot{Q}$. Assuming that $\dot{Q}_{\max}$ is an appropriate measure for the size of the plant, the running cost of the plant exploitation is defined as

$$C = a\dot{Q}_{\max} + b\dot{Q}, \tag{56}$$

where a and b are the weight coefficients and

$$\dot{Q} = \alpha(T_H - T_W), \tag{57}$$

$$\dot{Q}_{\max} = \alpha(T_H - T_L). \tag{58}$$

Then, the objective function can be expressed as

$$\omega = \frac{\dot{W}}{C}, \tag{59}$$

where

$$\dot{W} = \alpha\left(1 - \frac{T_L}{T_W}\right)(T_H - T_L). \tag{60}$$

Substituting Eqs. (57), (58) and (60) into Eq. (59) yields

$$\omega = \frac{1}{a}\frac{(T_W - T_L)(T_H - T_W)}{T_W(T_H - T_L) + r(T_H - T_W)}, \tag{61}$$

where r is the dimensionless ratio of b/a. The optimization of the objective function in Eq. (6) by $\partial\omega/\partial T_W = 0$ gives the optimum working fluid temperature

$$T_W = \sqrt{T_H T_L}\frac{\sqrt{1+r}(T_H - T_L) - r\sqrt{T_H T_L}}{T_H - (1+r)T_L} \tag{62}$$

and corresponding optimal efficiency as

$$\eta_{opt} = 1 - \frac{T_L}{T_W} = 1 - \sqrt{\frac{T_L}{T_H}}\frac{T_H - (1+r)T_L}{\sqrt{1+r}(T_H - T_L) - r\sqrt{T_H T_L}}. \tag{63}$$

De Vos [289] showed that the optimal efficiency η_{opt} depends on the economical parameter r. He also demonstrated that the optimal thermal efficiency lies between the mp and the Carnot efficiencies for $0 < r < \infty$, i.e. $\eta_{mp} < \eta_{opt} < \eta_C$.

De Vos [290] developed an analogous model to the Curzon–Ahlborn scheme for economic processes. He considered an endoreversible heat engine as shown in Fig. 2. By the aid of the first and second law of thermodynamics, he obtained the relationships for the working fluid temperatures, the heat input rate and the power output as follows

$$T_W = \left[\frac{\alpha_H(1-\eta)T_H^n + \alpha_L T_L^n}{\alpha_H(1-\eta) + \alpha_L(1-\eta)^n}\right]^{1/n}, \tag{64}$$

$$T_C = \left[\frac{\alpha_H(1-\eta)^n T_H^n + \alpha_L(1-\eta)^{n-1} T_L^n}{\alpha_H + \alpha_L(1-\eta)^{n-1}}\right]^{1/n}, \tag{65}$$

$$\dot{Q}_H = \alpha_H\alpha_L\frac{(1-\eta)^n T_H^n - T_L^n}{\alpha_H(1-\eta) + \alpha_L(1-\eta)^n}, \tag{66}$$

$$\dot{W} = \alpha_H\alpha_L\frac{\eta[(1-\eta)^n T_H^n - T_L^n]}{\alpha_H(1-\eta) + \alpha_L(1-\eta)^n}, \tag{67}$$

where α_H and α_L are thermal conductances of heat exchangers for hot and cold sides and the exponent n is related to the heat-transfer mode. Depending on $\dot{Q}_H(\eta)$ and $\dot{W}(\eta)$ characteristic curves for an endoreversible engine as shown in Fig. 28, it can be deduced that the engine works as a refrigerator when $\eta < 0$, as a heat engine when $0 < \eta < \eta_C$ and as a heat pump when $\eta_C < \eta$. For the special case solved by Curzon–Ahlborn [8], i.e. $n = 1$, De Vos showed that $\eta = \eta_{CNCA}$.

De Vos [290] also presented a model of an endoreversible economic engine as shown in Fig. 29 with two economic reservoirs one at the high worth V_1 and one at the low worth V_2 instead of heat reservoir temperatures, two goods flow rates $\dot{N}_1$ and $\dot{N}_2$ instead of heat fluxes, tax flow rates $\dot{W}_{ecn}$ instead of power output in a heat engine. $V\dot{N}$ is also defined as the price flow rates in this economic engine

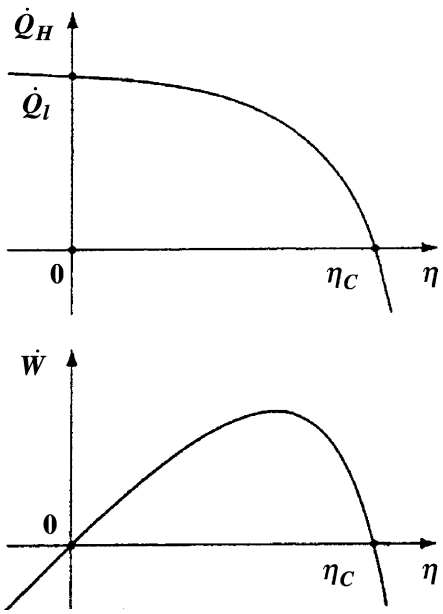

Fig. 28. Heat consumption-efficiency and work-efficiency characteristics of an endoreversible engine [290].

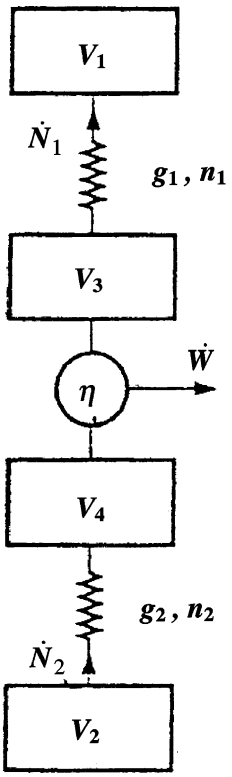

Fig. 29. Endoreversible economic engine model [290].

model. In order to determine the properties of this model he implemented two assumed economical laws equivalent to the two laws of thermodynamics. These assumptions are the conservation of matter

$$\dot{N}_1 = \dot{N}_2 \tag{68}$$

and the conservation of money

$$V_3\dot{N}_1 = \dot{W}_{\mathrm{ecn}} + V_4\dot{N}_2. \tag{69}$$

He introduced the tax rate

$$\eta = \frac{\dot{W}_{\mathrm{ecn}}}{V_4\dot{N}_2}, \tag{70}$$

to yield

$$\eta = \frac{V_3}{V_4} - 1. \tag{71}$$

He also introduced constitutive laws for the commercial conductors

$$\dot{N}_1 = g_1(V_1^{n1} - V_3^{n1}), \tag{72}$$

$$\dot{N}_2 = g_2(V_4^{n2} - V_2^{n2}), \tag{73}$$

where g_1 and g_2 are the economical market conductances. The exponents n_1 and n_2 in Eqs. (72) and (73) are closely related to the elasticity of demand and supply, respectively.

For the special case of equal elasticities, i.e. $n_1 = n_2 = n$, and considering the conservation of matter $\dot{N}_1 = \dot{N}_2$, Eqs. (71)–(73) yield

$$V_3 = (1+\eta)\left[\frac{g_1V_1^n + g_2V_2^n}{g_1(1+\eta)^n + g_2}\right]^{1/n}, \tag{74}$$

$$V_4 = \left[\frac{g_1V_1^n + g_2V_2^n}{g_1(1+\eta)^n + g_2}\right]^{1/n}. \tag{75}$$

Substituting Eq. (75) into Eq. (73) and $N_1 = N_2 = N$ gives

$$\dot{N} = g_1g_2\frac{V_1^n - (1+\eta)^nV_2^n}{g_1(1+\eta)^n + g_2} \tag{76}$$

and multiplication of Eq. (76) by ηV_4 yields

$$\dot{W} = g_1g_2\eta\frac{[V_1^n - (1+\eta)^nV_2^n][g_1V_1^n + g_2V_2^n]^{1/n}}{[g_1(1+\eta)^n + g_2]^{1+1/n}}. \tag{77}$$

Depending on the material consumption $\dot{N}(\eta)$ and the revenue rate $\dot{W}(\eta)$ characteristic curves for an endoreversible economic engine as shown in Fig. 30, it can also be deduced that the engine subsidizes consumption when $\eta < 0$, works as a true market engine when $0 < \eta < \eta_C$ and subsidizes restitution when $\eta_C < \eta$.

His analysis revealed an analogy between economics and thermodynamics where indirect tax revenue in economics plays the same role as work produced by a heat engine in thermodynamics.

Bera and Bandyopadhyay [291] studied the effect of combustion on the thermoeconomic performance of the

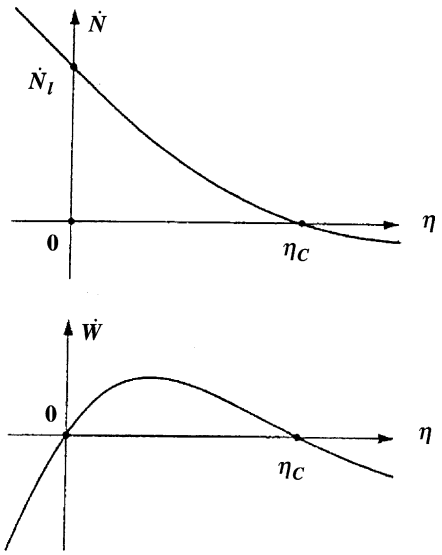

Fig. 30. Material consumption and revenue rate characteristics of an endoreversible economic engine [290].

endoreversible Otto and JB engines. In their work, the operating cost is used as an objective function for optimization. The operating cost of the engines is

$$\lambda = \dot{m}_a c_a T_f \frac{[g_1 - g_3 + \theta(g_2 + g_3)](\theta T_{max} - T_{min})}{(T_f - T_{max})\theta + T_{min}}, \quad (78)$$

where T_{max} and T_{min} are the limiting temperatures in the cycle and T_f is the adiabatic flame temperature, θ is the ratio of compressor inlet to outlet temperatures and g_1, g_2 and g_3 are the economical parameters which depend on the fuel cost, cooling utility cost and power selling price, respectively. The optimum value of θ that minimizes λ is

$$\theta_{opt} = \sqrt{\frac{T_{min}}{T_{max}}} \times \frac{\sqrt{T_f[(T_f - T_{max})(g_3 - g_1)/(g_2 + g_3) + T_{min}]} - \sqrt{T_{max} T_{min}}}{(T_f - T_{max})}. \quad (79)$$

They concluded that the efficiency of the heat engine at its minimum operating cost is always higher than the efficiency corresponding to the mp condition. As T_f approaches ∞ or T_{max}, the corresponding efficiency becomes

$$1 - \sqrt{[(g_3 - g_1)T_{min}]/[(g_2 + g_3)T_{max}]}$$

and

$$0.5\eta_C + 0.5 - (g_3 - g_1)/(g_2 + g_3),$$

respectively. Bandyopadhyay et al. [292] applied the thermoeconomical method introduced in Bera and Bandyopadhyay [291] for Otto and JB heat engines to a cascaded power cycle to determine the thermoeconomic performance. They observed that the efficiency of a multi-stage endoreversible cascaded cycle power plant corresponding to maximum power production or minimum operating cost is identical to that of a single endoreversible heat engine under the same operating conditions.

Wu et al. [293] carried out an exergoeconomic analysis for an endoreversible heat engine model based on general heat-transfer law, $\dot{Q} \propto \Delta(T^n)$. The profit obtained from the heat engine, which is defined as the difference between the revenue and the cost per unit time, is used as an objective function for optimization. They obtained the optimal profit and efficiency characteristics and the relation for the maximum profit at the corresponding efficiency range for three common heat-transfer laws, i.e. Newton's law, a linear phenomenological law in irreversible thermodynamics and the radiation heat-transfer law. Wu et al. [294] also carried out a finite-time exergoeconomic performance analysis for an endoreversible Carnot heat pump similar to their earlier work [293].

De Vos [295] demonstrated how endoreversible models can be applied to economic systems. He investigated whether extensive properties (such as energy, mass and entropy, etc.) and intensive properties (such as pressure, temperature and chemical potential, etc.) in physics have counterparts in economics. He described various endoreversible engines such as endoreversible engines in thermodynamics and endoreversible engines in economics. The endoreversible heat engine and the endoreversible chemical engine are discussed in detail and it is shown that their counterparts in economics are the endoreversible social engine and the endoreversible commercial engine, respectively.

Sahin and Kodal [296] introduced a new thermoeconomic performance analysis based on an objective function defined as the power output per unit total cost. Using this new criterion, they performed finite time thermoeconomic performance optimization for endoreversible [296] and irreversible [297] heat engines. In their study, fuel and investment cost items, having the major effect on the performance and design parameters, are considered for thermoeconomic optimization. They assumed that the investment cost of the plant is proportional to the total heat-transfer area and, the fuel consumption cost is proportional to the heat-transfer rate to the plant. In this context, the function to be optimized is defined as

$$F = \frac{\dot{W}}{a(A_H + A_L) + b\dot{Q}_H}, \quad (80)$$

where the proportionality coefficient for the investment cost, a is equal to the capital recovery factor times investment cost per unit heat-transfer area and the coefficient, b is equal to the annual operation hours times price per unit heat-transfer rate to the plant. Using the first and second laws of thermodynamics, the objective functions for endoreversible and irreversible heat engines are obtained as a function of working fluid temperatures and given, respectively, as follows

$$bF = \frac{T_W - T_C}{k\left[\frac{T_W}{U_H(T_H - T_W)} + \frac{T_C}{U_L(T_C - T_L)}\right] + T_W}, \quad (81)$$

$$bF = \frac{T_W - RT_C}{k\left[\frac{T_W}{U_H(T_H - T_W)} + \frac{RT_C}{U_L(T_C - T_L)}\right] + \left[1 + \frac{(T_H - T_L)C_l/(U_H A_H)}{T_H - T_W}\right]T_W}, \quad (82)$$

where R is the internal irreversibility parameter, $C_l/(U_H A_H)$ is the heat leakage parameter and $k = a/b$ is the economical parameter. They obtained the optimal working fluid temperatures and optimal heat-transfer area

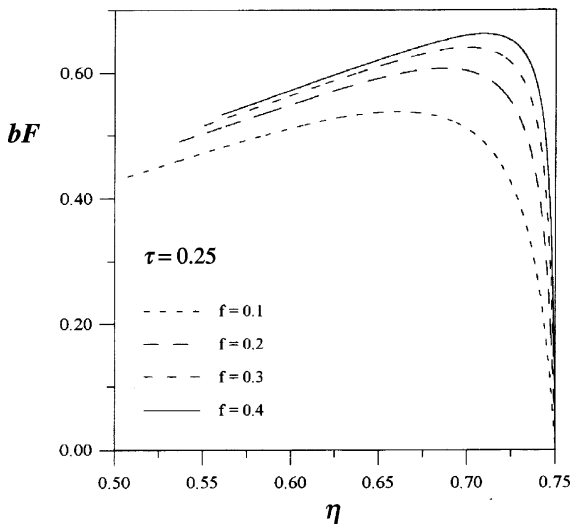

Fig. 31. Variation of the objective function for the endoreversible heat engine with respect to η for various $f = b/(a+b)$ values and the specified data set given in Ref. [296].

distributions to maximize the objective functions given in Eqs. (81) and (82) for endoreversible and irreversible cases, respectively. Thermoeconomic characteristic curves are given in Figs. 31 and 32 for endoreversible case and in Figs. 33 and 34 for irreversible case.

Antar and Zubair [298] performed a finite-time thermoeconomic analysis of an endoreversible heat engine, which is shown in Fig. 2, considering the total cost per unit power output as an objective function. They expressed the total cost of conductance, Γ in terms of unit cost parameters as

$$\Gamma = \zeta_H (UA)_H + \zeta_L (UA)_L, \tag{83}$$

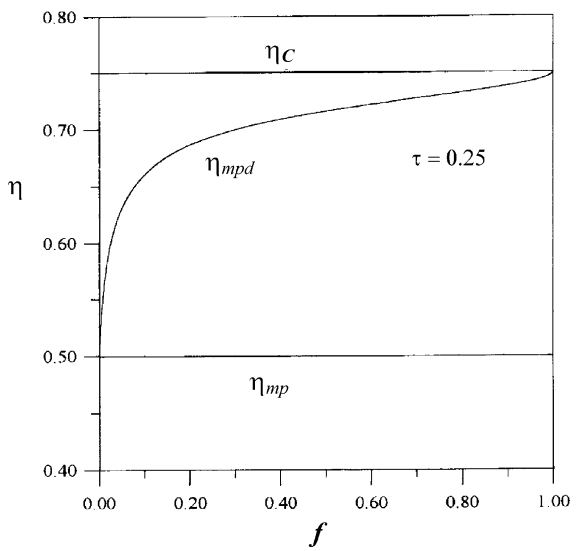

Fig. 32. Variation of the optimum thermal efficiency with respect to f for the specified data set given in Ref. [296].

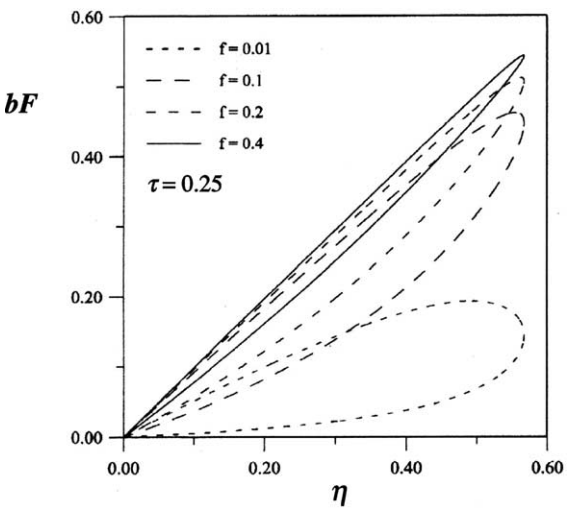

Fig. 33. Variation of the objective function for the irreversible heat engine with respect to η for various $f = b/(a+b)$ values and the specified data set given in Ref. [297].

where ζ_H and ζ_H are the unit conductance costs at hot and cold end heat exchangers, respectively. By the aid of the first and second laws of thermodynamics, they obtained

$$F = \frac{\Gamma}{\dot{W}/T_H} = \frac{\zeta_L}{1-\psi}\left(\frac{G}{1-\chi} + \frac{\psi}{\psi\chi - \tau}\right), \tag{84}$$

where the dimensionless absolute temperature ratios ψ, χ and τ are defined previously and G is defined as the ratio of the unit costs of the conductances of the hot side to the cold side of a power plant, $G = \zeta_H/\zeta_L$.

The dimensionless cost ratio F is minimized with respect to the temperature ratios of χ and ψ. Optimum values of the absolute temperature values are obtained and

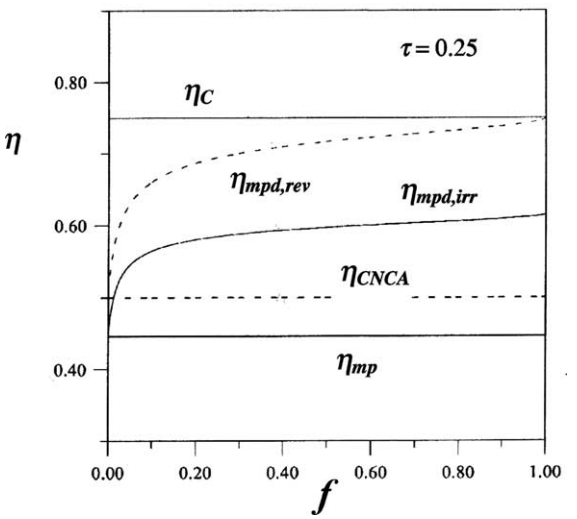

Fig. 34. Comparisons of the thermal efficiencies with respect to f for the specified data set given in Ref. [297].

the influences of G and ψ on the thermoeconomic performance are discussed.

Bejan et al. [266] also defined an objective function for the profit of a heat-driven refrigeration plant

$$P = p_L \dot{Q}_L - p_H \dot{Q}_H. \quad (85)$$

Here, p_L and p_H are the known prices of the refrigeration load and the heat input. They obtained numerically the optimal distribution of the total thermal conductance inventory UA to maximize the profit P. They showed that the condenser demands half of the total thermal conductance, regardless of the price ratio p_H/p_L. and the external temperature ratios.

Sahin and Kodal [299] introduced a new finite-time thermoeconomic performance criterion, defined as the cooling load of the refrigerator and the heating load of the heat pumps per unit total cost, which is the sum of the annual investment cost C_i and the energy consumption cost C_e. They investigated the economic design conditions based on this thermoeconomic performance criterion for endoreversible [299] and irreversible [300] single-stage vapour compression refrigeration and heat pump systems. The objective functions for endoreversible refrigeration and heat pump systems are defined, respectively, as

$$F_{ref} = \frac{\dot{Q}_L}{C_i + C_e}, \quad (86)$$

$$F_{hp} = \frac{\dot{Q}_H}{C_i + C_e}, \quad (87)$$

where the annual investment cost and the annual energy consumption cost of the system are written as

$$C_i = a(A_H + A_L) + b_1 \dot{W} = a(A_H + A_L) + b_1(\dot{Q}_H - \dot{Q}_L), \quad (88)$$

$$C_e = b_2 \dot{W} = b_2(\dot{Q}_H - \dot{Q}_L). \quad (89)$$

Here, the proportionality coefficients for the investment cost of the heat exchangers, a, is equal to the capital recovery factor times investment cost per unit heat-transfer area, for the investment cost of the compressor and its driver, b_1, is equal to the capital recovery factor times investment cost per unit power and the coefficient b_2 is equal to the annual operation hours times price per unit energy. They considered the investment costs of the main system components, which are the heat exchangers and the compressor together with its prime mover for the investment costs. The investment cost of the heat exchangers is assumed to be proportional to the total heat-transfer area. The investment cost of the compressor and its driver and, the energy consumption cost are assumed to be proportional to the compression capacity or the power input.

The variations of the objective functions with respect to COP for various $k = a/(b_1 + b_2)$ are shown in Figs. 35 and 36 for endoreversible and irreversible refrigerator and heat pump systems, respectively.

The finite-time thermoeconomic optimization technique introduced by Sahin and Kodal [299] has been extended to two-stage vapour compression and absorption refrigeration and heat pump systems [301–305]. In these works and also in Refs. [299,300], the optimum temperatures of the working fluids, optimum COP, optimum specific cooling or heating load and the optimal distribution of heat exchanger areas are determined in terms of technical and economical parameters.

Chen and Wu [306] carried out a thermoeconomic performance analysis of a multi-stage irreversible cascaded heat pump system. The operation of a heat pump is viewed as a production process with heat as its output. The profit of operating the heat pump system, which is taken as an objective function for optimization, is defined as

$$P = p_H \dot{Q}_1 - p_L \dot{Q}_{n+1} - p\dot{W}, \quad (90)$$

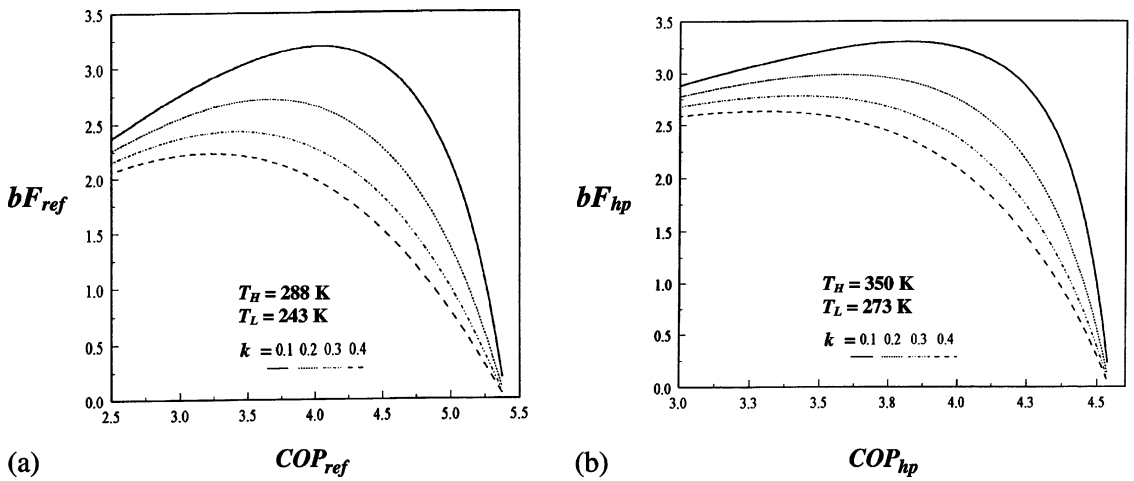

Fig. 35. Variations of the objective function for the endoreversible refrigerator (a) and for the endoreversible heat pump (b) with respect to COP for various k values and the specified data set given in Ref. [299].

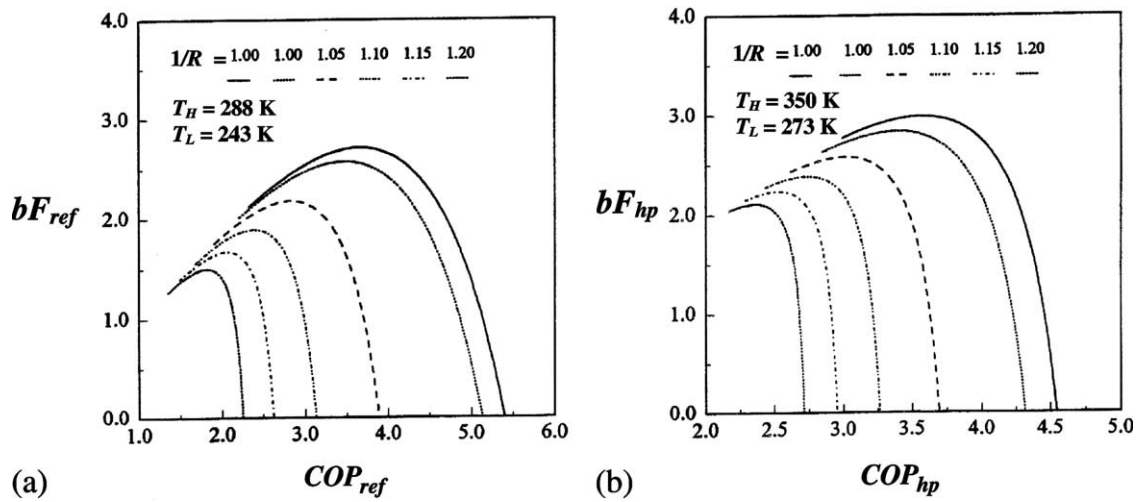

Fig. 36. Variations of the objective function for the refrigerator (a) and for the heat pump (b) with respect to COP for various $1/R$ values and the specified data set given in Ref. [300].

where $\dot{Q}_1 = \dot{Q}_H$ is the heating load of the heat pump, $\dot{Q}_{n+1} = \dot{Q}_L$ is the heat-transfer rate from the cold thermal reservoir to the heat pump, $\dot{W}$ is the total power input required by the cascaded heat pump system, p_H is the price of heat supplied by the heat pump to the users, p_L is the price of heat absorbed by the heat pump from the low temperature thermal reservoir and p is the price of work input. They determined the optimal COP, heating load and power input at the maximum profit together with the optimal distribution of the heat-transfer areas or the thermal conductances of the heat exchangers and the optimal temperature ratios of the working fluids of two adjacent cycles.

Antar and Zubair [307] applied a similar procedure used in Antar and Zubair [298] to investigate the optimum allocation of heat-transfer inventory for heat exchangers in a refrigeration system with specified power input or cooling capacity, and for a heat pump with specified heating capacity considering the cost of both heat exchanger conductances as an additional design parameter. They employed the dimensionless cost ratio F, which is derived similar to the one in Eq. (29), as an objective function and minimized it with respect to χ.

7. Final remarks and conclusions

The Carnot cycle is a completely reversible heat engine cycle having the ideal thermal efficiency of $\eta = 1 - T_L/T_H$, which is called the Carnot efficiency. The thermal efficiency for any heat engine cycle, operating between the fixed temperature limits of T_H and T_L cannot exceed this efficiency. However, the Carnot cycle is not a practical power cycle due to two reasons: (1) the two reversible isothermal processes need infinitely long execution time to maintain the thermodynamic equilibrium between the working fluid and the thermal reservoirs having finite heat exchanger areas, (2) the Carnot cycle requires infinitely large heat exchanger area to transfer a finite amount of heat in finite time. Hence, the Carnot cycle, although constituting an upper limit of thermal efficiency for heat engines, produces a finite amount of work but no power. Therefore, the processes in a real heat engine cycle must be executed in finite time to produce some power.

In addition to this, in classical thermodynamic analyses, the first law of thermodynamics has been used incorporating the concept of conservation of energy under the assumption of thermodynamic quasi-equilibrium during processes, together with the second law of thermodynamics as an additional constraint. A quasi-equilibrium process can be viewed as a sufficiently slow process, which allows the system to adjust itself internally so that properties in one part of the system do not change any faster than those at the other parts. However, real processes are non-equilibrium processes, and they are approximated by ideal processes in a quasi-static manner under the classical thermodynamic approach. Therefore, in the analysis of real thermal systems, the application of thermodynamic laws in rate form must be taken into account, i.e. power instead of work. Following this argument, it can be deduced that the duration of any process is of primary importance as power is more important commodity in daily life than energy.

Therefore, to provide a new perspective on the application of thermodynamics to the analysis of real thermal systems, FTT theory has been put forward in which the irreversibilities in real thermal systems are included in the analysis in a simple way and the optimizations are carried out in a straightforward procedure. From the reviewed studies in this paper, it can be

observed that FTT has found a wide area of application since 1970s and taken its place in general thermodynamics as the classical, the statistical and the non-equilibrium thermodynamics.

Thermodynamic optimization studies have recently been extended to focus on the generation of optimal geometric form (shape, structure and topology) in flow systems and applied to design in both mechanical and civil engineering. The optimization of global system performance (e.g. minimum flow resistance, minimum irreversibility) subject to global finiteness constraints (volume, weight, time) was identified as principle for the generation of geometric form (shape and structure) in systems with internal flows. The geometric structures derived from this principle for engineering applications have been named constructural designs. The thought that the same principle serves as basis for the occurrence of geometric form in natural flow systems has been named constructural theory. Recent developments on these topics are reviewed in a book by Bejan [308], who is the pioneering researcher, and in a review article by Bejan and Lorente [309].

Some critiques and comments on the fundamental concepts and applications of FTT were also provided by Gyftopoulos [310,311], Moran [312], Chen et al. [313] and on the role and limitations of FTT by Ishida [314]. Denton [315] provided a critical overview of thermal cycles in classical thermodynamics, non-equilibrium thermodynamics and FTT. Bejan [316,317] also pointed out that the heat input is assumed to be freely variable during the optimization procedure, which is a modelling limitation in endoreversible heat engine performance analyses leading to the CNCA efficiency.

The studies on the determination of efficiency at maximum power for externally irreversible Carnot heat engine cycle may be regarded as the very first works of FTT. Many different objective functions, such as thermal efficiency, specific power, power density for heat engines, cooling load, heating load, coefficient of performance for refrigerators and heat pumps, exergy rate, ecological rate, economical rate, for the optimization of thermal systems are taken into consideration and studied in detail. These optimization studies are extended to the other single, cascaded and combined heat engine, refrigerator and heat pump systems and also to the direct energy conversion systems considering irreversibilities due to not only finite-rate external heat transfer but also internal irreversibilities and heat leakage.

FTT combines thermodynamics, heat transfer and fluid mechanics, and covers an interdisciplinary field of research. The particular laws of heat transfer need to be used together with the fundamental principles of classical thermodynamics and mechanics to consider the irreversibilities in FTT analyses.

One of the major results of FTT analyses is the determination of optimal performance range, e.g. the optimal efficiency lies between the maximum efficiency and the efficiency at maximum power for an irreversible heat engine, $\eta_{mp} \leq \eta_{opt} \leq \eta_{max}$ which corresponds to $\dot{W}_{max} \geq \dot{W}_{opt} \geq \dot{W}_{mef} \geq 0$. It should be noted here that $\dot{W}_{mef} = 0$ applies to the case with no heat leak and $\dot{W}_{mef} > 0$ with heat leak (Figs. 8 and 9). This result shows that the thermal efficiency at maximum power constitutes the lower limit for rational design of thermal systems. As it can be concluded from the reviewed studies, the optimal efficiencies depending on different performance criterion other than the maximum power and efficiency are placed in the same efficiency interval.

There appears to be very limited publications on addressing the environmental concerns such as covering reduction of thermal pollution and exergy destruction by FTT analyses, therefore, new optimization criteria may be introduced for the ecological and exergetic performance optimization of thermal systems. The fundamental analysis of rate dependent processes introduced by FTT may be extended to the problems in other disciplines through analogies, such as chemistry, economics and other social field of studies. Finite-time thermoeconomic analysis is still in its early stages, in progress and it needs more effort in fundamental theory development and for its applications.

References

[1] Carnot S. Réflections sur la puissance motrice du feu. Paris: Bachelier; 1824.

[2] Chambadal P. Les Centrales Nucléaires. Paris: Armand Colin; 1957. p. 41–58.

[3] Chambadal P. Le choix du cycle thermique dans une usine génératrice nucléaire. Rev Gén Élect 1958;67:332–45.

[4] Novikov II. Atomnaya Energiya 1957;409–12. [in Russian].

[5] Novikov II. The efficiency of atomic power stations (a review). J Nucl Energy 1958;125–8.

[6] El-Wakil MM. Nuclear power engineering. New York: McGraw-Hill; 1962. p. 162–5.

[7] El-Wakil MM. Nuclear energy conversion. International Textbook Company; 1971. p. 31–5.

[8] Curzon FL, Ahlborn B. Efficiency of a Carnot engine at maximum power output. Am J Phys 1975; 43(1):22–4.

[9] Bejan A. Entropy generation through heat and fluid flow. New York: Wiley; 1982.

[10] Andresen B. Finite-time thermodynamics. Physics Laboratory II, University of Copenhagen; 1983.

[11] Sieniutycz S, Salamon P. In: Sieniutycz S, Salamon P, editors. Advances in thermodynamics: finite-time thermodynamics and thermoeconomics, vol. 4. New York: Taylor & Francis; 1990.

[12] De Vos A. Endoreversible thermodynamics of solar energy conversion. Oxford: Oxford University Press; 1992.

[13] Bejan A. Entropy generation minimization. Boca Raton, FL: CRC Press; 1996.

[14] Bejan A, Tsatsaronis G, Moran M. Thermal design and optimization. New York: Wiley; 1996.

[15] Bejan A, Mamut E, editors. Thermodynamic optimization of complex energy systems. London: Kluwer Academic Publishers; 1999.
[16] Wu C, Chen L, Chen J, editors. Recent advances in finite-time thermodyanmics. New York: Nova Science Publishers; 1999.
[17] Berry RS, Kazakov V, Sieniutycz S, Szwast Z, Tsirlin AM. Thermodynamic optimization of finite-time processes. New York: Wiley; 2000.
[18] Radcenco V. Generalized thermodynamics. Bucharest: Editura Techica; 1994.
[19] Sieniutycz S, Shiner JS. Thermodynamics of irreversible processes and its relation to chemical engineering: second law analyses and finite-time thermodynamics. J Non-Equilib Thermodyn 1994;1:303–48.
[20] Bejan A. Entropy generation minimization: the new thermodynamics of finite-size devices and finite-time processes. J Appl Phys 1996;79(3):1191–218.
[21] Chen L, Wu C, Sun F. Finite-time thermodynamic optimization or entropy generation minimization of energy systems. J Non-Equilib Thermodyn 1999;2:327–59.
[22] Hoffmann KH, Burzler JM, Schubert S. Endoreversible thermodynamics. J Non-Equilib Thermodyn 1997;2:311–55.
[23] Bejan A. Advanced engineering thermodynamics. 2nd ed. New York: Wiley; 1997.
[24] Van Wylen G, Sonntag R, Borgnakke C. Fundamentals of classical thermodynamics. 4th ed. New York: Wiley; 1994. p. 214–6.
[25] Winterbone D. Advanced thermodynamics for engineers. London: Butterworth–Heinemann; 1996. p. 85–99.
[26] Andresen B, Salamon P, Berry RS. Thermodynamics in finite time: extremals for imperfect heat engines. J Chem Phys 1977;66(4):1571–7.
[27] Salamon P, Andresen B, Berry RS. Thermodynamics in finite time. II. Potentials for finite-time processes. Phys Rev A 1977;15(5):2094–102.
[28] Gutkowicz-Krusin D, Procaccia I, Ross J. On the efficiency of rate processes. Power and efficiency of heat engines. J Chem Phys 1978;69(9):3898–906.
[29] Rubin MH. Optimal configuration of a class of irreversible heat engines, I. Phys Rev A 1979;19(3):1272–6.
[30] Rubin MH. Optimal configuration of a class of irreversible heat engines, II. Phys Rev A 1979;19(3):1277–89.
[31] Rubin MH. Optimal configuration of an irreversible heat engine with fixed compression ratio. Phys Rev A 1980;22(3): 1741.
[32] Salamon P, Nitzan A, Andresen B, Berry RS. Minimum entropy production and the optimization of heat engines. Phys Rev A 1980;21(6):2115–29.
[33] Andresen B, Gordon JM. Optimal paths for minimizing entropy generation in a common class of finite-time heating and cooling processes. Int J Heat Fluid Flow 1992;13(3): 294–9.
[34] Salamon P, Nitzan A. Finite time optimizations of a Newton's law Carnot cycle. J Chem Phys 1981;74(6): 3546–60.
[35] Rubin MH, Andresen B. Optimal staging of endoreversible heat engines. J Appl Phys 1982;53(1):1–7.
[36] Ondrechen MJ, Rubin MH, Band YB. The generalized Carnot cycle: a working fluid operating in finite time between finite heat sources and sinks. J Chem Phys 1983;78(7): 4721–7.
[37] Rebhan E, Ahlborn B. Frequency-dependent performance of a nonideal Carnot engine. Am J Phys 1987;55(5):423–8.
[38] Wu C. Output power and efficiency upper bound of real solar heat engines. Int J Ambient Energy 1988;9(17):17–21.
[39] Wu C, Walker TD. Finite-time thermodynamics and its potential naval shipboard application. Naval Engrs J 1989; 101(1):35–9.
[40] DeVos A. Efficiency of some heat engines at maximum power conditions. Am J Phys 1985;5:570–3.
[41] Wu C. Power optimization of a finite-time Rankine heat engine. Int J Heat Fluid Flow 1989;1:134–8.
[42] Bejan A. Theory of heat-transfer irreversible power-plants. Int J Heat Mass Transm 1988;31(6):1211–9.
[43] Wu C, Kiang RL, Lopardo VJ, Karpouzian GN. Finite-time thermodynamics and endoreversible heat engines. Int J Mech Engng Educ 1993;21(4):337–46.
[44] Wu C. Power optimization of a finite time Carnot heat engine. Energy 1988;13(9):681–7.
[45] Nulton JD, Salamon P, Pathria RK. Canot-like processes in finite time. I. Theoretical limits. Am J Phys 1993;61(10): 911–6.
[46] Pathria RK, Nulton JD, Salamon P. Canot-like processes in finite time. II. Applications to model cycles. Am J Phys 1993; 61(10):916–24.
[47] Gordon JM. Maximum power point characteristics of heat engines as a general thermodynamic problem. Am J Phys 1989;57(12):1136–42.
[48] De Mey G, De Vos A. On the optimum efficiency of endoreversible thermodynamic processes. J Phys D: Appl Phys 1994;27:736–9.
[49] Bejan A. Maximum power from fluid flow. Int J Heat Mass Transfer 1996;3(6):1175–81.
[50] Bejan A, Errera MR. Maximum power from a hot stream. Int J Heat Mass Transfer 1998;4(13):2025–35.
[51] Vargas JVC, Bejan A. Thermodynamic optimization of the match between two streams with phase change. Energy 2000; 25:15–33.
[52] Andresen B, Berry RS, Nitzan A, Salamon P. Thermodynamics in finite time. I. The step Carnot cycle. Phys Rev A 1977;15:2086–93.
[53] Orlov VN. Optimum irreversible Carnot cycle containing three isotherms. Sov Phys Dokl 1985;30:506–8.
[54] Yan Z, Chen L. Optimal performance of a generalized Carnot cycle for another linear heat transfer law. J Chem Phys 1990; 9(3):1994–8.
[55] Castans M. Bases físicasdel approvechamiento de la energía solar Revista Geofis 1976;35:127–39.
[56] Jeter S. Maximum conversion efficiency for the utilization of direct solar radiation. Solar Energy 1981;26(3):231–6.
[57] De Vos A, Pauwels H. On the thermodynamic limit of photovoltaic energy conversion. J Appl Phys 1981;25(2):119–25.
[58] Chen L, Yan Z. The effect of heat-transfer law on performance of a two-heat-source endoreversible cycle. J Chem Phys 1989;9(7):3740–3.
[59] Gordon JM. Observations on efficiency of heat engines operating at maximum power. Am J Phys 1990;58(4): 370–5.
[60] Gordon JM. On optimized solar-driven heat engines. Solar Energy 1988;40(5):457–61.

[61] Gordon JM, Zarmi Y. Wind energy as a solar-driven heat engine: a thermodynamic approach. Am J Phys 1989;(11): 995–8.
[62] Agnew B, Anderson A, Frost TH. Optimisation of a steady-flow Carnot cycle with external irreversibilities for maximum specific output. Appl Therm Engng 1997;1(1):3–15.
[63] Erbay LB, Yavuz H. An analysis of an endoreversible heat engine with combined heat transfer. J Phys D: Appl Phys 1997;30:2841–7.
[64] Badescu V. Optimum design and operation of a dynamic solar power system. Energy Convers Mgmt 1996;37(2): 151–60.
[65] Sahin AZ. Optimum operating conditions of solar driven heat engines. Energy Convers Mgmt 2000;41:1335–43.
[66] Gordon JM, Huleihil M. On optimizing maximum-power heat engines. Am J Phys 1991;6(1):1–7.
[67] Goktun S, Ozkaynak S, Yavuz H. Design parameters of a radiative heat engine. Energy 1993;1(6):651–5.
[68] Wu C, Kiang RL. Finite-time thermodynamic analysis of a Carnot engine with internal irreversibility. Energy 1992; 1(12):1173–8.
[69] Chen J, Wu C, Kiang RL. Maximum specific power output of an irreversible radiant heat engine. Energy Convers Mgmt 1996;37:17–22.
[70] Goktun S. Finite-time optimization of a solar-driven heat engine. Solar Energy 1996;5(6):617–20.
[71] Ozkaynak S, Goktun S, Yavuz H. Finite-time analysis of a radiative heat engine with internal irreversibility. J Phys D: Appl Phys 1994;27:1139–43.
[72] Ozkaynak S. Maximum power operation of a solar-powered heat engine. Energy 1995;2(8):715–21.
[73] Ait-Ali MA. Maximum power and thermal efficiency of an irreversible power cycle. J Appl Phys 1995;7(7):4313–8.
[74] Bejan A. Thermodynamic optimization alternatives: minimization of physical size subject to fixed power. Int J Energy Res 1999;23:1111–21.
[75] Salah El-Din MM. Second law analysis of irreversible heat engines with variable temperature heat reservoirs. Energy Convers Mgmt 2001;42:189–200.
[76] Gordon JM, Huleihil M. General performance characteristics of real heat engines. J Appl Phys 1992;7(3):829–37.
[77] Chen J. The maximum power output and maximum efficiency of an irreversible Carnot heat engine. J Phys D: Appl Phys 1994;27:1144–9.
[78] Chen L, Sun F, Wu C. Generalised model of a real heat engine and its performance. J Inst Energy 1996;69:214–22.
[79] Chen L, Sun F, Wu C. Influence of internal heat leak on the power versus efficiency characteristics of heat engines. Energy Convers Mgmt 1997;38:1501–7.
[80] Moukalled F, Nuwayhid RY, Noueihed N. The efficiency of endoreversible heat engines with heat leak. Int J Energy Res 1995;19:377–89.
[81] Moukalled F, Nuwayhid RY, Fattal S. A universal model for studying the performance of Carnot-like engines at maximum power conditions. Int J Energy Res 1996;20:203–14.
[82] Sahin B, Kodal A, Yavuz H. Efficiency of a Joule–Brayton engine at maximum power-density. J Appl Phys 1995;28: 1309–13.
[83] Sahin B, Kodal A, Yavuz H. Maximum power density for an endoreversible Carnot heat engine. Energy 1996;2(12): 1219–25.
[84] Kodal A, Sahin B, Yilmaz T. A comparative performance analysis of irreversible Carnot heat engines under maximum power density and maximum power conditions. Energy Convers Mgmt 2000;41:235–48.
[85] Angulo-Brown F. An ecological optimization criterion for finite-time heat engines. J Appl Phys 1991;6(11):7465–9.
[86] Comment onYan Z. Comment on An ecological optimization criterion for finite-time heat engines. J Appl Phys 1993;73(7):3583.
[87] Cheng CY, Chen CK. The ecological optimization of an irreversible Carnot heat engine. J Phys D: Appl Phys 1997; 30:1602–9.
[88] Arias-Hernandez LA, Angulo-Brown F. A general property of endoreversible thermal engines. J Appl Phys 1997;81(7): 2973–9.
[89] Angulo-Brown F, Arias-Hernandez LA, Paez-Hernandez R. A general property of non-endoreversible thermal cycles. J Phys D: Appl Phys 1999;32:1415–20.
[90] Ares de Parga G, Angulo-Brown F, Navarrete-Gonzalez TD. A variational optimization of a finite-time thermal cycle with a nonlinear heat transfer law. Energy 1999;24: 997–1008.
[91] Velasco S, Roco JMM, Medina A, White JA, Hernandez AC. Optimization of heat engines including the saving of natural resources and the reduction of thermal pollution. J Phys D: Appl Phys 2000;33:355–9.
[92] Andresen B, Rubin MH, Berry RS. Availability for finite-time processes. General theory and a model. J Chem Phys 1983;87:2704–13.
[93] Mironova VA, Tsirlin AM, Kazakov VA, Berry RS. Finite-time thermodynamics: exergy and optimization of time-constrained processes. J Appl Phys 1994;76:629–36.
[94] Yan Z, Chen L. Optimization of the rate of exergy output for an endoreversible Carnot refrigerator. J Phys D: Appl Phys 1996;29:3017–21.
[95] Sahin B, Kodal A, Ekmekci I, Yilmaz T. Exergy optimization for an endoreversible cogeneration cycle. Energy 1997;22: 551–7.
[96] Sieniutycz S, Von Spakovsky MR. Finite time generalization of thermal exergy. Energy Convers Mgmt 1998;39(14): 1423–47.
[97] Wu C, Karpouzian G, Kiang L. The optimal power performance of an endoreversible combined cycle. J Inst Energy 1992;65:41–5.
[98] Chen J, Wu C. Maximum specific power output of a two-stage endoreversible combined cycle. Energy 1994;20: 305–9.
[99] Chen J, Wu C. General performance characteristics of an *n*-stage endoreversible combined power cycle system at maximum specific power output. Energy Convers Mgmt 1996;37(9):1401–6.
[100] Sahin B, Yavuz H, Kodal A. The overall efficiency of a combined endoreversible engine at maximum power output conditions. ECOS'95; July 11–15, 1995. p. 116–20.
[101] Bejan A. Theory of heat transfer-irreversible power plants. II. The optimal allocation of heat exchange equipment. Int J Heat Mass Transfer 1995;3(3):433–44.
[102] Ozkaynak S. The theoretical efficiency limits for a combined cycle under the condition of maximum power output. J Phys D: Appl Phys 1995;28:1–5.

[103] Chen J. The efficiency of an irreversible combined cycle at maximum specific power output. J Appl Phys 1996;29: 2818–22.
[104] Chen J. A universal model of an irreversible combined Carnot cycle system and its general performance characteristics. J. Phys A: Math. Gen. 1998;31:3383–94.
[105] Sahin B, Kodal A. Steady-state thermodynamic analysis of a combined Carnot cycle with internal irreversibility. Energy 1995;20(12):1285–9.
[106] Leff HS. Thermal efficiency at maximum work output: New results for old heat engines. Am J Phys 1987;55(7): 602–10.
[107] Landsberg PT, Leff HS. Thermodynamic cycles with nearly universal maximum-work efficiencies. J Phys A: Math Gen 1989;22:4019–26.
[108] Joule JP, Joule's scientific papers, vol. 1. London: Dawson of Pall Mall; 1963. p. 331.
[109] Wu C, Kiang RL. Work and power optimization of a finite-time Brayton cycle. Int J Ambient Energy 1990;11:129–36.
[110] Wu C. Power optimization of an endoreversible Brayton gas heat engine. Energy Convers Mgmt 1991;3(6):561–5.
[111] Wu C, Kiang RL. Power performance of a nonisentropic Brayton cycle. J Engng Gas Turbines Power 1991;11(4): 501–4.
[112] Ibrahim OM, Klein SA, Mitchell JW. Optimum heat power cycles for specified boundary-conditions. J Engng Gas Turbines Power 1991;11(4):514–21.
[113] Cheng CY, Chen CK. Power optimization of an irreversible Brayton heat engine. Energy Sources 1997;1(5):461–74.
[114] Blank DA. Analysis of a combined law power-optimized open Joule–Brayton heat engine cycle with a finite interactive heat source. J Phys D: Appl Phys 1999;32: 769–76.
[115] Gandhidasan P. Thermodynamic analysis of a closed-cycle, solar gas turbine plant. Energy Convers Mgmt 1993;3(8): 657–61.
[116] Cheng CY, Chen CK. Power optimization of an endoreversible regenerative Brayton cycle. Energy 1996;2(4): 241–7.
[117] Cheng CY, Chen CK. Maximum power of an endoreversible intercooled Brayton cycle. Int J Energy Res 2000;2(6): 485–94.
[118] Hernandez AC, Medina A, Roco JMM. Power and efficiency in a regenerative gas-turbine. J Phys D: Appl Phys 1995; 2(10):2020–3.
[119] Wu C, Chen L, Sun F. Performance of a regenerative Brayton Heat Engine. Energy 1996;2(2):71–6.
[120] Roco JMM, Velasco S, Medina A, Hernandez AC. Optimum performance of a regenerative Brayton thermal cycle. J Appl Phys 1997;8(6):2735–41.
[121] Hernandez AC, Roco JNM, Medina A. Power and efficiency in a regenerative gas-turbine cycle with multiple reheating and intercooling stages. J Phys D: Appl Phys 1996;2(6): 1462–8.
[122] Chen LG, Sun FR, Wu C, Kiang RL. Theoretical analysis of the performance of a regenerative closed Brayton cycle with internal irreversibilities. Energy Convers Mgmt 1997;3(9): 871–7.
[123] Vecchiarelli J, Kawall JG, Wallace JS. Analysis of a concept for increasing the efficiency of a Brayton cycle via isothermal heat addition. Int J Energy Res 1997;2(2):113–27.
[124] Goktun S, Yavuz H. Thermal efficiency of a regenerative Brayton cycle with isothermal heat addition. Energy Convers Mgmt 1999;4(12):1259–66.
[125] Sahin B, Kodal A, Yilmaz T, Yavuz H. Maximum power-density analysis of an irreversible Joule–Brayton Engine. J Phys D: Appl Phys 1996;29:1162–7.
[126] Medina A, Roco JMM, Hernandez AC. Regenerative gas turbines at maximum power density conditions. J Phys D: Appl Phys 1996;29:2802–5.
[127] Sahin B, Kodal A, Kaya SS. A comparative performance analysis of irreversible regenerative reheating Joule–Brayton engines under maximum power density and maximum power conditions. J Phys D: Appl Phys 1998;31:2125–31.
[128] Chen LG, Zheng JL, Sun FR, Wu C. Optimum distribution of heat exchanger inventory for power density optimization of an endoreversible closed Brayton cycle. J Phys D: Appl Phys 2001;3(3):422–7.
[129] Chen LG, Zheng JL, Sun FR, Wu C. Performance comparison of an endoreversible closed variable temperature heat reservoir Brayton cycle under maximum power density and maximum power conditions. Energy Convers Mgmt 2002;4(1):33–43.
[130] Chen LG, Zheng JL, Sun FR, Wu C. Power density analysis and optimization of a regenerated closed variable-temperature heat reservoir Brayton cycle. J Phys D: Appl Phys 2001; 3(11):1727–39.
[131] Erbay LB, Goktun S, Yavuz H. Optimal design of the regenerative gas turbine engine with isothermal heat addition. Appl Energy 2001;6(3):249–64.
[132] Cheng CY, Chen CK. Ecological optimization of an endoreversible Brayton cycle. Energy Convers Mgmt 1998; 3(1-2):33–44.
[133] Chen CY, Chen CK. Ecological optimization of an irreversible Brayton heat engine. J Phys D: Appl Phys 1999;32:350–7.
[134] Huang YC, Hung CI, Chen CK. An ecological exergy analysis for an irreversible: Brayton engine with an external heat source. Proc Inst Mech Engrs A, J Power 2000;21(A5): 413–21.
[135] Reader GT. Stirling regenerators. Heat Transfer Engng 1994; 15(2):19–25.
[136] Walker G. Stirling engines. Oxford: Oxford University Press; 1980.
[137] Daub EE. The regenerator principle in the Stirling and Ericsson hot air engines. Br J Hist Sci 1974;7(27): 529–77.
[138] Badescu V. Optimum operation of a solar converter in combination with a Stirling or Ericsson heat engine. Energy 1992;17(6):601–7.
[139] Ladas HG, Ibrahim OM. Finite-time view of the Stirling engine. Energy 1994;19(8):837–43.
[140] Senft JR. Theoretical limits on the performance of Stirling engines. Int J Energy Res 1998;22:991–1000.
[141] Blank DA, Davis GW, Wu C. Power optimization of an endoreversible Stirling cycle with regeneration. Energy 1994;19:125–33.
[142] Blank DA, Wu C. Power limit of an endoreversible Ericsson cycle with regeneration. Energy Convers Mgmt 1996;37: 59–66.
[143] West CD. Principles and applications of Stirling engines. New York: Van Nostrand-Reinhold; 1986.

[144] Blank DA, Wu C. Power optimization of an extra-terrestrial solar radiant Stirling heat engine. Energy 1995;20(6): 523–30.
[145] Blank DA, Wu C. Finite-time power limit for solar-radiant Ericsson engines in space applications. Appl Therm Eng 1998;18:1347–57.
[146] Erbay LB, Yavuz H. Analysis of the Stirling heat engine at maximum power conditions. Energy 1997;7:645–50.
[147] Erbay LB, Yavuz H. Analysis of an irreversible Ericsson engine with a realistic regenerator. Appl Energy 1999;62: 155–67.
[148] Erbay LB, Yavuz H. Optimization of the irreversible Stirling heat engine. Int J Energy Res 1999;23:863–73.
[149] Wu F, Chen L, Wu C, Sun F. Optimum performance of irreversible Stirling engine with imperfect regeneration. Energy Convers Mgmt 1998;39(8):727–32.
[150] Chen J, Yan Z, Chen L, Andresen B. Efficiency bound of a solar-driven Stirling heat engine system. Int J Energy Res 1998;22:805–12.
[151] Feidt M, Costea M, Popescu G. Optimal design of Stirling engine using a generalized heat transfer law model. Proceedings of the Workshop on Second Law Analysis of Energy System Symposium; 1995. p. 431–41.
[152] Feidt M, Costea M, Belabbas B. Influence of the regenerator on the optimal distribution of the heat transfer surface conductance in a Stirling engine. ECOS'96; June 25–27, 1996. p. 179–86.
[153] Costea M, Feidt M. The effect of the overall heat transfer coefficient variation on the optimal distribution of the heat transfer surface conductance or area in a Stirling engine. Energy Convers Mgmt 1998;16–18: 1753–61.
[154] Blank DA. Generalized mixed-mode heat transfer studies to enhance power and work at optimum power in reciprocating regenerative Stirling-like and Carnot heat engines with interactive finite thermal reservoirs. J Phys D: Appl Phys 1999;32:2515–25.
[155] Bhattacharyya S, Blank DA. A universal expression for optimum specific work of reciprocating heat engines having endoreversible Carnot efficiencies. Int J Energy Res 1999;23: 327–34.
[156] Gu CJ, Lin L. A heat-power cycle for electricity generation from hot water with non-azeotropic mixtures. Energy 1988; 13:529–36.
[157] Lee WY, Kim SS. The maximum power from a finite reservoir for a Lorentz cycle. Energy 1992;17:275–81.
[158] Mozurkewich M, Berry RS. Optimal paths for thermodynamic systems: the ideal otto cycle. J Appl Phys 1982;5(1): 34–42.
[159] Hoffman KH, Watowich SJ, Berry RS. Optimal paths for thermodynamic systems: the ideal Diesel cycle. J Appl Phys 1985;5(6):2125–34.
[160] Band YB, Kafri O, Salamon P. Finite time thermodynamics: optimal expansion of a heated working fluid. J Appl Phys 1982;5(1):8–27.
[161] Aizenbud BM, Band YB, Kafri O. Optimization of a model internal combustion engine. J Appl Phys 1982;5(3): 1277–82.
[162] Klein SA. An explanation for observed compression ratios in internal combustion engines. J Engng Gas Turbines Power 1991;113:511–3.
[163] Wu C, Blank DA. The effects of combustion on a work-optimized endoreversible Otto cycle. J Inst Energy 1992; 6(1):86–9.
[164] Blank DA, Wu C. The effect of combustion on a power optimized endoreversible Diesel cycle. Energy Convers Mgmt 1993;3(6):493–8.
[165] Chen XY. Optimization of the dual cycle considering the effect of combustion on power. Energy Convers Mgmt 1997; 3(4):371–6.
[166] Wu C, Blank DA. Optimization of the endoreversible Otto cycle with respect to both power and mean effective pressure. Energy Convers Mgmt 1993;3(12):1255–9.
[167] Orlov VN, Berry RS. Power and efficiency limits for internal combustion engines via methods of finite-time thermodynamics. J Appl Phys 1993;7(10):4317–22.
[168] Angulo-Brown F, Fernandez-Betanzos J, Diaz-Pico CA. Compression ratio of an optimized air standard Otto cycle model. Eur J Phys 1994;15:38–42.
[169] Hernandez AC, Medina A, Roco JMM, Velasco S. On an irreversible air standard Otto cycle model. Eur J Phys 1995; 16:73–5.
[170] Angulo-Brown F, Rocha-Martinez JA, Navarrete-Gonzalez TD. A non-endoreversible Otto cycle model: improving power output and efficiency. J Phys D: Appl Phys 1996;29: 80–3.
[171] Aragon-Gonzalez G, Canales-Palma A, Leon-Galicia A. Maximum irreversible work and efficiency in power cycles. J Phys D: Appl Phys 2000;33:1403–9.
[172] Chen L, Lin J, Sun F, Wu C. Efficiency of an Atkinson engine at maximum power density. Energy Convers Mgmt 1998; 3(3/4):337–41.
[173] Chen L, Zeng F, Sun F, Wu C. Heat transfer effects on net work and/or power as functions of efficiency for air standard Diesel cycles. Energy 1996;2(12):1201–5.
[174] Akash BA. Effect of heat transfer on the performance of an air-standard Diesel cycle. Int Commun Heat Mass 2001;2(1): 87–95.
[175] Chen L, Wu C, Sun F, Cao S. Heat transfer effects on the net work output and efficiency characteristics for an air standard Otto cycle. Energy Convers Mgmt 1998;3(7):643–8.
[176] Lin J, Chen L, Wu C, Sun F. Finite-time thermodynamic performance of a dual cycle. Int J Energy Res 1999;2(9): 765–72.
[177] Bhattacharyya S. Optimizing an irreversible Diesel cycle: fine tuning of compression ratio and cut-off ratio. Energy Convers Mgmt 2000;41:847–54.
[178] Chen LG, Lin JX, Luo J, Sun F, Wu C. Friction effect on the characteristic performance of Diesel engines. Int J Energy Res 2002;2(11):965–71.
[179] Wang W, Chen L, Sun F, Wu C. The effect of friction on the performance of an air standard dual cycle. Exergy 2002;2: 340–4.
[180] Sahin B, Kesgin U, Kodal A, Vardar N. Performance optimization of a new combined power cycle based on power density analysis of the dual cycle. Energy Convers Mgmt 2002;4(15):2019–31.
[181] Sahin B, Ozsoysal OA, Sogut OS. A comparative performance analysis of endoreversible dual cycle under maximum ecological function and maximum power conditions. Exergy 2002;2:173–85.

[182] Aydin M, Yavuz H. Application of finite-time thermodynamics to MHD power cycles. Energy 1993;9:907–11.
[183] Sahin B, Kodal A, Yavuz H. A performance analysis for MHD power cycles operating at maximum power density. J Phys D: Appl Phys 1996;29:1473–5.
[184] Sahin B, Kodal A, Oktem AS. Optimal performance analysis of irreversible regenerative MHD power cycles. J Phys D: Appl Phys 1999;32:1832–41.
[185] Wu C. Optimal power from a radiating solar-powered thermionic engine. Energy Convers Mgmt 1992;3(4): 279–82.
[186] Gordon JM. Generalized power versus efficiency characteristics of heat engines: the thermoelectric generator as an instructive illustration. Am J Phys 1991;59(6):551–5.
[187] Wu C. Specific cooling load of thermoelectric refrigerators. Proceedings of the XI International Conference on Thermoelectrics, Arlington, TX; 1992. p. 136–9.
[188] Wu C, Schulden W. Specific heating load of thermoelectric heat pumps. Energy Convers Mgmt 1994;35:459–64.
[189] Ozkaynak S, Goktun S. Effect of irreversibilities on the performance of a thermoelectric generator. Energy Convers Mgmt 1994;35(12):1117–21.
[190] Goktun S. Design considerations for a thermoelectric refrigerator. Energy Convers Mgmt 1995;36:1197–200.
[191] Goktun S. Optimal performance of a thermoelectric refrigerator. Energy Sources 1996;18:531–6.
[192] Agrawal DC, Menon VJ. The thermoelectric generator as an endoreversible Carnot engine. J Phys D: Appl Phys 1997;30: 357–9.
[193] Nuwayhid RY, Moukalled F, Noueihed N. On entropy generation in thermoelectric devices. Energy Convers Mgmt 2000;41:891–914.
[194] Leff HS, Teeters WD. EER and 2nd law efficiency for air-conditioners. Am J Phys 1978;46:19–22.
[195] Blanchard CH. Coefficient of performance for finite-speed heat pump. J Appl Phys 1980;51:2471–2.
[196] Yan Z, Chen J. A class of Irreversible Carnot refrigeration cycles with a general heat transfer law. J Phys D: Appl Phys 1990;23:136–41.
[197] De Vos A. Reflections on the power delivered by endoreversible engines. J Phys D: Appl Phys 1987;20(2):232–6.
[198] Bejan A. Theory of heat transfer-irreversible refrigeration plants. Int J Heat Mass Transfer 1989;32:1631–9.
[199] Klein SA. Design considerations for refrigeration cycles. Rev Int Froid 1992;15(3):181–5.
[200] Bejan A. Power and refrigeration plants for minimum heat exchanger inventory. J Energy Resour Technol 1993;115: 148–50.
[201] Bejan A. Power generation and refrigeration models with heat transfer irreversibilities. J Heat Transfer Soc Jpn 1994; 33(128):68–75.
[202] Radcenco V, Vargas JVC, Bejan A, Lim JS. Two design aspects of defrosting refrigerators. Int J Refrig 1995;18(2): 76–86.
[203] Agrawal DC, Menon VJ. Performance of a Carnot refrigerator at maximum cooling power. J Phys A: Math Gen 1990; 23(22):5319–26.
[204] Agrawal DC, Menon VJ. Finite-time Carnot refrigerators with wall gain and product loads. J Appl Phys 1993;74: 2153–8.
[205] Grazzini G. Irreversible refrigerators with isothermal heat exchangers. Int J Refrig 1993;16:101–6.
[206] Ait-Ali MA. Finite-time optimum refrigeration cycles. J Appl Phys 1995;77(9):4280–4.
[207] Wu C. Maximum obtainable specific cooling load of a refrigerator. Energy Convers Mgmt 1995;36:7–10.
[208] Wu C. Performance of an endoreversible Carnot refrigerator. Energy Convers Mgmt 1996;37(10):1509–12.
[209] Chiou JS, Liu CJ, Chen CK. The performance of an irreversible Carnot refrigeration cycle. J Phys D: Appl Phys 1995;28:1314–8.
[210] Chen WZ, Sun FR, Cheng SM, Chen LG. Study on optimal performance and working temperatures of endoreversible forward and reverse Carnot cycles. Int J Energy Res 1995;19: 751–9.
[211] Ait-Ali MA. A class of internally irreversible refrigeration cycles. J Phys D: Appl Phys 1996;29:593–9.
[212] Ait-Ali MA. The maximum coefficient of performance of internally irreversible refrigerators and heat pumps. J Phys D: Appl Phys 1996;29:975–80.
[213] Salah El-Din MM. Optimization of totally irreversible refrigerators and heat pumps. Energy Convers Mgmt 1999; 40:423–36.
[214] Chen J. New performance bounds of a class of irreversible refrigerators. J Phys A: Math Gen 1994;27:6395–401.
[215] Cheng CY, Chen CK. Performance optimization of an irreversible heat pump. J Phys D: Appl Phys 1995;28:2451–4.
[216] Chen L, Wu C, Sun F. Influence of internal heat leak on the performance of refrigerators. Energy Convers Mgmt 1998; 39(1/2):45–50.
[217] Chen L, Sun F, Ni N, Wu C. Optimal configuration of a class of two-heat-reservoir refrigeration cycles. Energy Convers Mgmt 1998;39:767–73.
[218] Chen L, Sun F, Wu C, Kiang RL. A generalized model of a real refrigerator and its performance. Appl Therm Engng 1997;17:401–12.
[219] Davis GW, Wu C. Optimal performance of a geothermal heat-engine-driven heat-pump system. Energy 1994;12: 1219–33.
[220] Davis GW, Wu C. Finite time analysis of a geothermal heat engine driven air conditioning system. Energy Convers Mgmt 1997;38:263–8.
[221] Chen J, Yan Z. Optimal performance of an endoreversible-combined refrigeration cycle. J Appl Phys 1988;63: 4795–9.
[222] Chen L, Sun F, Chen W. Optimization of the specific rate of refrigeration in combined refrigeration cycles. Energy 1995; 20:1049–53.
[223] Chen L, Wu C, Sun F. Optimization of specific rate of heat pumping in combined heat pump cycles. Energy Convers Mgmt 1998;39(1/2):113–6.
[224] Chen J, Wu C. Performance of a cascade endoreversible heat pump system. J Inst Energy 1995;68:137–41.
[225] Chen J, Wu C. Optimization of a two-stage combined refrigeration system. Energy Convers Mgmt 1996;7(3):353–8.
[226] Chen L, Wu C, Sun F. Steady flow combined refrigeration cycle performance with heat leak. Appl Therm Engng 1997; 17:639–45.
[227] Chen J. Performance characteristics of a two-stage irreversible combined refrigeration system at maximum coefficient of performance. Energy Convers Mgmt 1999;40:1939–48.

[228] Chen J. The general performance characteristics of an *n*-stage combined refrigeration system affected by multi-irreversibilities. J Phys D: Appl Phys 1999;32:1462–8.
[229] Goktun S. Coefficient of performance for an irreversible combined refrigeration cycle. Energy 1996;21:721–4.
[230] Kaushik SC, Kumar P, Jain S. Performance evaluation of irreversible cascaded refrigeration and heat pump cycles. Energy Convers Mgmt 2002;43:2405–24.
[231] Wu C. Heat exchanger effect on a gas refrigeration cycle. Energy Convers Mgmt 1996;37:1513–6.
[232] Wu C, Chen L, Sun F. Optimization of steady flow refrigeration cycles. Int J Ambient Energy 1996;17: 199–206.
[233] Chen L, Wu C, Sun F. Finite-time thermodynamic performance of an isentropic closed regenerated Brayton refrigeration cycle. Int J Energy Environ Econ 1997;4:261–74.
[234] Chen L, Wu C, Sun F. Cooling load vs. COP characteristics for an irreversible air refrigeration cycle. Energy Convers Mgmt 1998;39:117–25.
[235] Chen L, Zhou S, Sun F, Wu C. Performance of heat-transfer irreversible regenerated Brayton refrigerators. J Phys D: Appl Phys 2001;34:830–7.
[236] Ni N, Chen L, Wu C, Sun F. Performance analysis for endoreversible closed regenerated Brayton heat pump cycles. Energy Convers Mgmt 1999;40:393–406.
[237] Chen L, Ni N, Wu C, Sun F. Performance analysis of a closed regenerated Brayton heat pump with internal irreversibilities. Int J Energy Res 1999;23:1039–50.
[238] Yan Z, Chen J. The characteristics of polytropic magnetic refrigeration cycles. J Appl Phys 1991;70(4): 1911–4.
[239] Chen J, Yan Z. The effect of field-dependent heat capacity on regeneration in magnetic Ericsson cycles. J Appl Phys 1991; 69(9):6245–7.
[240] Yan Z, Chen J. A note on the Ericsson refrigeration cycle of paramagnetic salt. J Appl Phys 1989;66(5):2228–9.
[241] Dai W. Regenerative balance in magnetic Ericsson refrigeration cycles. J Appl Phys 1995;78(5):5272–4.
[242] Yan Z. On the criterion of perfect regeneration for a magnetic Ericsson cycle. J Appl Phys 1995;78(5):2903–5.
[243] Chen J, Yan Z. The effect of thermal resistances and regenerative losses on the performance characteristics of a magnetic Ericsson refrigeration cycle. J Appl Phys 1998; 84(4):1791–5.
[244] Chen J, Yan Z. The general performance characteristics of a Stirling refrigerator with regenerative losses. J Phys D: Appl Phys 1996;29:987–90.
[245] Chen J, Yan Z. The influence of regenerative losses on the maximum cooling rate of a Stirling refrigerator. Proceedings of ECOS'96, Stockholm: Royal Institute of Technology; 1996. p. 147–51.
[246] Chen J. Minimum power input of irreversible Stirling refrigerator for given cooling rate. Energy Convers Mgmt 1998;39:1255–63.
[247] Petrescu S, Harman C, Petrescu V. Stirling cycle optimization including the effects of finite speed operation. Proceedings of ECOS'96, Stockholm: Royal Institute of Technology; 1996. p. 167–73.
[248] Kaushik SC, Tyagi SK, Bose SK, Singhal MK. Performance evaluation of irreversible Stirling and Ericsson heat pump cycles. Int J Therm Sci 2002;41:193–200.
[249] Wu C. Analysis of an endoreversible Rallis cycle. Energy Convers Mgmt 1994;35:79–85.
[250] Yan Z, Chen J. An optimal endoreversible three-heat-source refrigerator. J Appl Phys 1989;65:1–4.
[251] Chen J, Yan Z. Equivalent combined systems of three-heat-source heat pumps. J Chem Phys 1989;90:4951–5. see also p. 1–4.
[252] Wu C. Maximum cooling load of a heat-engine-driven refrigerator. Energy Convers Mgmt 1993;34:691–6.
[253] Davis GW, Wu C. Endoreversible analysis of a heat-engine-driven heat pump system utilizing low grade thermal energy. Circus, second law analysis of energy systems: towards the 21st century; July 1995. p. 223–31.
[254] D'Accadia MD, Sasso M, Sibilio S. Design consideration for irreversible heat-engine-driven heat pumps. ECOS'96; June 25–27, 1996. p. 135–40.
[255] D'Accadia MD, Sasso M, Sibilio S. Optimum performance of heat-engine-driven heat pumps: finite-time approach. Energy Convers Mgmt 1997;38(4):401–13.
[256] Chen J. The equivalent cycle system of an endoreversible absorption refrigerator and its general performance characteristics. Energy 1995;20:995–1003.
[257] Chen J, Andresen B. Optimal analysis of primary performance parameters for an endoreversible absorption heat pump. Heat Recovery Syst CHP 1995;15: 723–31.
[258] Chen J, Schouten JA. Optimum performance characteristics of an irreversible absorption refrigeration system. Energy Convers Mgmt 1998;39:999–1007.
[259] Chen J. The optimum performance characteristics of a four-temperature-level irreversible absorption refrigerator at maximum specific cooling load. J Phys D: Appl Phys 1999; 32:3085–91.
[260] Chen J. The general performance characteristics of an irreversible absorption heat pump operating between four temperature levels. J Phys D: Appl Phys 1999;32: 1428–33.
[261] Wijeysundera NE. Analysis of the ideal absorption cycle with external heat-transfer irreversibilities. Energy 1995; 20(2):123–30.
[262] Goktun S. The effect of irreversibilities on the performance of a three-heat-source heat pump. J Phys D: Appl Phys 1996; 29:2823–5.
[263] Goktun S. Optimal performance of an irreversible refrigerator with three heat sources (IRWTHS). Energy 1997;22: 27–31.
[264] Bhardwaj PK, Kaushik SC, Jain S. Finite time optimization of an endoreversible and irreversible vapour absorption refrigeration system. Energy Convers Mgmt 2003;44: 1131–44.
[265] Goktun S, Yavuz H. The performance of irreversible combined heat pump cycles. J Phys D: Appl Phys 1997;30: 2848–52.
[266] Bejan A, Vargas JVC, Sokolov M. Optimal allocation of a heat exchanger inventory in heat driven refrigerators. Int J Heat Mass Transfer 1995;38(16):2997–3004.
[267] Chen J. Optimal performance characteristics of a solar-driven heat pump at maximum COP. Energy Convers Mgmt 1994; 35(12):1009–14.
[268] Chen J. Optimal heat-transfer areas for endoreversible heat pumps. Energy 1994;19(10):1031–6.

[269] Chen J. Optimal performance analysis of irreversible cycles used as heat pumps and refrigerators. J Phys D: Appl Phys 1997;30:582–7.
[270] Lin G, Yan Z. The optimal performance of an irreversible solar-driven heat pump system. ECOS'96; June 25–27, 1996. p. 141–5.
[271] Lin G, Yan Z. The optimal operating temperature of the collector of an irreversible solar-driven refrigerator. J Phys D: Appl Phys 1999;32:94–8.
[272] Wu C, Chen L, Sun F, Cao S. Optimal collector temperature for solar-driven heat pumps. Energy Convers Mgmt 1998; 39(1/2):143–7.
[273] Goktun S, Ozkaynak S. Optimum performance of a corrugated collector-driven irreversible Carnot heat engine and absorption refrigerator. Energy 1997;22(5):481–5.
[274] Goktun S, Yavuz H. The optimum performance of an irreversible solar-driven Carnot refrigerator and combined heat engine. J Phys D: Appl Phys 1997;30:3317–21.
[275] Goktun S. Optimization of irreversible solar assisted ejector-vapor compression cascaded systems. Energy Convers Mgmt 2000;41:625–31.
[276] Goktun S. Optimal performance of an irreversible, heat engine-driven, combined vapour compression and absorption refrigerator. Appl Energy 1999;62:67–79.
[277] Chen J. The influence of multi-irreversibilities on the performance of a heat transformer. J Phys D: Appl Phys 1997;30:2953–7.
[278] Chen J. Equivalent combined cycle of an endoreversible absorption heat transformer and optimal analysis of primary performance parameters. Energy Convers Mgmt 1997;38: 705–12.
[279] Chen T, Yan Z. An ecological optimization criterion for a class of irreversible absorption heat transformers. J Phys D: Appl Phys 1998;31:1078–82.
[280] Huang FF. Performance assessment parameters of a cogeneration system. In: Alvfors P, Eidensten L, Svedberg G, Yan J, editors. Proceedings of ECOS'96. Stockholm: Royal Institute of Technology; 1996. p. 2255–29.
[281] Goktun S. Finite-time thermodynamic analysis of an irreversible cogeneration refrigerator. In: Wu C, Chen L, Chen J, editors. Recent advances in finite-time thermodynamics. Commarck, NY: Nova Science; 1999. p. 127–34.
[282] Goktun S. Performance analysis of an irreversible cogeneration heat pump cycle. Int J Energy Res 1998;22:1299–304.
[283] Goktun S. Solar powered cogeneration system for air conditioning and refrigeration. Energy 1999;24:971–7.
[284] Goktun S, Ozkaynak S. Performance parameters for the design of a solar-driven cogeneration system. Energy 2001; 26:57–64.
[285] Goktun S, Yavuz H. Performance of irreversible combined cycles for cryogenic refrigeration. Energy Convers Mgmt 2000;41:449–59.
[286] Wu C. Analysis of an endoreversible Stirling cooler. Energy Convers Mgmt 1993;34(12):1249–53.
[287] Gordon JM, Ng KC. Thermodynamic modelling of reciprocating chillers. J Appl Phys 1994;75(6):2769–74.
[288] Bejan A. Power and refrigeration plants for minimum heat-exchanger inventory. ASME Trans J Energy Resour Technol 1993;115(2):148–55.
[289] De Vos A. Endoreversible thermoeconomics. Energy Convers Mgmt 1995;3(1):1–5.
[290] De Vos A. Endoreversible economics. Energy Convers Mgmt 1997;3(4):311–7.
[291] Bera NC, Bandyopadhyay S. Effect of combustion on the economic operation of endoreversible Otto and Joule–Brayton engine. Int J Energy Res 1998;2(3):249–56.
[292] Bandyopadhyay S, Bera NC, Bhattacharyya S. Thermoeconomic optimization of combined cycle power plants. Energy Convers Mgmt 2001;4(3):359–71.
[293] Wu C, Chen L, Sun F. Effect of the heat transfer law on the finite-time exergoeconomic performance of heat engines. Energy 1996;21(12):1127–34.
[294] Wu C, Chen L, Sun F. Effects of heat transfer law on finite-time exergoeconomic performance of Carnot heat pump. Energy Convers Mgmt 1998;39(7):579–88.
[295] De Vos A. Endoreversible thermodynamics versus economics. Energy Convers Mgmt 1999;4(10):1009–19.
[296] Sahin B, Kodal A. Performance analysis of an endoreversible heat engine based on a new thermoeconomic optimization criterion. Energy Convers Mgmt 2001;4(9): 1085–93.
[297] Kodal A, Sahin B. Finite size thermoeconomic optimization for irreversible heat engines. Int J Therm Sci 2003;4: 777–82.
[298] Antar MA, Zubair SM. Thermoeconomic considerations in the optimum allocation of heat exchanger inventory for a power plant. Energy Convers Mgmt 2001;4(10):1169–79.
[299] Sahin B, Kodal A. Finite time thermoeconomic optimization for endoreversible refrigerators and heat pumps. Energy Convers Mgmt 1999;4(9):951–60.
[300] Kodal A, Sahin B, Yilmaz T. Effects of internal irreversibility and heat leakage on the finite time thermoeconomic performance of refrigerators and heat pumps. Energy Convers Mgmt 2000;4(6):607–19.
[301] Kodal A, Sahin B, Oktem AS. Performance analysis of two stage combined heat pump system based on thermoeconomic optimization criterion. Energy Convers Mgmt 2000;4(18): 1989–98.
[302] Sahin B, Kodal A, Koyun A. Optimal performance characteristics of a two-stage irreversible combined refrigeration system under maximum cooling load per unit total cost conditions. Energy Convers Mgmt 2001; 4(4):451–65.
[303] Kodal A, Sahin B, Erdil A. Performance analysis of a two-stage irreversible heat pump under maximum heating load per unit total cost conditions. Exergy 2003;2(3): 159–66.
[304] Sahin B, Kodal A. Thermoeconomic optimization of a two stage combined refrigeration system: a finite-time approach. Int J Refrig 2002;2(7):872–7.
[305] Kodal A, Sahin B, Ekmekci I, Yilmaz T. Thermoeconomic optimization for irreversible absorption refrigerators and heat pumps. Energy Convers Mgmt 2003;4(1):109–23.
[306] Chen JC, Wu C. Thermoeconomic analysis on the performance characteristics of a multi-stage irreversible combined heat pump system. J Energy Resour, ASME 2000;12(4): 212–6.
[307] Antar MA, Zubair SM. Thermoeconomic considerations in the optimum allocation of heat transfer inventory for refrigeration and heat pump systems. J Energy Resour, ASME 2002;12(1):28–33.
[308] Bejan A. Shape and structure, from engineering to nature. Cambridge: Cambridge University Press; 2000.

[309] Bejan A, Lorente S. Thermodynamic optimization of flow geometry in mechanical and civil engineering. J Non-Equilib Thermodyn 2001;2(4):305–54.
[310] Gyftopoulos EP. Fundamentals of analyses of processes. Energy Convers Mgmt 1997;3(15-17):1525–33.
[311] Gyftopoulos EP. Infinite time (reversible) versus finite time (irreversible) thermodynamics: a misconceived distinction. Energy 1999;24:1035–9.
[312] Moran MJ. On second-law analysis and the failed promise of finite-time thermodynamics. Energy 1998;2(6):517–9.
[313] Chen J, Yan Z, Lin G, Andresen B. On the Curzon–Ahlborn efficiency and its connection with the efficiencies of real heat engines. Energy Convers Mgmt 2001;42:173–81.
[314] Ishida M. The role and limitations of endoreversible thermodynamics. Energy 1999;24:1009–14.
[315] Denton JC. Thermal cycles in classical thermodynamics and nonequilibrium thermodynamics in contrast with finite time thermodynamics. Energy Convers Mgmt 2002;43: 1583–617.
[316] Bejan A. Models of power plants that generate minimum entropy while operating at maximum power. Am J Phys 1996;6(8):1054–9.
[317] Bejan A. Method of entropy generation minimization, or modeling and optimization based on combined heat transfer and thermodynamics. Rev Gén Therm 1996;35: 637–46.